AD-A088 160 TRANSPORTATION SYSTEMS CENTER CAMBRIDGE MA F/G 20/1
DETECTION AND ASSESSMENT OF SECONDARY SONIC BOOMS IN NEW ENGLAN--ETC(U)
MAY 80 E J RICKLEY, A D PIERCE
UNCLASSIFIED TSC-FAA-80-10 FAA-AEE-80-22 NL

1 OF 2
AD88 160

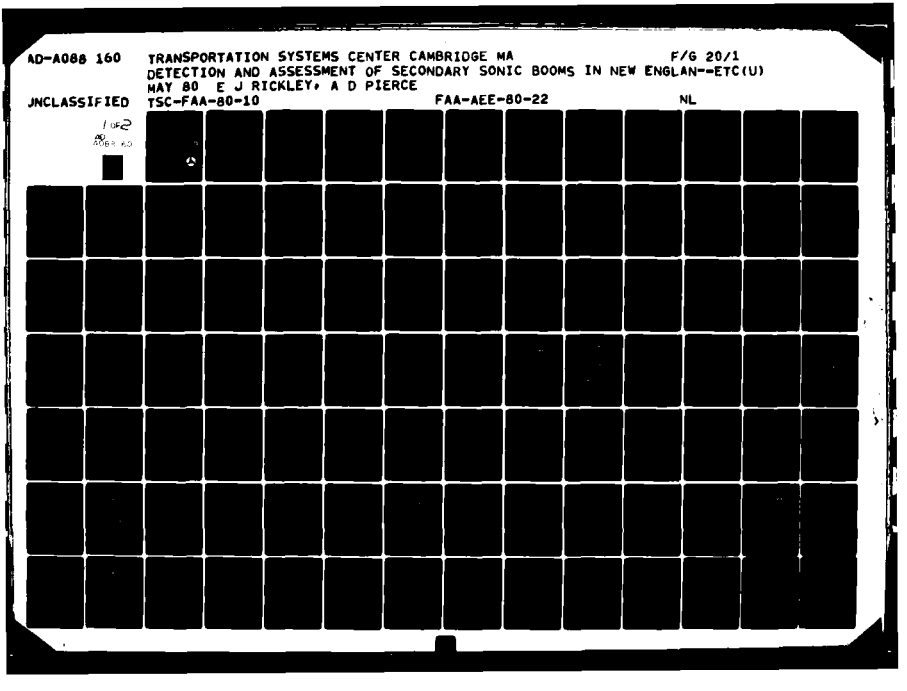

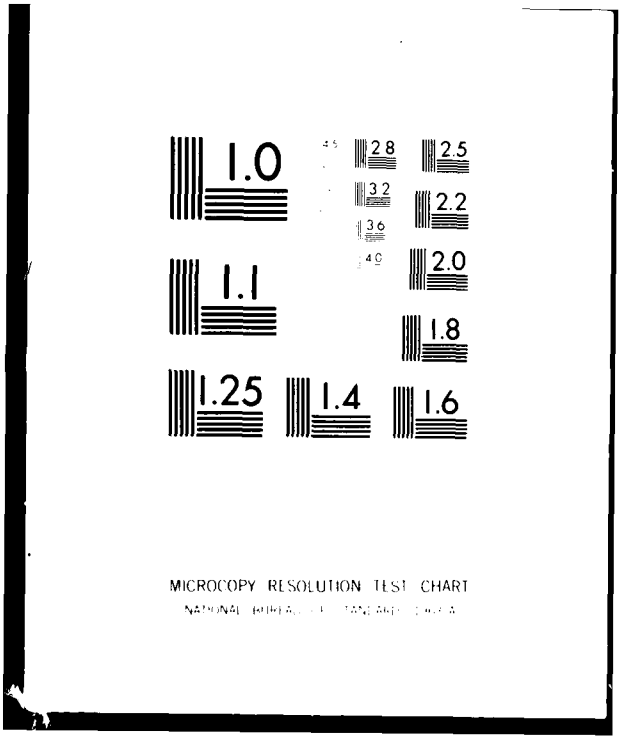
1.0
2.8
2.5
3.2
2.2
3.6
4.0
2.0
1.1
1.8
1.25
1.4
1.6
MICROCOPY RESOLUTION TEST CHART

LEVEL II

FAA-AEE-80-22

DETECTION AND ASSESSMENT OF SECONDARY SONIC BOOMS IN NEW ENGLAND

MAY 1980

U.S. DEPARTMENT OF TRANSPORTATION

RESEARCH AND SPECIAL PROGRAMS ADMINISTRATION
TRANSPORTATION SYSTEMS CENTER • CAMBRIDGE MA 02142

PREPARED FOR FEDERAL AVIATION ADMINISTRATION
OFFICE OF ENVIRONMENT AND ENERGY • WASHINGTON DC 20591

NOTICE

This document is disseminated under the sponsorship of the Department of Transportation in the interest of information exchange. The United States Government assumes no liability for its contents or use thereof.

NOTICE

The United States Government does not endorse products or manufacturers. Trade or manufacturers' names appear herein solely because they are considered essential to the object of this report.

Technical Report Documentation Page

1. Report No.	2. Government Accession No.	3. Recipient's Catalog No.
FAA-AEE-80-22	AD-A088160	

4. Title and Subtitle
DETECTION AND ASSESSMENT OF SECONDARY SONIC BOOMS IN NEW ENGLAND

5. Report Date
May 1980

6. Performing Organization Code
DOT/TSC

7. Author(s)
Edward J. Rickley, Allan D. Pierce*

8. Performing Organization Report No.
DOT-TSC-FAA-80-10

9. Performing Organization Name and Address
U.S. Department of Transportation
Research and Special Programs Administration
Transportation Systems Center
Kendall Square, Cambridge, MA 02142

10. Work Unit No. (TRAIS)
R0110/FA-053

11. Contract or Grant No.

12. Sponsoring Agency Name and Address
Department of Transportation
Federal Aviation Administration
800 Independence Ave., S.W.
Washington, DC 20591

13. Type of Report and Period Covered
Final Report

14. Sponsoring Agency Code
FAA

15. Supplementary Notes
*Faculty Fellow, on detail from Georgia Institute of Technology
Atlanta, GA 30332

16. Abstract

This report documents the results of a secondary sonic boom detection and assessment program conducted by the U.S. Department of Transportation, Transportation Systems Center in New England during the summer of 1979. Measurements of both acoustic and infrasonic signals were made. Measurement data and ray trace computations demonstrate that the secondary sonic booms frequently reported by New England residents are created by the Concorde passenger flight off the New England coast enroute to Kennedy Airport in New York City.

Signal amplitudes show wide fluctuations from flight to flight, from day to day, and with geographic locations.

A brief set of measurements were made in Applebachsville PA, show a similar day to day variability and are correlated with Concorde flights into Dulles Airport in Virginia.

17. Key Words	18. Distribution Statement
Acoustics, Aeroacoustics, Aircraft Noise, Atmospheric Acoustics, Concorde, Infrasound, Ray Acoustics, Sonic Boom, SST, Supersonic Transport	DOCUMENT IS AVAILABLE TO THE PUBLIC THROUGH THE NATIONAL TECHNICAL INFORMATION SERVICE, SPRINGFIELD, VIRGINIA 22161

19. Security Classif. (of this report)	20. Security Classif. (of this page)	21. No. of Pages	22. Price
Unclassified	Unclassified	142	

Form DOT F 1700.7 (8-72) Reproduction of completed page authorized

PREFACE

Appreciation is expressed to British Airways, Air France, and the personnel and officials of the New England and New York Regions of the FAA for their cooperation and for supplying operational information and tracking data; the personnel of the Air Resources Laboratory of the National Oceanic and Atmospheric Administration for supplying high altitude weather data; the Director of Parks and Recreation Division, Metropolitan District Commission, Boston MA; the Director of Parks and Recreation, Bucks County PA; and the Massachusetts Division of Forests and Parks for permission for the use of public, wooded areas as measurement sites; and the officials of the FAA Office of Environment and Energy for their helpful suggestions in this measurement and assessment program.

The following members of the Noise Measurement and Assessment Laboratory of the Transportation Systems Center contributed to the preparation of this report: G. Ameral, W. Cobb, A. Dahlgren, R. Quinn, N. Rice, and R. Salamone.

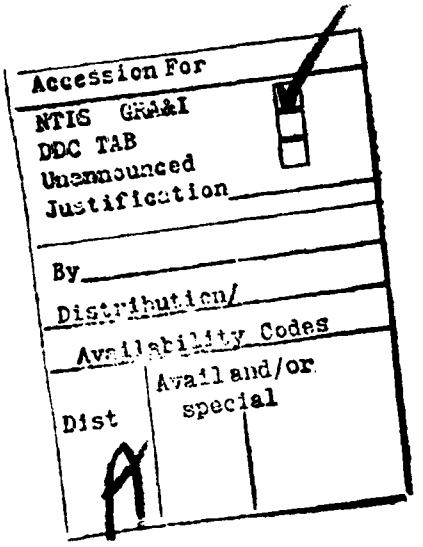

METRIC CONVERSION FACTORS

Approximate Conversions to Metric Measures

Symbol	When You Know	Multiply by	To Find	Symbol
		LENGTH		
in	inches	*2.5	centimeters	cm
ft	feet	30	centimeters	cm
yd	yards	0.9	meters	m
mi	miles	1.6	kilometers	km
		AREA		
in^2	square inches	6.5	square centimeters	cm^2
ft^2	square feet	0.09	square meters	m^2
yd^2	square yards	0.8	square meters	m^2
mi^2	square miles	2.6	square kilometers	km^2
	acres	0.4	hectares	ha
		MASS (weight)		
oz	ounces	28	grams	g
lb	pounds	0.45	kilograms	kg
	short tons (2000 lb)	0.9	tonnes	t
		VOLUME		
tsp	teaspoons	5	milliliters	ml
Tbsp	tablespoons	15	milliliters	ml
fl oz	fluid ounces	30	milliliters	ml
c	cups	0.24	liters	l
pt	pints	0.47	liters	l
qt	quarts	0.95	liters	l
gal	gallons	3.8	liters	l
ft^3	cubic feet	0.03	cubic meters	m^3
yd^3	cubic yards	0.76	cubic meters	m^3
		TEMPERATURE (exact)		
°F	Fahrenheit temperature	5/9 (after subtracting 32)	Celsius temperature	°C

*1 in = 2.54 (exactly). For other exact conversions and more detailed tables, see NBS Misc. Publ. 286, Units of Weights and Measures. Price $2.25, SD Catalog No. C13.10:286

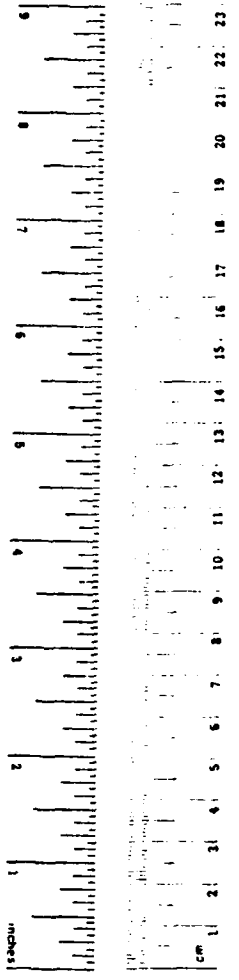

Approximate Conversions from Metric Measures

Symbol	When You Know	Multiply by	To Find	Symbol
		LENGTH		
mm	millimeters	0.04	inches	in
cm	centimeters	0.4	inches	in
m	meters	3.3	feet	ft
m	meters	1.1	yards	yd
km	kilometers	0.6	miles	mi
		AREA		
cm^2	square centimeters	0.16	square inches	in^2
m^2	square meters	1.2	square yards	yd^2
km^2	square kilometers	0.4	square miles	mi^2
ha	hectares (10,000 m^2)	2.5	acres	
		MASS (weight)		
g	grams	0.035	ounces	oz
kg	kilograms	2.2	pounds	lb
t	tonnes (1000 kg)	1.1	short tons	
		VOLUME		
ml	milliliters	0.03	fluid ounces	fl oz
l	liters	2.1	pints	pt
l	liters	1.06	quarts	qt
l	liters	0.26	gallons	gal
m^3	cubic meters	35	cubic feet	ft^3
m^3	cubic meters	1.3	cubic yards	yd^3
		TEMPERATURE (exact)		
°C	Celsius temperature	9/5 (then add 32)	Fahrenheit temperature	°F

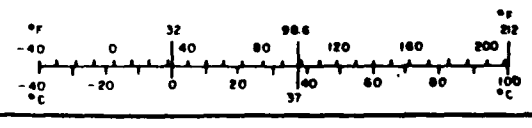

TABLE OF CONTENTS

LIST OF ILLUSTRATIONS

LIST OF ILLUSTRATIONS (CONTINUED)

LIST OF ILLUSTRATIONS (CONTINUED)

LIST OF ILLUSTRATIONS (CONTINUED)

LIST OF TABLES

ABBREVIATIONS

CPA	-	Closest Point of Approach
dB	-	decibel
dBA	-	decibels-A Weight
DOT/TSC	-	Department of Transportation, Transportation Systems Center
EDST	-	Eastern Daylight Savings Time
FAA	-	Federal Aviation Administration
GMT	-	Greenwich Mean Time
Hz	-	Hertz
JFK	-	John F. Kennedy International Airport
kHz	-	kilohertz
km	-	kilometer
lbs/ft^2	-	pounds per square foot
mb	-	millibar
m/s	-	meter per second
NOAA	-	National Oceanic and Atmospheric Administration
NWS	-	National Weather Service
rms	-	root mean square
SPL	-	Sound Pressure Level
SST	-	Supersonic Transport
uPa	-	microPascal

SUMMARY

Measurements of acoustic signals in the Boston area during summer 1979 are reported. The measurements demonstrate that the secondary sonic boom events frequently reported by New England residents during the summer are created by Concorde flights off the New England coast en route to Kennedy Airport in New York City. Reception times for such events are highly correlated with Concorde flight times; the time delay between aircraft time at closest point of approach to Hyannis MA and signal reception at Malden MA is constant within 53 seconds. Ray trace computations, based on best available meteorological data and on Federal Aviation Administration (FAA) radar measurements of Concorde flight profiles, predict signal arrival times within 20 seconds of that observed and predict wave front azimuthal angles within 4°.

Signal amplitudes show wide fluctuations from flight-to-flight and from day-to-day. The average measured event maximum peak-to-peak pressure amplitude for May, June, July, August, and the first half of September are 0.15, 0.14, 0.19, 0.20, and 0.11 pounds per square foot (lbs/ft^2). The largest individual values are 0.63, 0.69, 0.65, 0.59, and 0.35 for the five months, respectively. Simultaneous measurements carried out at other locations in the Boston area show that there are also wide variations with geographic location for the same event. A brief set of measurements for four days in July were made at Applebachsville PA. These measurements show similar day-to-day variability and are correlated with Concorde flights into Dulles Airport.

The ray trace computations indicate that the events with larger amplitudes are associated with strong focusing of the secondary boom at the reception site. Although the locations where strongest focusing occur vary significantly with meteorological conditions, the ray theory computations show that they generally fall within the greater Boston area during the summer months.

The data taken during this measurement program and the theoretical interpretation of the results provide the basis for evaluating the effectiveness of alternate operational procedures to reduce the frequency and intensity of secondary sonic booms within the U.S. mainland.

1. INTRODUCTION

This report documents the results of a Secondary Sonic Boom Detection and Assessment program conducted in New England during the summer of 1979 by the U.S. Department of Transportation - Transportation Systems Center (DOT/TSC) for the Office of Environment and Energy of the Federal Aviation Administration.

Secondary sonic boom events were reported in the New England area during the summer of 1978. These events were reported as muffled "thumps" and low-frequency "rumbles" and occurred predominantly in the morning hours between 8:00 and 10:30 am. Reports were received from citizens as far north as Maine and along New England coastal regions of New Hampshire, Massachusetts, and Rhode Island. Because of the widespread nature of the reported events and their low frequency nature, it was speculated at that time that these events originated from the shock wave of supersonic aircraft operating off the New England coast.

Preliminary investigation of the phenomena by DOT/TSC during September 1978 showed that there was some correlation in timing between boom data measured north of Boston and visual sightings of the New York-bound Concorde at Chatham MA. However, at that time data was insufficient to clearly establish the Concorde as the primary source of these secondary sonic booms.

A measurement program was thus devised to determine conclusively the source of the energy that precipitated the public reports and to provide an overall assessment of the propagation and disturbance mechanism.

2. TECHNICAL BACKGROUND

FAA flight rules require supersonic transports (SSTs) to fly at subsonic speeds over U.S. land areas in order to prevent sonic booms from impacting the U.S. environment. For aircraft approaching U.S. boundaries, flight rules specify operational procedures be such that direct sonic shock waves do not encroach upon the U.S.

Although these requirements are adequate to prevent primary shock waves from impacting U.S. population centers, secondary long distance effects are known to occur.[1,2,3] A principal propagation mechanism causing such long distance effects is refraction caused by wind and temperature gradient effects at altitudes between 20 and 60 km (the mesosphere). Sound rays that carry upward traveling sonic booms to such altitudes can be bent back toward the ground if these gradients cause the effective sound speed to increase with height; the basic mechanism has been understood for some time in connection with the abnormal zones[4] of audibility associated with the sound heard at large distances from gunfire and explosions. Such downward refraction can also take place in the thermosphere[5,6] (altitudes above 80 km); but the high attentuation and the lengthening of the shock duration at such high altitudes would render such thermospheric refracted arrivals much less likely to be audible by the time they return to the ground.

The secondary booms that arrive via a refracted path that bends downward in the mesosphere can be of two basic types (see Figure 1). Type I originates in the shock wave that is generated by the airplane and initially travels obliquely upward. Type II is initiated from a downward shock wave that reflects from the sea surface relatively close to the aircraft's trajectory, then travels up to the thermosphere and returns to the ground. In either case, it is possible for the propagation to be such that perceivable acoustic events occur in restricted on-shore regions. This refractive mode of low frequency acoustic propagation extends the possible impact region of an SST's supersonically generated acoustical disturbance

beyond its primary boom carpet. The ranges at which such secondary paths may reach the ground can be anywhere from 50 to 200 miles beyond the primary carpet.

Meteorological conditions play an important role in this long-range propagation of acoustical shock waves. Of the family of rays that leave the aircraft and are refracted, only a small fraction reach the ground. Only when the sum of the component of the wind velocity in the direction of propagation and the sound speed (at some altitude above the flight altitude) exceeds the corresponding sum at the ground, is it possible for these rays to reach the ground beyond the primary carpet area. The geometry of the paths may be such that large areas on the ground are not reached by any rays (creating quiet zones), while in areas further from the flight trajectory, rays may touch down, such that energy is received. This phenomenon, known as anomalous or abnormal sound, has been studied on various occasions in connection with large explosions near the ground. Up to now it has not been studied in much detail in connection with sonic boom propagation. The extreme sensitivity of the propagation paths to the sound speed and wind velocity profiles and large scale turbulence in the atmosphere suggests that the energy received at any point will vary substantially with meteorological conditions.

This effect of upper atmospheric wind currents explains the absence of reports in New England during the winter months when the stratospheric winds are predominantly westerly, thus inhibiting refractive propagation. On the other hand, during the summer months when strong easterly winds predominate, the secondary sonic boom events become evident.

An important consquence of these meteorological influences is that the energy reaching the ground via such long paths is unequally spread over the ground and that it is virtually impossible to predict precisely where the energy will be most concentrated. Given the atmosphere's basic structure, only a relatively small fraction of the acoustic energy created by the Concorde's supersonic flight should reach the ground via paths that are refracted

downwards in the upper atmosphere. If this energy were uniformly spread over a wide range of lateral distances, then it is doubtful that the secondary booms would ever be audible. However, focusing can produce an audible effect in a relatively small area. Thus, the reported events in New England are caused by circumstances when wind and temperature profiles, aircraft heading, speed, and location in the right combination produce an augmentation (or focusing) of acoustic energy at the location of the observer.

3. EXPERIMENTAL APPROACH

3.1 BASIC APPROACH

Low-frequency pressure changes were measured with three microphone measuring systems deployed in a triangular array during the period May 3, 1979 to September 14, 1979. The signals from each of the microphones along with a time code signal were recorded on a multitrack, FM tape recorder. The differences in arrival time among microphones and the position and dimensions of the array were used to compute the direction of the arriving wave front. This arriving ray vector was then used to project back to the signal source.

In addition to the three microphone array deployed, a single microphone recording system with time code synchronization was also deployed on occasion at several sites throughout the Greater Boston area. Measurements were made simultaneously with the multi-microphone and the single microphone systems to show the variability of the signals measured with site location.

3.2 MEASUREMENT SITES

A prime measurement site was selected within the expected "first bounce" impact area in the Middlesex Fells Reservation in Malden MA (Figure 2). A lightly wooded area was selected to provide natural wind reduction with relatively little attenuation of the expected signals.

Six other sites were chosen within a 25 mile radius of Boston to show the variability of the data with site location. These sites, Wilmington, Georgetown, Marlboro, Medfield, Sharon, and Cohasett MA, are shown in Figure 2.

A measurement site was also sought with coordinates relative to the flight track of inbound Concorde flights to Dulles International Airport similar to those of the Malden site relative to

inbound Concorde flight to Kennedy Airport (JFK). Measurements were made during the week of July 23, 1979 at a site in Applebachsville PA that met this requirement (see Figure 3).

3.3 INSTRUMENTATION AND DEPLOYMENT

Low-frequency (infrasonic) microphone systems, consisting of B&K 4146 one-inch condenser microphones and B&K 2631 Microphone Carrier System were used (Figure 4). The infrasonic data was band-filtered (0.5 to 30 Hz) and recorded on a four-track FM Instrumentation Tape Recorder HP Model 3960A. The microphones were enclosed in a weather proof wooden enclosure (30" x 20" x 16") to further reduce the effects of wind noise. An acoustic calibration signal of 125 Hertz (Hz) at a level of 114 decibels (db) re 20 micro-Pascal was recorded on tape to provide a reference level for the data reduction instrumentation.

Three low-frequency microphone systems were placed in a triangular array 250 feet apart (Figure 4). This triad was deployed at the Malden MA site except during the weeks of July 9-13, 1979 and July 23-26, 1979, when it was deployed at Georgetown MA and Applebachsville PA respectively.

A single low-frequency microphone system was deployed at the Malden MA site during these two weeks to provide continuity of the data. Occasionally, the single system was also deployed at sites in Wilmington, Marlboro, Medfield, Sharon, and Cohasett MA to provide an indication of the variability of the secondary boom that occurs within a 25 mile radius of Boston.

A vibration-measuring system consisting of an Endevco Accelerometer Model 2217E with signal conditioners was deployed in a residential home in Wilmington MA on June 20, 1979. The accelerometer was cemented to the center of a 54 by 60 inch by one-quarter inch plate glass window located in a room, facing east, at the rear of the house. Lateral acceleration levels (2 Hz to 1 kilohertz (kHz)) of the glass were recorded in synchronism with the infrasonic data from the low-frequency microphone system located outside approximately 100 feet from the window.

To measure and record events as perceived by a listener, an acoustic measuring system using a half inch, General Radio 1962-9610 Electret condenser microphone was also deployed on occasion. Measured outdoor acoustic data in the frequency band 15 Hz to 20 kHz was recorded on a Nagra model IVSJ instrumentation tape recorder.

A time code signal was recorded on all recorders for exact time synchronization.

3.4 FLIGHT DATA

Flight track data was obtained from the FAA Data Systems Office in Nashua NH from the air traffic control radar system. This data includes aircraft flight number, speed, altitude, position, and time of day. Physical data from the on-board recorders of several selected flights was obtained from British Airways and Air France to supplement the radar data. (See typical tracks to JFK and Dulles Airports in Figures 2 and 3, respectively.)

In addition, an aircraft receiver tuned to Boston Air Route Traffic Control Center was used to assist in aircraft identification.

3.5 WEATHER DATA

Local weather was recorded continuously on site. High altitude data were obtained from rocketsonde observations from Wallops Island VA. Local high altitude data were obtained from balloon observations and from satellite-infrared radiance data - all obtained through the courtesy of the Air Resources Laboratory of the National Oceanic and Atmospheric Administration (NOAA).

3.6 DATA ANALYSIS

Utilizing a Nicolet Scientific Dual Channel Fast Fourier Transform (FFT) Analyzer Model 411A, cross-correlation techniques yielded time differences and chronology for the signals received by the microphones of the triangular array. Since the microphones

were deployed in a triangular array and one side of the triangle ran north to south, this data could be used to calculate the azimuth and elevation angles of the arriving ray vector as follows:

$$\text{Azimuth angle } (\theta) = \tan^{-1} \frac{\Delta t_{21}}{\Delta t_{23}}$$

where Δt_{21} = time difference between microphone 2 and 1

Δt_{23} = time difference between microphone 2 and 3

$$\text{Elevation angle} = \cos^{-1} \frac{c\Delta t_{23}}{d \cos\theta}$$

where c = local speed of sound

d = the distance between microphones 2 and 3

The narrow-band frequency spectra and peak pressure of the signals were also obtained. The absolute level of this data was referenced to the recorded calibration signal, i.e., 114 dB sound pressure level corresponds to a pressure of 0.33 peak lbs/ft^2. The narrow band frequency spectrum was referenced to a narrow band measurement (1.25 Hz line width) of the recorded calibration signal (114 dB re 20 microPascal).

Graphic history recordings of the measured infrasonic peak pressure changes were made using a SAN-EL Instruments Rectigraph model 8S. (Selected representative events recorded are included in Section 4.2.)

4. MEASUREMENT DATA

During the period May 3, 1979 to September 14, 1979, infrasonic measurements were made at Malden MA, at six other sites in the Greater Boston area (See Figure 2), and at a site in Applebachsville PA (see Figure 3). Measurements were made on a daily basis throughout the period at the Malden site with measurements simultaneously made (one site at a time) at each of the other sites to obtain a measure of the variability of the data with geographic location.

4.1 SUMMARY DATA

Tables 1 through 1D contain summary data of the events recorded on a daily basis at the Malden site for May, June, July, August, and September 1979, respectively. Table 1E summarizes the data measured at the remaining seven sites.

An inspection of these tables shows the variability of the measured peak-to-peak pressure change resulting from the unstable stratospheric winds. Of the events measured, seven were recorded with peak-to-peak pressure changes in excess of 0.5 lbs/ft^2. The largest signal (0.69 lbs/ft^2) was measured on June 14, 1979. The lowest signals were measured during September, 1979, and signaled the end of the 1979 season of easterly stratospheric winds and the uninhibited propagation of secondary sonic booms that were generated off shore. The 1979 measurement program was therefore terminated on September 14, 1979.

On September 6, 1979, Air France Flight AF-001 flew a track approximately 40 miles south of the usual JFK-bound flight track. The new flight track, operational procedures, and the absence of easterly stratospheric winds on that particular day resulted in the low pressure levels measured for that particular flight.

A comparison of data in Table 1E (Miscellaneous Sites) with data at the Malden site during the same time frame shows the variability of the data because of geographic location. It is seen

that the levels measured in Georgetown were generally greater than those in Malden. At the remaining five sites in Massachusetts, the reverse was generally true. This is further illustrated in Section 4.2 in the comparison of pressure time histories.

Angular dimensions of the arriving ray vector are also included in these tables. The azimuth angle is the calculated heading of the arriving ray vector measured clockwise from true north. The measured azimuth angle averaged approximately 278 degrees re true north at Malden. If the aircraft is taken to have a 250 degree heading, the azimuth angle indicates (see Section 4.4, Ray Tracing) the aircraft was traveling at approximately Mach 1.31 when the shock wave was launched (see Figure 2).

The elapsed time tabulated is the difference between the time of the measured maximum peak-to-peak pressure change and the time of the closest point of approach (CPA) of the aircraft to Hyannis MA, as determined by radar. The statistical consistency of the elapsed time over the summer indicates conclusively that these JFK bound flights are the source of the secondary shock waves in New England. Further, it indicates that the shock waves in question are launched from a specific portion of the flight track of the aircraft.

Technicians on site heard the majority of the signals measured and in some cases were able to obtain a sound level meter reading (on the fast scale) unencumbered by local disturbances. These have also been tabulated. The highest sound pressure level (SPL) measured on June 18, 1976, overloaded a sound level meter set for a full scale reading of 60 dBA. A peak-to-peak pressure change of 0.68 lbs/ft^2 was recorded for this event, one of the highest levels measured during the summer.

4.2 PRESSURE SIGNATURES

Representative time histories of pressure changes recorded are presented. Figures 5 to 16 show the day-to-day as well as the hour-to-hour (or flight-to-flight) variability of the signals measured at the Malden measurement site during the 1979 measurement

program. Extremes in the hour-to-hour variability can be seen in Figures 10 and 12 for July 18 and 26, 1979, while Figure 13 for August 15, 1979 shows a marked similarity in the two events measured.

An examination of the Malden signatures shows that not only do the amplitudes change but the complexity, duration, and multiplicity of the waveforms also vary. The waveforms appear less complex in May and September than those in the intervening months. Azimuth calculations of various portions of the pressure signatures show the waveforms are made up of signals arriving from a variety of azimuth angles. When the upper level winds begin to inhibit the refracted wave from touching down, as in early May and late September, the number of paths are reduced and the pressure signatures become less complex (see Figures 15 and 16).

A direct comparison can be made in Figures 17 through 24 of the signals measured at Malden with the simultaneous measurements recorded at Marlboro, Medfield, Cohasset, Georgetown, and Sharon MA. Both the amplitude and shape of the signatures are seen to be significantly different. The larger of the levels was measured in Malden, with the exception of those measured in Marlboro and Georgetown.

Figures 25 and 26 show pressure time histories of data recorded in Applebachsville PA from Concorde flights in-bound to Dulles International Airport. The signatures shown have the same degree of day-to-day variability as have the Malden data. The phenomenon is similar to that observed in New England.

Figure 27 contains time histories of both exterior infrasonic pressure changes and window vibration accelerations measured on June 20, 1979, at a residential home in Wilmington MA. The lateral accelerations of the 54 by 60 by one-quarter inch plate glass window are seen to be in synchronism with the outside pressure changes resulting from the secondary sonic boom. In this instance, technicians both inside and outside the home heard the event.

Figure 28 presents expanded pressure time histories of two reasonably uncomplicated sonic signals measured on May 3 and 14, 1979. In addition, synchronous histories are shown in Figure 28A of the pressure measured with the triangular array of infrasonic sensors. Note that the differences between times of occurrence are clearly discernable in the three time histories.

The time difference between the traces for microphone 2 and microphone 1 shows that the wave front arrived from an easterly direction, i.e., the wave front arrived at microphone 1 prior to microphone 2. In addition, the signal arrived at microphone 2 prior to microphone 3 (as shown), which indicates a ray direction from the south. This combined information shows the signal arrived roughly from a southeasterly direction. Actual geometric calculations of time differences (obtained more precisely by cross-correlation techniques) shows the azimuth angle or heading of the arriving ray vector to be in this case 279 degrees corrected to true north.

Pressure time histories of selected more complex signals are shown in Figures 29-33. Each figure supplements the overall pressure time history of the event with expanded segments of the history, showing the fine detail of the complex pressure changes.

4.3 FREQUENCY SPECTRA

A narrow-band frequency analysis was performed, averaging a 4-second period of data centered at the time of the maximum recorded pressure change. The frequency spectra for several representative events are presented in Figures 34-41. The signal drop-off above 30 Hz is characteristic of the TSC infrasonic measuring system, which was adjusted for a high frequency cutoff at 30 Hz. The narrow band frequency spectrum of the acoustic event recorded on May 14, 1979 is presented in Figure 35 for comparison with the narrow band spectrum of the infrasonic signal measured simultaneously (Figure 34B). Note that Figure 35A shows the presence of acoustic energy up to approximately 100 Hz. An expansion of the low-frequency portion of this spectra is shown in Figure 35B. It is seen to be an extension of the data measured by the infrasonic

system (Figure 34B). Note that the low-frequency roll-off of the data in Figure 35B is characteristic of the acoustic measuring system, which has a flat response above 20 Hz and is approximately 6 dB down at 15 Hz. The measured "A" weighted SPL of this signal was 46 dBA in an environment with low level ambient of 40 dBA. Narrow band analysis of various other acoustic signals measured during the program (acoustic instrumentation was not deployed every day) did not exhibit any significant increase in the high frequency (greater than 100 Hz) portion of the spectra.

Figures 36-39 contain the narrow band frequency spectra for representative events measured in Malden MA during June, July, August, and September, 1979. (See Figures 8, 9, 13 and 16 for pressure time history data.) Figure 40 contains frequency data for events measured on July 11, 1979, in Georgetown MA and can be compared with the frequency spectra (Figure 37) for the same events measured in Malden MA. (Also see the pressure histories in Figures 22 and 9.)

Figure 41 contains frequency spectra for signals from two flights measured in Applebachsville PA. (See Figures 25 and 26 for the pressure time histories).

Figure 42 contains the frequency spectra for the infrasonic event measured on June 20, 1979 in Wilmington MA, and the spectra of the window pane vibrations. (See Figure 27 for the corresponding time histories.)

5. PUBLIC REPORTS AND ACOUSTIC DATA

Several hundred reports were received by the FAA from citizens in the Greater Boston area of sounds indicative of secondary sonic booms during the summer of 1978. The Planning and Appraisal Staff of the New England Region FAA called several of these citizens during the latter part of May, 1979, to solicit their assistance in observing the phenomena and to keep records of their observations for correlation with the measurements program. Table 2 includes observations from five citizens plus some unsolicited reports received during May, 1979, by the FAA New England Region.

Note that the reported observation times coincide very closely with the measured data as shown in Table 2. Reports received by the FAA from May through July, 1979, constitute the basis for Figure 43, that shows geographically the area from which the reports were received.

Citizen reports indicate the secondary booms were "heard." TSC technicians at the measurement site indicate they "heard" many of the secondary booms recorded. As shown in the Summary Data (Tables 1-1E), the technicians "heard" the secondary booms when the maximum peak-to-peak pressure changes exceed approximately 0.1 lb/ft^2. On several days, sound level meter measurements were made on site and levels up to 58 dBA (fast scale) were measured. On one occasion (July 18, 1970) the sound level meter overloaded and indicated a level in excess of 60 dBA. It should be noted from Table 1B that one of the largest peak-to-peak pressures measured was recorded that day (0.68 lbs/ft^2).

Frequency analysis of these data in narrow band (see Figure 35) and in one third octave (data not shown) shows little, if any, energy above a level of 30 to 40 dB re 20 micro Pascal (uPa) in the frequency range above 100 Hz. One third octave analysis was done using a Gen Rad One Third Octave Real Time Analyzer.

As shown in the expanded pressure time history, Figure 33D, the rise time of the signal is less than 10 milliseconds. For an impulse, this would indicate a cutoff frequency of approximately 100 Hz, which agrees with the above frequency analysis.

6. DATA INTERPRETATION

Many of the features of the data measured in the field experiments can be interpreted using basic acoustical principles.

6.1 WAVEFORM SEGMENTS

While the pressure time histories recorded in the field show a great amount of variability, it is possible with guidance from theory and ray computations to perceive three different types of arrivals in most of the time histories. The data (Figures 8B and 31) received at Malden that was caused by the BA-171 flight (see Figure 44) of June 20, provides an illustration of such a classification. The segments B and C in Figure 31A correspond to a *ground wave* and to a *type I secondary sonic boom,* respectively. The segments D, E, and F correspond collectively to a *type II secondary sonic boom.*

The *ground wave* is of very small amplitude and, in many of the studied events, is either too small to be detected or else requires careful scrutiny of the recording before it is found. It is always the first arrival and typically arrives about 1 minute before the type I secondary boom. The propagation path of the ground wave goes from the flight trajectory of the airplane to the edge of the primary carpet along a direct (but refracted) geometrical acoustic ray. However, at the edge of the primary carpet, the energy carried by impinging direct rays splits. Most of the energy reflects back into the atmosphere, but a portion continues to propagate along the ground in the same general direction as a *creeping wave.* The creeping wave continuously sheds energy into the atmosphere and therefore dies out exponentially with increasing propagation distance. Consequently, very little amplitude remains by the time it reaches the Malden site. The theory of this ground wave dates back to fundamental papers by C. L. Pekeris[7] (1946) and by D.C. Pridmore-Brown and U. Ingard[8] (1955). The application of the theory to sonic booms has been subsequently discussed by R. Onyeonwu[9] (1975).

The type I secondary sonic boom arrival travels along a geometric acoustic ray path (see Figures 1 and 44) that initially goes obliquely upward from the flight trajectory, but bends downward as it propagates upward until eventually the ray is turned back toward the ground. Typically the turning point is at 45,000 to 55,000 meters in altitude. Amplitudes at Malden of type I arrivals are highly variable, but usually the type I arrival is weaker than the type II arrival. The tentative explanation for this tendency is that the energy associated with shocks propagating obliquely downwards from a Concorde in supersonic flight is substantially more than that associated with shocks propagating obliquely upwards.

The type II secondary sonic boom waveform segment typically arrives about 30 to 50 seconds after the type I segment. The delay is because it travels a longer path, going from aircraft trajectory to ground (impacting within primary carpet), then reflecting and propagating up to the stratosphere and mesosphere, and refracting downward back to the ground.

6.2 EFFECT OF UPPER ATMOSPHERIC WINDS

The simplest model of sonic boom propagation is based on geometrical acoustics. This model predicts type I and type II sonic boom arrivals beyond the primary carpet area only when the sum of the wind velocity component in the direction of propagation and the sound speed at an altitude above the flight altitude, exceeds the corresponding sum at the ground. (See Figure 45.) This implies that the presence in the Boston area of secondary booms caused by inbound Concorde flights is strongly affected by the east-west component of the wind velocity at heights of 30 to 60 kilometers (km). Strong winds blowing east to west at such altitudes should be associated with the presence of secondary booms. The very small amplitudes received during early May can be explained by observing meteorological conditions of the upper atmospheric winds that are blowing in the wrong direction or are very light at the time.

To test the hypothesis just mentioned the scatter plot in Figure 46 was prepared. Each point corresponds to an event recorded at the Malden site during May or June. The amplitudes that constitute the vertical coordinates are the peak-to-peak maxima listed in Tables 1 and 1A. The horizon coordinates are east-to-west wind components at 55,000 meter altitude for the corresponding day of flight. The latter numbers come from estimates based on meteorological data obtained from satellites; these estimates are for the Boston area and are supplied to us by the NOAA Air Resources Laboratory (see Appendix A). The accuracy of such meteorological estimates is not known, so the scatter plot also constitutes a rough test of the veracity of the NOAA estimates.

Figure 46 demonstrates that the probability of receiving a large amplitude event is small unless the east-to-west wind speed at the considered altitude exceeds 16 meters per second (m/s). There is one large amplitude event (associated with the BA-171 flight of May 9) that is a drastic exception to this rule, but the day to day reliability of the NOAA predictions is unknown. It is expected, however, that statistically, they are valid predictions.

Even when the upper atmospheric winds are of high amplitude and blowing in the right direction, there is no binding theoretical reason that the amplitudes of secondary booms at a specified measurement site should be large. The detailed geographical distribution of the received secondary boom energy has a complicated and even somewhat erratic dependence on the details of the meteorological structure all along the propagation path as well as on the flight profile, so any simple rules for predicting large amplitude secondary sonic booms must be regarded in a statistical sense. From this point of view, Figure 46 would appear to give substantial confirmation of the hypothesis that occurrence of such events is strongly associated with stronger magnitude east-to-west winds in the upper atmosphere.

6.3 MEASURED AND PREDICTED ARRIVAL TIMES

Given sufficient meteorological data and sufficient data concerning the aircraft's flight profile, it is possible to compute predictions for the arrival times of the ground wave and of the type I and type II secondary sonic boom waveforms at any given measurement site. The meteorological data needed consists of temperature, wind speed, and wind direction versus height up to an altitude of at least 50 km. Some sample profiles are shown in Figures 47, 48, and 49. Flight profile data required consists of aircraft position, altitude, speed, and heading versus time.

Meteorological profiles for the months of May, June, and July were furnished to TSC by the NOAA Air Resources Laboratory; flight profiles (radar trackings of inbound Concordes) were furnished by the FAA (see Appendix A for a fuller discussion). From the subset of events for which both meteorological data and flight profile data were available, the thirteen listed in Table 3 were selected for detailed computational study.

With the exception of two subtleties (described below), the calculation of arrival times at the Malden site involves a straightfoward (although nontrivial) application of sonic boom and geometrical acoustics principles. Rays are continously being "shed" along the flight profile and they obey certain constraints in their possible initial directions that are related to the aircraft's heading and Mach number. Subsequent propagation of the shedded rays is affected by the meteorological profiles and follows the basic rules of geometrical acoustics. The computer program written by TSC for this purpose is summarized in Appendix A.

One of the problems that had to be overcome was that the Malden site was invariably too close to the flight profile for the geometrical acoustics model per se to predict the arrival time of the type II secondary sonic boom. All of the computed ray paths that left the flight profile would fall beyond Malden. The miss distance of Malden from the nearest such type II ray impact point, however, was typically not large, being usually only about 10 to 20 percent of the total propagation distance.

The geometrical acoustics model of sonic boom propagation is approximate and valid at best only in the limit of very high frequencies and negligible attenuation, so it is not surprising to find a type II arrival at Malden when the simplistic model doesn't yield any ray path connecting the flight trajectory with Malden. A proper theoretical interpretation of the geometrical acoustics theory is that it furnishes the basic "super-structure" of the wavefield to which the "billowing sails" of the full-wave theory are "sewn."

It was observed from the computed results that, at those more distant points, where the geometrical acoustics model did predict both type I and type II ray arrivals, the time difference in their arrivals along a given azimuth direction was nearly independent of range. Consequently, it was argued that the same difference would apply to the Malden site. The computed type II arrival times at Malden shown in Table 3 are therefore sums of the corresponding computed type I arrival times and increments based on parameters of type II rays that reach further points.

Another modification made in the computation was to assume that winds had no effect on the ground wave transit speed, so the appropriate speed is simply the sound speed on the ground. The reason for leaving out the wind speed is that the NOAA estimates of wind velocities are based on the geostrophic assumption rather than direct measurements. Such an assumption, although good at moderate to high altitudes, is inappropriate near the ground and within the earth's boundary layer. With regard for the frictional effect of the ground and in absence of other data, zero wind speed at the ground seems to be the most rational assumption of comparable simplicity.

The measured arrival times with which the computed arrival times in Table 3 are compared are times of maximum amplitude for the corresponding waveform segment. In some cases, the actual waveform portion corresponding to a given propagation mode had a duration of as much as 30 seconds. If a single time must be selected to compare with theory, however, the time of maximum amplitude should be least biased.

The discrepancies between computed and measured times are very small compared to a representative travel time, aircraft trajectory to Malden, of an arriving acoustic ray. The latter is of the order of 750 to 800 seconds. In contrast, the average (absolute) discrepancies in Table 3 are 12 seconds, 18 seconds, and 24 seconds for the ground wave, type I and type II arrivals, respectively. (The latter are 1.6 percent, 2.3 percent, and 3.0 percent of 800 seconds.)

The agreement strongly supports identification of Concorde flights bound for JFK as the cause of the events recorded at Malden. It also supports the suppositions that divide the total waveforms into ground wave, type I, and type II segments.

The arrival time agreements do not, however, constitute a sensitive test of the accuracy of the meteorological data because the travel time, equal to path integral of reciprocal of wave speed, tends to be insensitive to minor fluctuations in atmospheric properties. Neither do they provide a thorough test of the accuracy of ray path predictions because *Fermat's principle* guarantees that acoustic travel time along a path connecting two points should be insensitive to small variations in the path.

The May 30 meteorological data was such that no type I or type II ray paths are predicted that touch the ground anywhere to the northwest of the flight track. This does not necessarily mean that such arrivals are precluded by the full wave theory, but the development of a scheme for estimating their arrival times did not seem warranted in the present study. The small amplitudes recorded for the AF 001 event for this particular date suggest, however, that the meteorological conditions were not favorable for the occurrence of strong secondary sonic booms.

6.4 RAY AZIMUTHS AND ELEVATIONS

The measured azimuths and elevations (shown in Tables 1-1E) of the arriving rays correspond to the waveform segment with greatest amplitude. Usually, as explained in Section 6.1, this is the type II arrival waveform segment. The arrival azimuths for

successive waveform segments were measured for a number of events; the results show some variation but the type I arrival characteristically arrives with an azimuth 2° less than that of the type II arrival. (Smaller azimuths correspond to arrivals that leave the flight track earlier.)

Our computer predictions for points where both types of rays are expected according to the geometrical acoustics model are consistent with this trend; differences for points just to the west of Malden are typically 1.5° to 2°.

The plot in Figure 50 of computed versus measured arrival ray azimuth angles takes the computed numbers to be those for the type I rays, since the geometrical acoustics model usually does not yield such a number for type II arrivals at the Malden site. Adding 2° to each computed azimuth (as might be suggested by the remarks in the preceding paragraph) would not change the slope of the linear least squares fit line, but would raise it. This would change the point of its intersection to 282° instead of 278°. From either point of view, the agreement seems substantial.

Table 4 lists computed and measured elevation angles for the events selected for analysis. Here again, the computed numbers correspond to type I rays arriving at Malden; the measured values are based for the most part on the local horizontal transit speed of the type II waveform segment across the array at the Malden site. The measured ray elevation angle is the arc-cosine of the ratio of the sound speed at the ground to the measured transit speed across the array. The computed elevation angles are derived from the geometrical acoustics ray paths computed by the program.

Because the elevation angles are small and because the cosine (approximately 1) of a small angle is relatively insensitive to small variations, the measured elevation angles are probably not too accurate. Also, the computed elevation angles are very sensitive to small variations in the assumed meteorological model's sound speed and wind velocity on the ground. For these reasons, the poor correlation of measured and computed values in Table 4 is to be expected. The results, however, are of

comparable magnitudes and consequently support the hypothesis that the secondary booms at the Malden site have traveled along paths that reached stratospheric altitudes before returning to the ground.

A related comparison of measured and computed quantities is shown in Figure 51; local horizontal transit speeds (*phase velocities*) of waveforms across the microphone array are predicted by the basic theory to be the same as the sum (at the highest altitude reached by the incident ray) of the sound speed and wind velocity component in propagation direction. This prediction is in accord with the extension of Snell's law that takes winds into account. The comparison of the measured and computed local horizontal transit speeds should therefore be insensitive to the local meteorological conditions and topography at the array site; the comparison tests instead the reliability of the meteorological profiles at turning point altitudes (35 km to 50 km above the earth's surface).

6.5 SECONDARY BOOM FOCUS LINES

The geometrical acoustics theory predicts, for type I secondary boom arrivals, a line (*secondary boom focus line*) that divides regions where no type I rays hit the ground from regions where they do hit the ground. An analogous line is predicted that separates regions struck by type II geometrical acoustics rays from regions where they do not strike. (The reasons for referring to such lines as focus lines are stated further below.)

Figure 44 shows the two secondary boom focus lines computed by the TSC computer program (see Appendix A) for the BA 171 flight of June 30. Similar computational results are depicted in Figures 52, 53, 54, and 55 for the May 31 BA 171 flight, the June 27 AF 001 flight, and the July 18 AF 001 and BA 171 flights.

The type I secondary boom focus line is always closer to the flight track than is the type II focus line. The separation distance between the two lines is typically about 30 nautical miles. The locations and shapes of the two lines depend on the details of the aircraft's flight profile as well as on the

meteorological data. That small variations in flight profile may affect the lines, even when the meteorology does not change, is evident from a comparison of Figures 54 and 55.

For all the events analyzed, the predicted type II focus line always lies further from the flight track than does the Malden site. The Malden site typically falls between the two lines, but in some instances the type I focus line passes through some point west of Malden. Figure 54 for the July 18 AF-001 flight exemplifies the latter possibility. Far to the east-north-east of the Boston area, the two lines, as indicated in Figure 44, eventually approach asymptotes that are parallel to the flight track and correspond to the region of level rectilinear flight at a constant Mach number of 2.

It is possible that type I and type II lines exist south of the flight track but the meteorological conditions (upper atmosphere winds blowing east to west) for the considered events are likely to prevent the secondary sonic boom ray from returning to the ground south of the flight track. Our computations, however, have been confined to disturbances in the New England area.

The southernmost tips of the type I and type II focus lines that appear in the figures are associated with the last point in the corresponding FAA radar track tabulation for which the aircraft was flying at supersonic speed relative to the ground. The FAA tabulations are at time intervals of 12.5 seconds, so any extensions of the secondary boom focus lines to points further south must correspond to less than 12.5 seconds of flight (or to less than 2 miles of flight). The lines, if extended, would resemble arcs of circles with radii of approximately 200 km and 260 km, respectively, extending down to the flight track. However, because the secondary boom energy generated per unit time is roughly constant and because the energy generated during the last few seconds is spread over such a wide geographical area, the amplitudes at points south of where the computed lines stop are expected to be relatively low.

The identification of the computed lines as focus lines results because they describe lines along which the geometrical acoustics rays converge. The ray density (number of rays per unit area) formally become infinite and the ray tube area goes to zero along such lines. The geometrical acoustics theory breaks down at these focus lines but predicts large amplitudes near the lines. On the illuminated side the amplitude should fluctuate somewhat because of interference between rays that have touched and have not yet touched the caustic surface, but the general trend is for amplitude to decrease as the inverse fourth root of distance from the focus line.

On the side of the focus line where the geometrical acoustics theory predicts an absence of impinging rays, the full wave theory[10] predicts that the amplitude dies off with distance y from the focus line roughly as

$$\exp\left[-(4\pi/3)(2/\lambda^2 R)^{1/2}(\tan\theta)^{3/2}\, y^{3/2}\right]$$

where λ is the wavelength, R is a distance of the order of 200 km, and the angle θ is of the order of 10°. The distance

$$L = (3/4\pi)^{2/3}(\lambda^2 R/2)^{1/3}/\tan\theta$$

can be taken as a measure of the half-width of the strip over which the influence of the focus extends on either side. For λ = 340 m (f = 1 Hz), L is of the order of 5 km. (The choice of 1 Hz for a representative frequency follows from an examination of the expanded pressure time histories in Figures 28-33.)

The hypothesis that larger amplitudes are associated with the proximity of the measurement site to a focus line is tested by the scatter plots in Figures 56 and 57.

The former, Figure 56, plots the measured maximum, peak-to-peak, pressure change for the type I waveform segments versus computed perpendicular distance of the Malden site from the type I focus line (which is the focus line closer to the flight track). Here, positive distance implies Malden lies on the far side of the focus line in relation to the flight track or, equivalently,

that the focus line lies between Malden and the flight track. For simplicity, the least squares fit line, which is included to indicate the general trend rather than to approximate the functional dependence predicted by theory, is based on the assumption that maximum amplitude is symmetrical about the focus line.

The general trend supports the hypothesis, but there is considerable scatter. Our interpretation of this scatter is that the amplitude dependence on distance from a focus line must be viewed in terms of probabilities. Proximity to the focus line increases the probability that a high amplitude will be measured, but does not guarantee it. One reason for the absence of a deterministic relationship is because focusing is also affected by turbulence[11] and by departures of the atmosphere from perfect stratification.

Another source of fluctuations is that our predictions of focus line locations are of dubious accuracy. The meteorological information available is not sufficiently detailed to allow such lines to be pinpointed. A rough guess is that the accuracy in focus line prediction is of the order of ± 20 km. If this is so, then the actual sharpness of the focusing will be considerably blurred when one plots amplitude versus computed distance to focus line rather than versus true distance to focus line. From this perspective, the rather weak slope of the linear least squares fit line in Figure 56 is not surprising, even though the characteristic scale for the width of the focus region that is predicted by theory is only of the order of 10 km.

The preceding remarks apply also for the plot in Figure 57, in which maximum peak-to-peak pressure changes for type II waveform segments are plotted versus distance to the type II secondary boom focus line. Here, however, the positive sense of direction is opposite to that adopted in Figure 56. For all the events studied, Malden was always closer to the flight track than was the computed type II focus line. A positive distance of, for example, 30 km in Figure 57 means the type II focus line passed through a point northwest of Malden that was roughly 30 km distant from the measurement site. Also, because the type II focus line

is more distant from the track than is the type I focus line, it is expected that its computed location is even less precise. The estimate is that the accuracy in focus line prediction in this case is of the order of ± 30 km.

7. CONCLUSIONS

Low frequency acoustic signals arrived at regular intervals in the New England area during the late spring and summer months of 1979. Arrival times and detailed analysis of the measured signals leave no doubt that they are caused by inbound Concorde flights into JFK International Airport in New York City. During every period when the measurement system was in operation from May 3 to September 14, 1979, and when a Concorde was in an inbound approach path to JFK, a signal was recorded. A similar statement applies to the measurements at Applebachsville PA (July 23 to 27, 1979) in regard to Concorde flights into Dulles.

For the New England events, the measured arrival times of peak signal amplitudes correlated extremely well with time of Concorde passage to the closest point of approach to Hyannis MA. Knowledge of the latter gives the former with an rms error of only 53 seconds. Furthermore, if account is taken of the detailed flight profile of the aircraft, the event arrival times can be predicted to within 20 seconds using acoustic propagation theory and available meteorological data.

During May, 55 percent of the measured events at Malden were audible to the field technicians. In June, 94 percent were audible; in July, 97 percent; in August, 86 percent; in the first half of September, 53 percent. Consequently, it is concluded that, for the approach profiles currently being flown, almost every Concorde flight into JFK during the summer months generates audible sound in the Boston area. The four measurements at Applebachsville PA during July suggest a similar conclusion concerning flights into Dulles.

The preponderance of reports during the summer months is well explained in terms of acoustic propagation theory by the seasonal changes in stratospheric wind direction. During summer, the winds in the altitude region, 30 km to 60 km, blow east to west and cause secondary sonic booms propagating high above the aircraft flight

altitude to refract back down to the ground. Detailed calculations based on radar trackings of Concordes and on best available meteorological data for 13 events yield respectable agreement with data in regard to arrival times, azimuth angles, and local horizontal transit speeds. Therefore, the basic mechanisms by which the secondary booms are conveyed to the Boston area can be regarded as well understood.

The computations and the data yield the conclusions that the signals received in the Boston area from the Concorde flights are generated during the last minute of supersonic flight, when the aircraft is off the New England coast between 68° and 69° W longitude.

Although there are noticeable similarities among the waveforms received from different flights and on different dates, there are wide variations in details of signature shape and in amplitudes. The maximum (within a given waveform) pressure change, peak-to-peak, for events measured at Malden in May ranged from 0.02 to 0.63 lbs/ft^2; in July, they ranged from 0.04 to 0.68 lbs/ft^2; in August, they ranged from 0.07 to 0.59 lbs/ft^2; in September, they ranged from less than 0.01 to 0.32 lbs/ft^2.

The large amplitude events are ascribed to an uneven distribution of acoustic energy impinging on the ground; a region receiving an abnormally large amplitude is a region of acoustic focusing. Just where such focusing occurs is highly sensitive to details in the atmosphere's meteorological structure, but the basic theoretical model that neglects longitudinal and latitudinal variations of weather profiles predicts two focus lines along which abnormally high amplitudes may be expected. Both lines typically pass through the Boston area with a separation distance of about 30 nautical miles. The Malden measurement site typically lies between the focus lines, but small variations in flight profile and in meteorological structure can cause the focus lines to move in either direction by as much as 35 nautical miles. The comparison of

measured peak amplitudes with distances of the Malden site from the computed focus lines supports the hypothesis that larger amplitudes are caused by focusing.

The data taken during this measurement program and the theoretical interpretation of the results provide the basis for evaluating the effectiveness of alternate operational procedures to reduce the frequency and intensity of secondary sonic booms within the U.S. mainland.

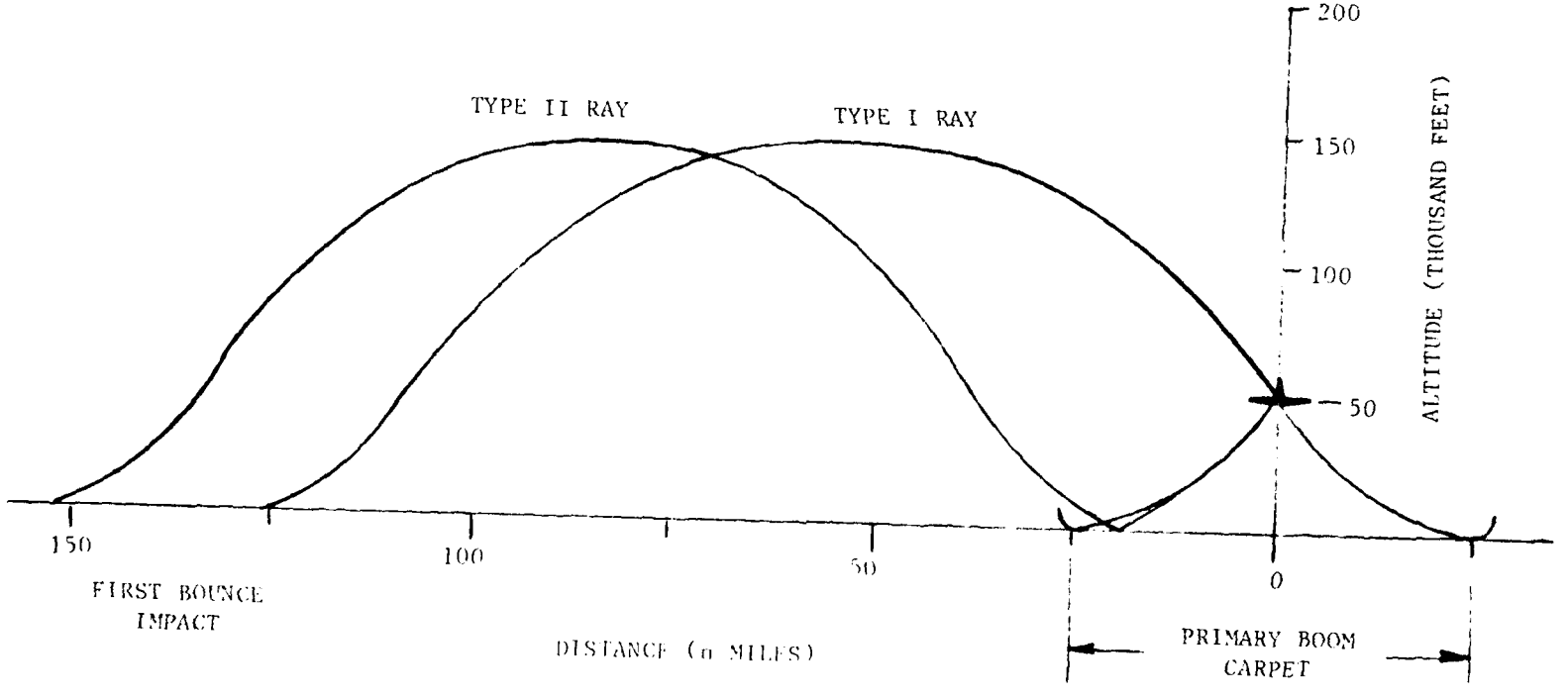

FIGURE 1. SCHEMATIC OF REFRACTIVE SONIC BOOM PROPAGATION
Source: BA 171, June 20, 1979, Ray Vector Azimuth Angle 278 Degrees

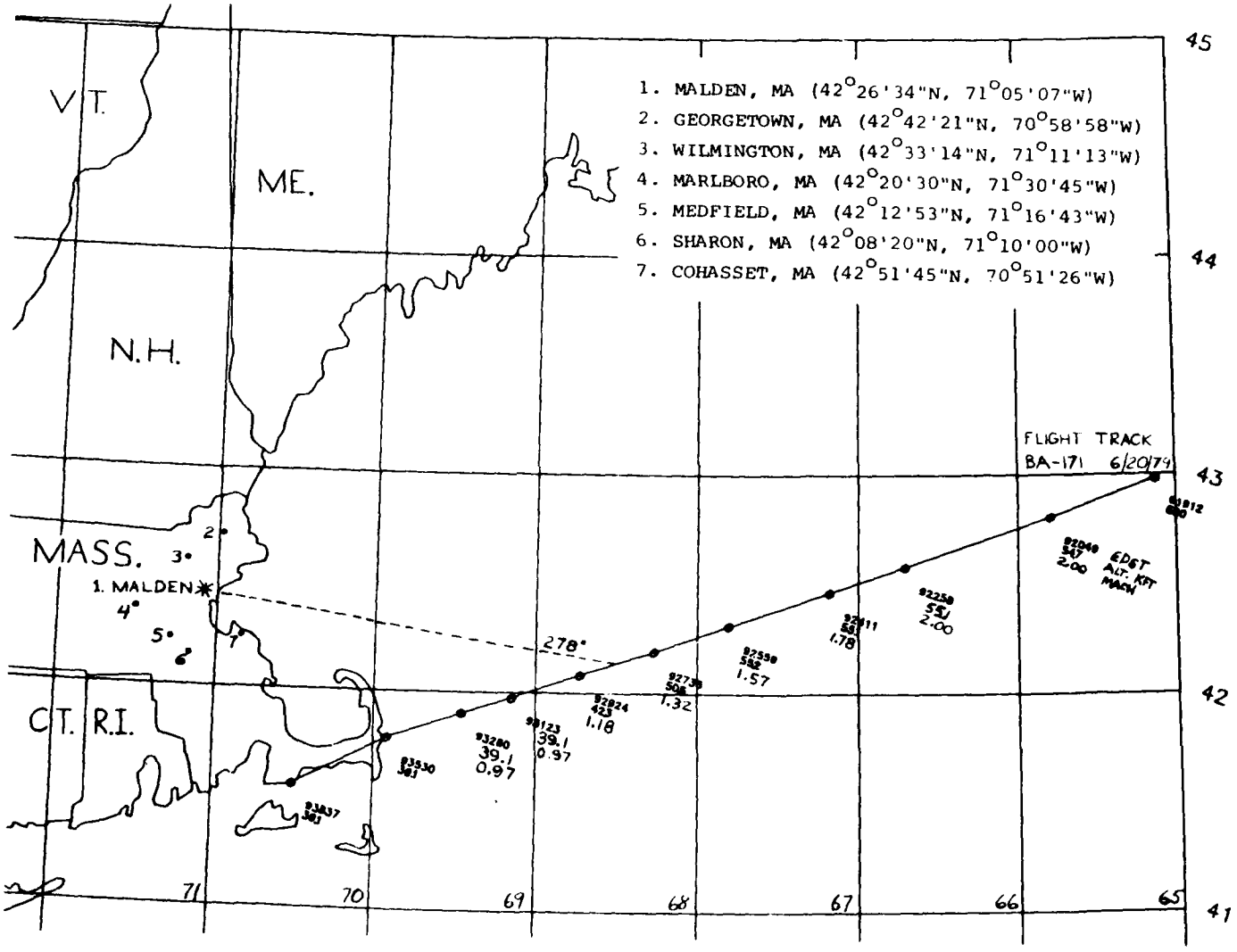

FIGURE 2. FLIGHT TRACK - JFK-BOUND FLIGHT BRITISH AIRWAYS FLIGHT BA-171 JUNE 20, 1979

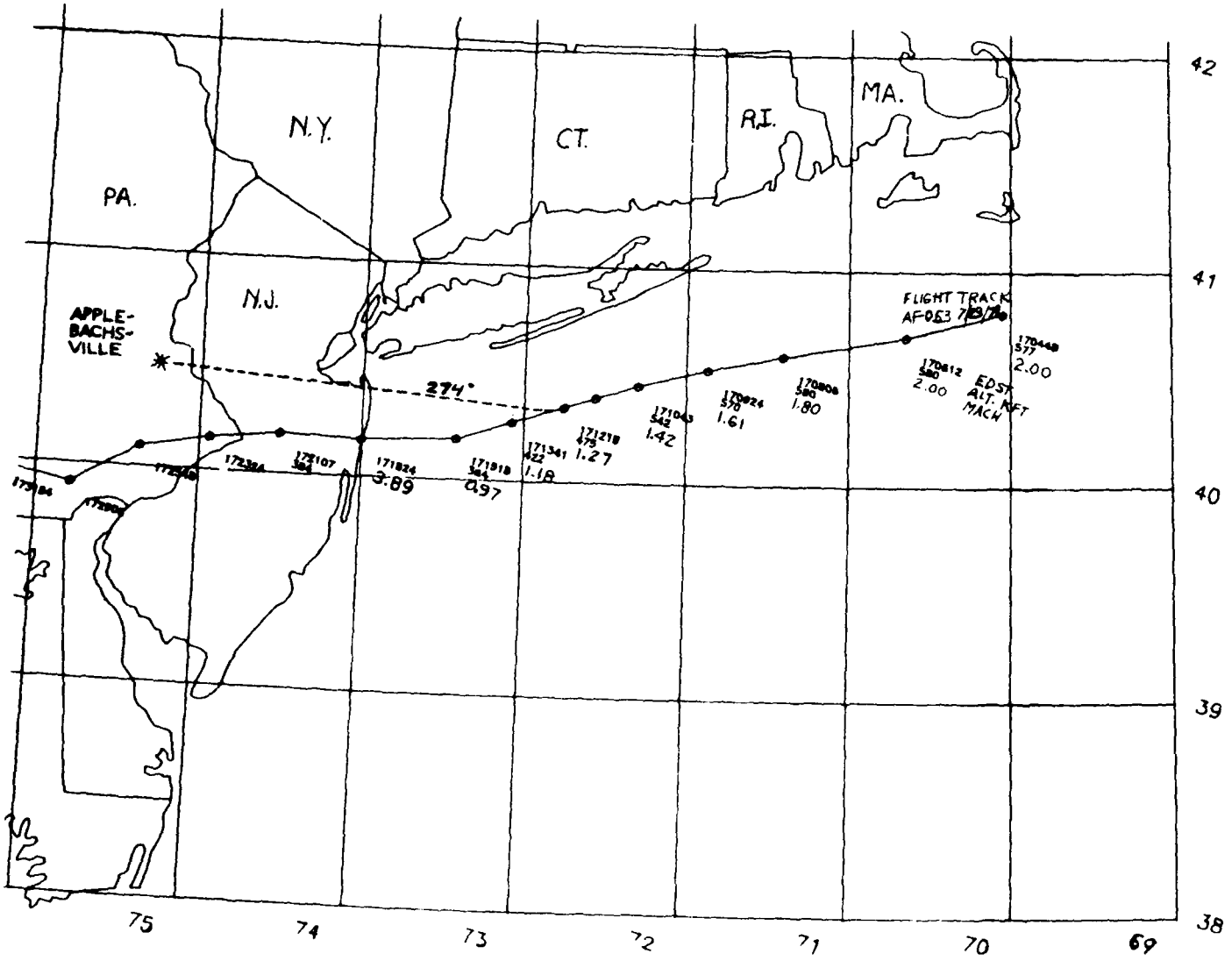

FIGURE 3. FLIGHT TRACK - DULLES-BOUND FLIGHT AIR FRANCE FLIGHT AF-053 JULY 23, 1979 APPLEBACHSVILLE PA. (40° 29' 12" N, 75° 15' 56' W)

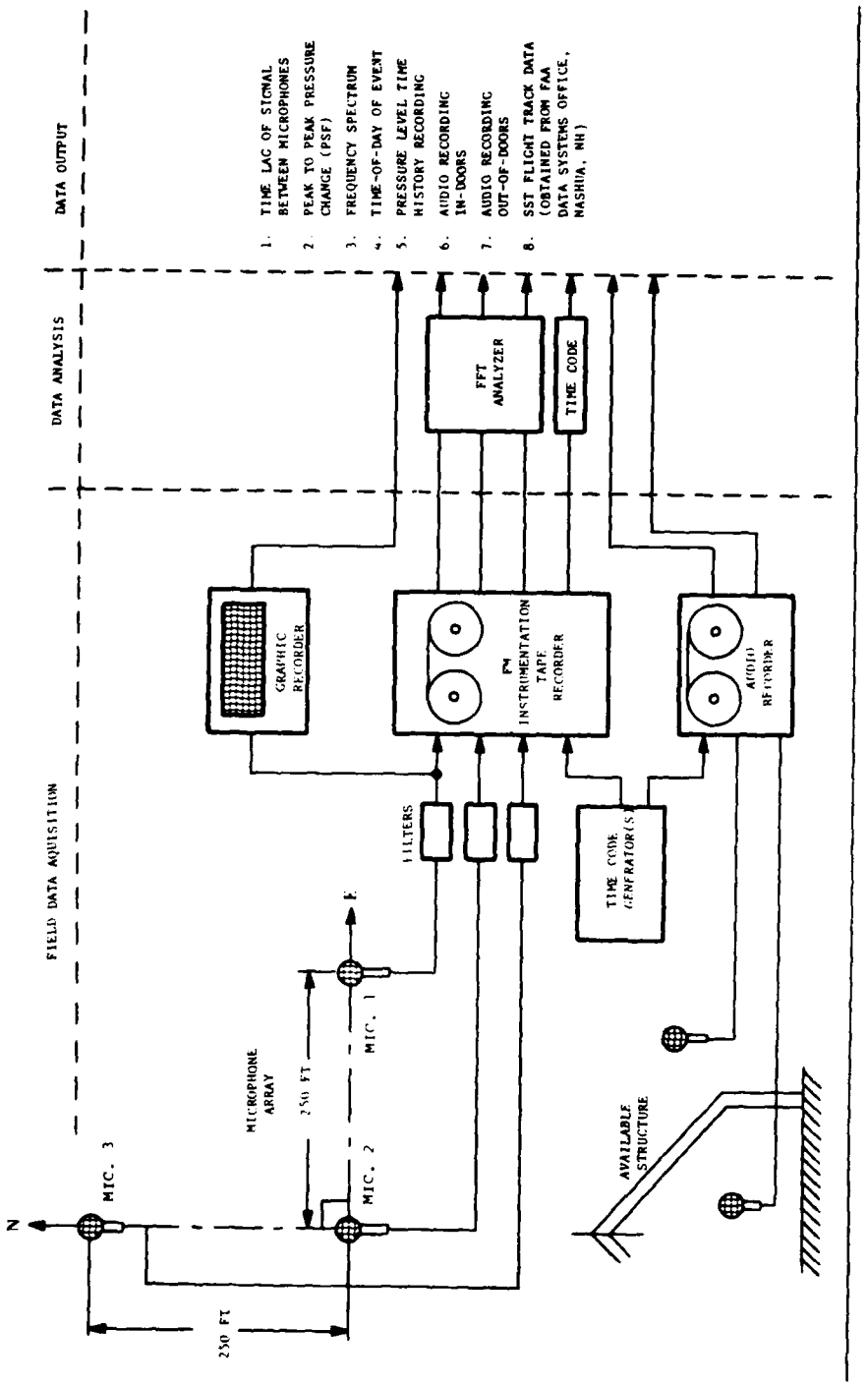

FIGURE 4. SYSTEM SCHEMATIC DIAGRAM

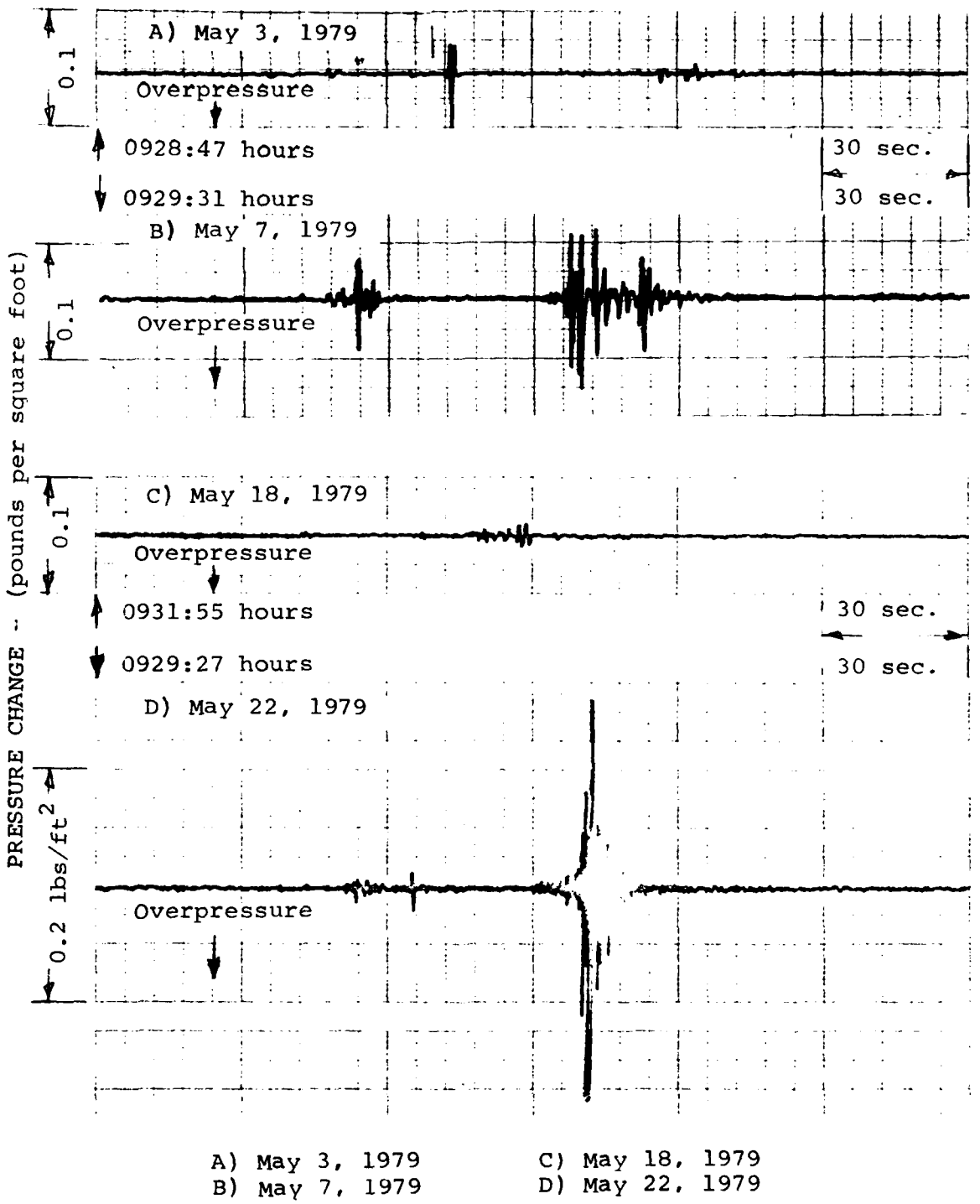

FIGURE 5. PRESSURE TIME HISTORIES SOURCE: BRITISH AIRWAYS FLIGHT BA-171 MALDEN MA

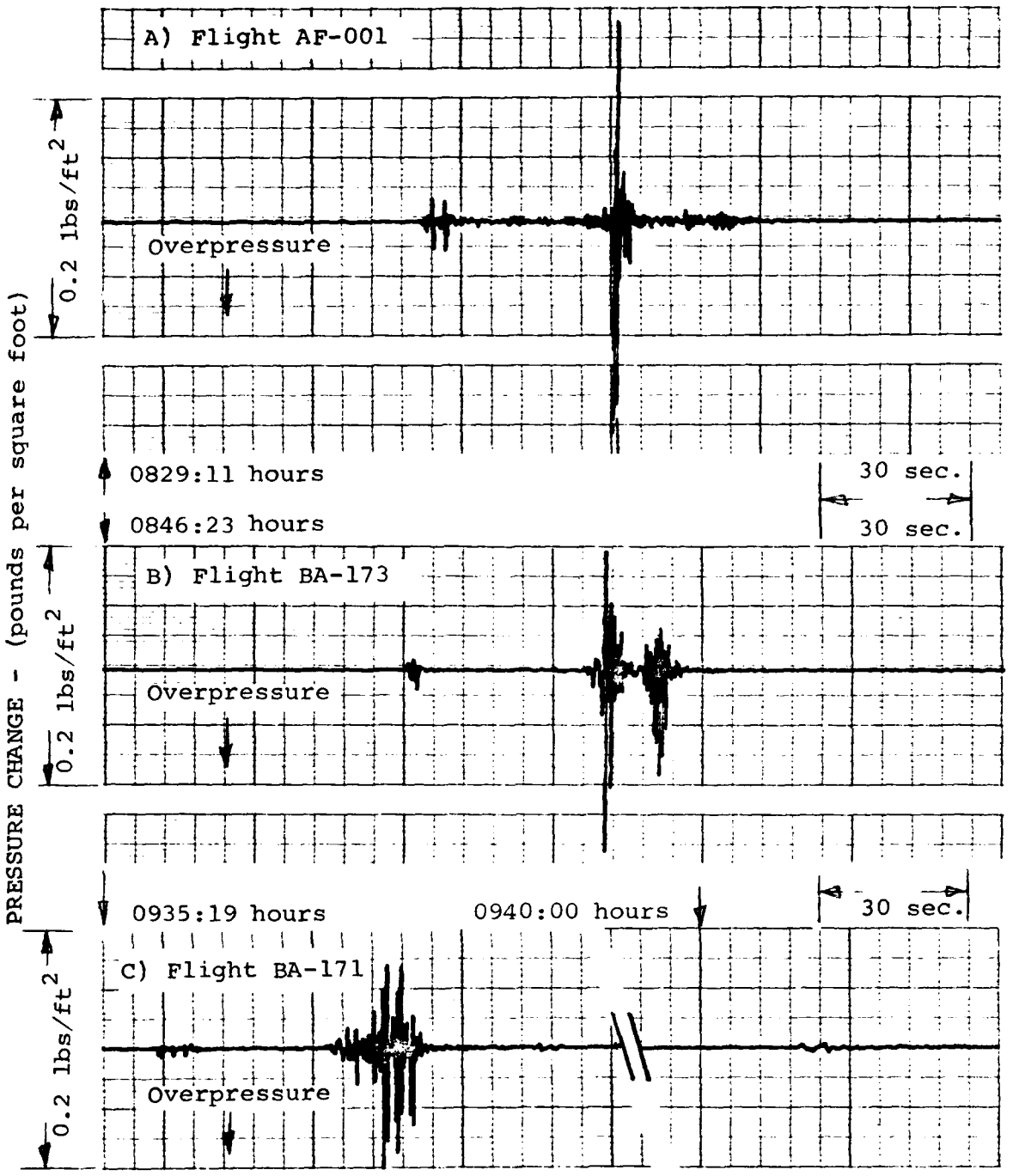

A) Source: Air France Flight AF-001
B) Source: British Airways Flight BA-173
C) Source: British Airways Flight BA-171

FIGURE 6. PRESSURE TIME HISTORIES MALDEN MA - MAY 29, 1979

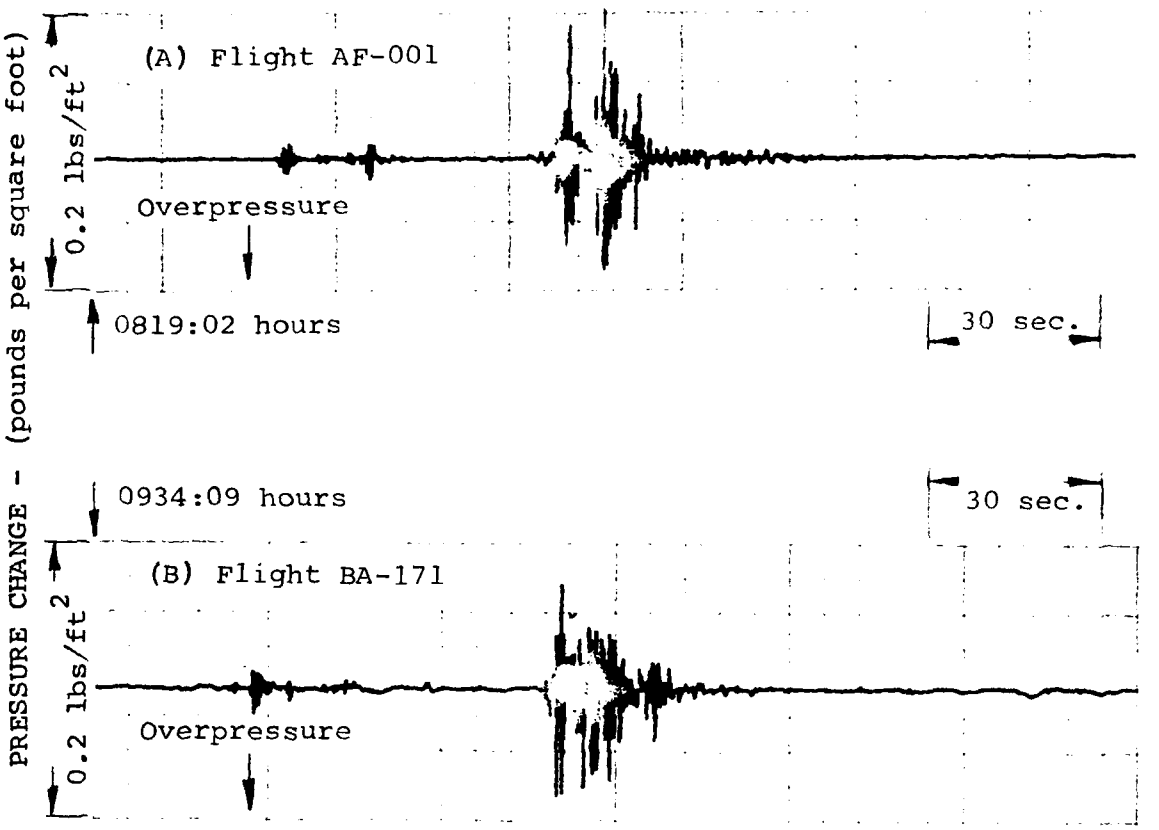

A) Source: Air France Flight AF-001
B) Source: British Airways Flight BA-171

FIGURE 7. PRESSURE TIME HISTORIES MALDEN MA - JUNE 13, 1979

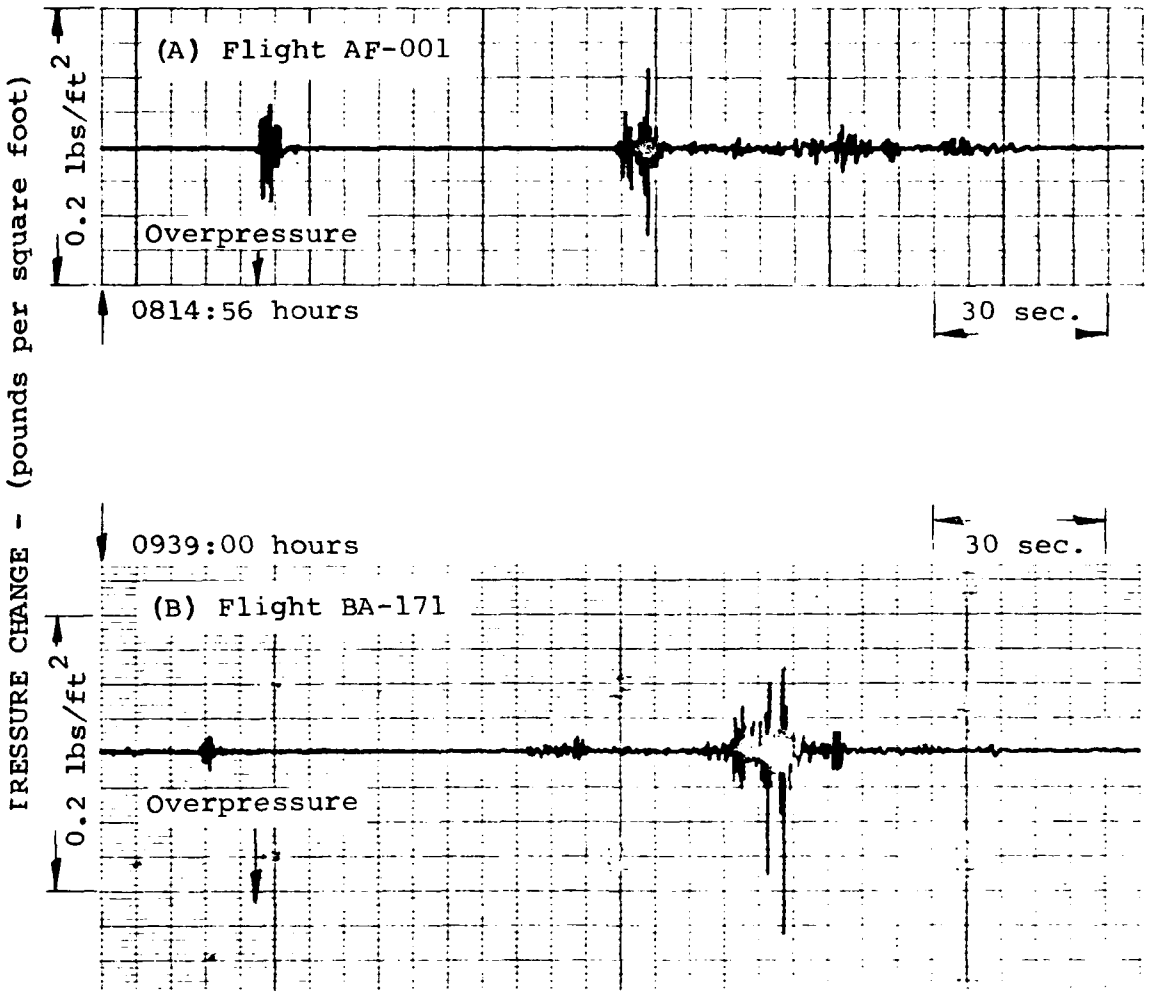

A) Source: Air France Flight AF-001
B) Source: British Airways Flight BA-171

FIGURE 8. PRESSURE TIME HISTORIES MALDEN MA - JUNE 20, 1979

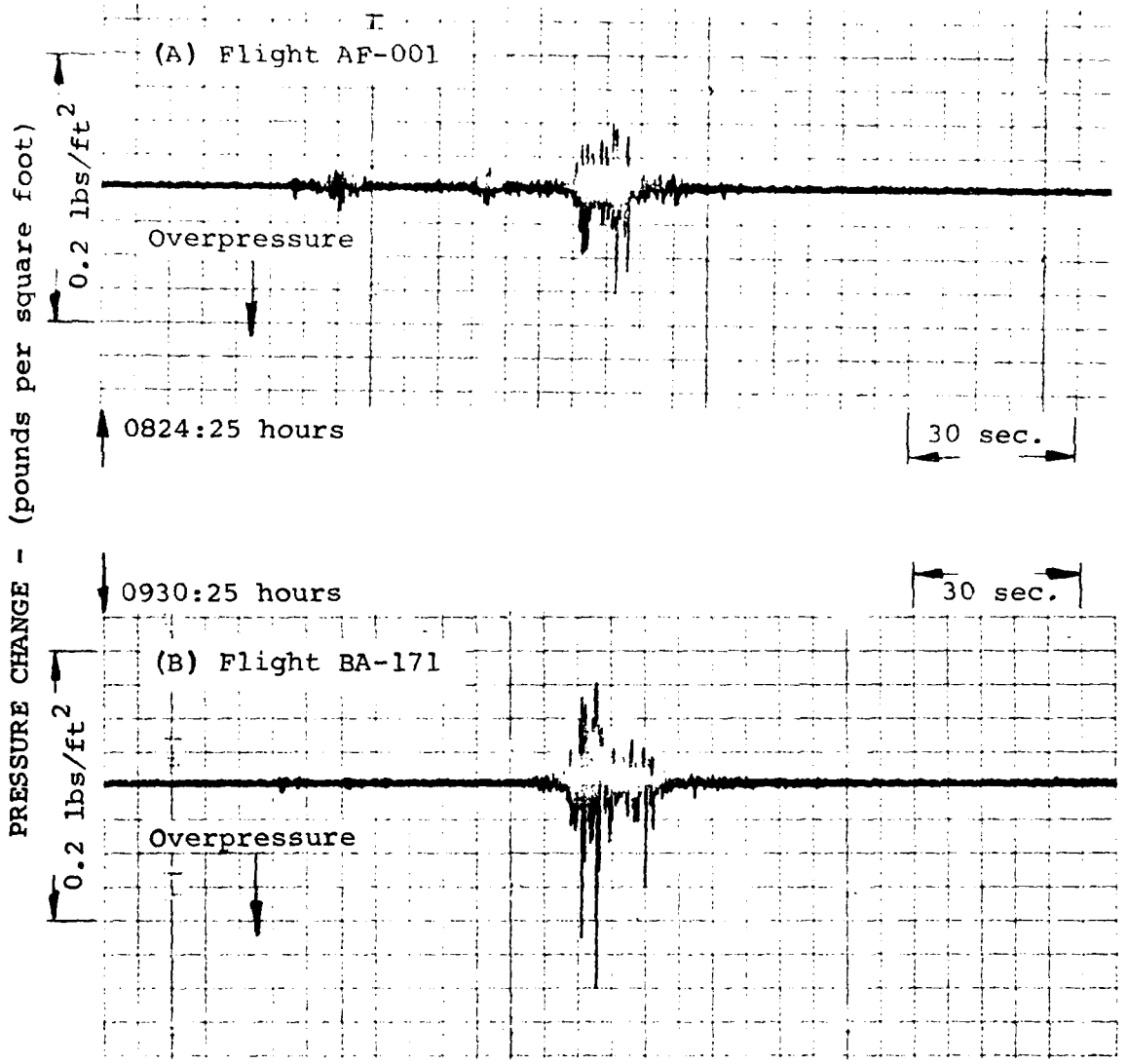

A) Source: Air France Flight AF-001
B) Source: British Airways Flight BA-171

FIGURE 9. PRESSURE TIME HISTORIES MALDEN MA - JULY 11, 1979

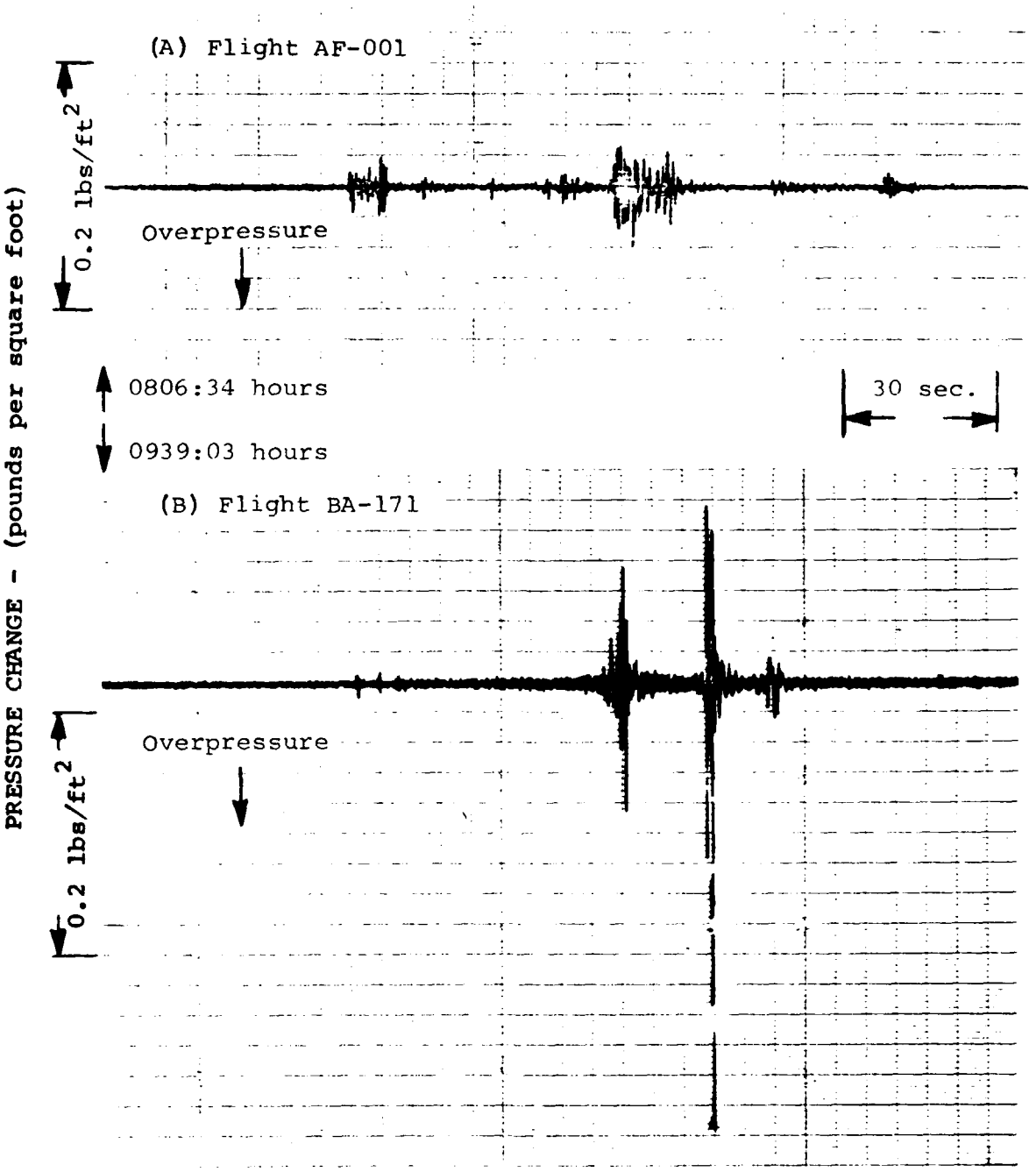

A) Source: Air France Flight AF-001
B) Source: British Airways Flight BA-171

FIGURE 10. PRESSURE TIME HISTORIES MALDEN MA - JULY 18, 1979

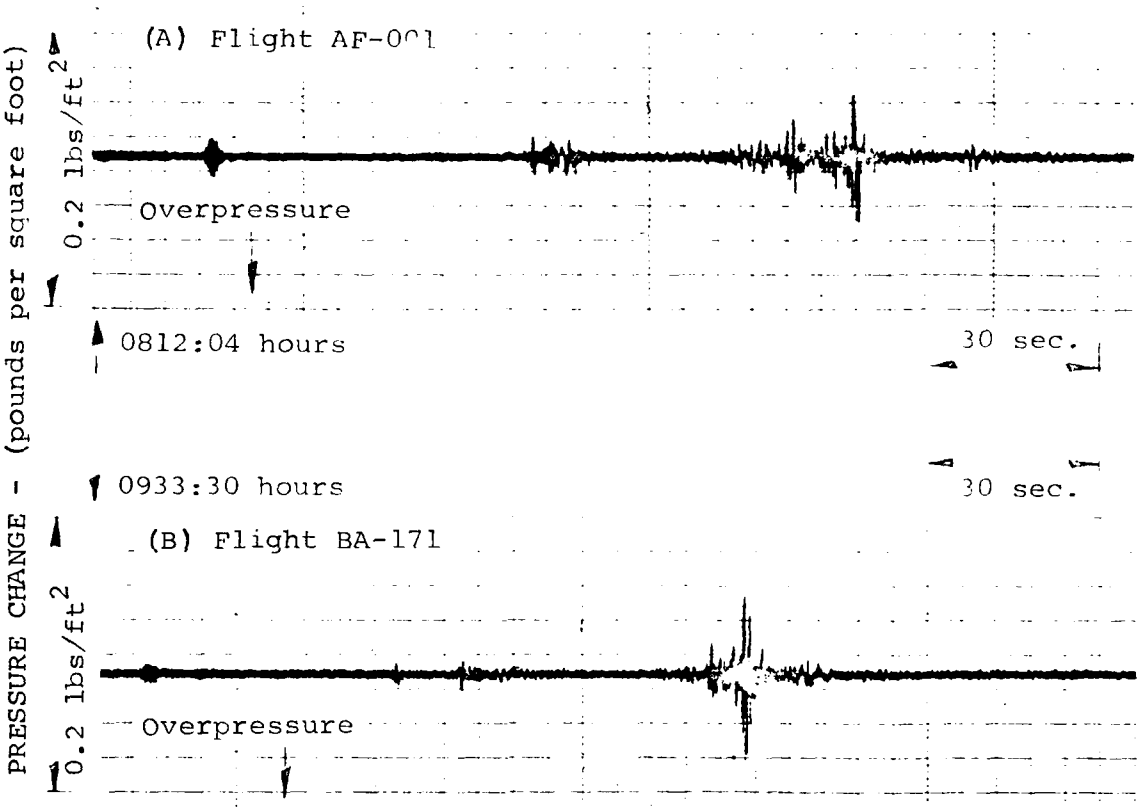

A) Source: Air France Flight AF-001
B) Source: British Airways Flight BA-171

FIGURE 11. PRESSURE TIME HISTORIES MALDEN MA - JULY 23, 1979

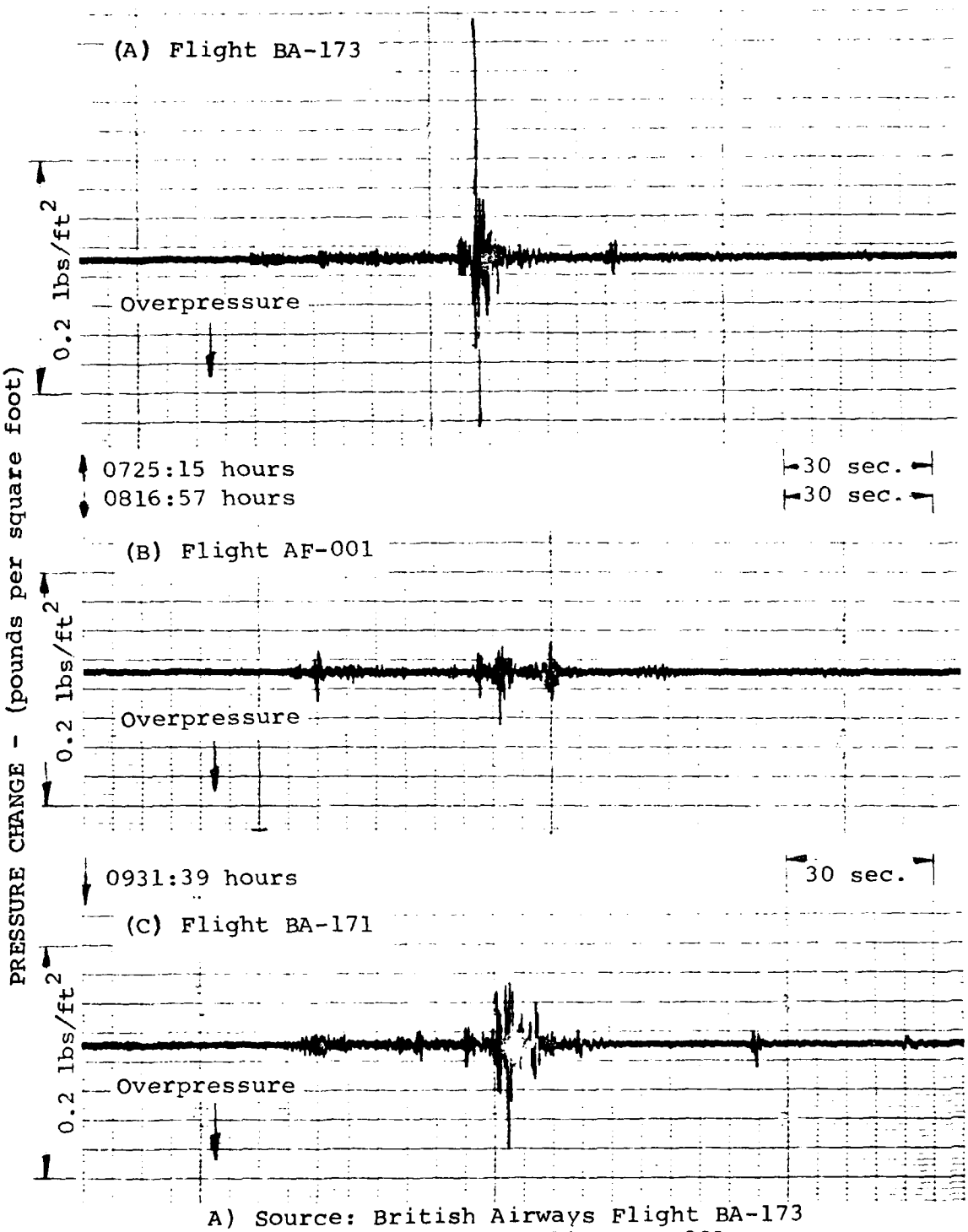

A) Source: British Airways Flight BA-173
B) Source: Air France Flight AF-001
C) Source: British Airways Flight BA-171

FIGURE 12. PRESSURE TIME HISTORIES MALDEN MA - JULY 26, 1979

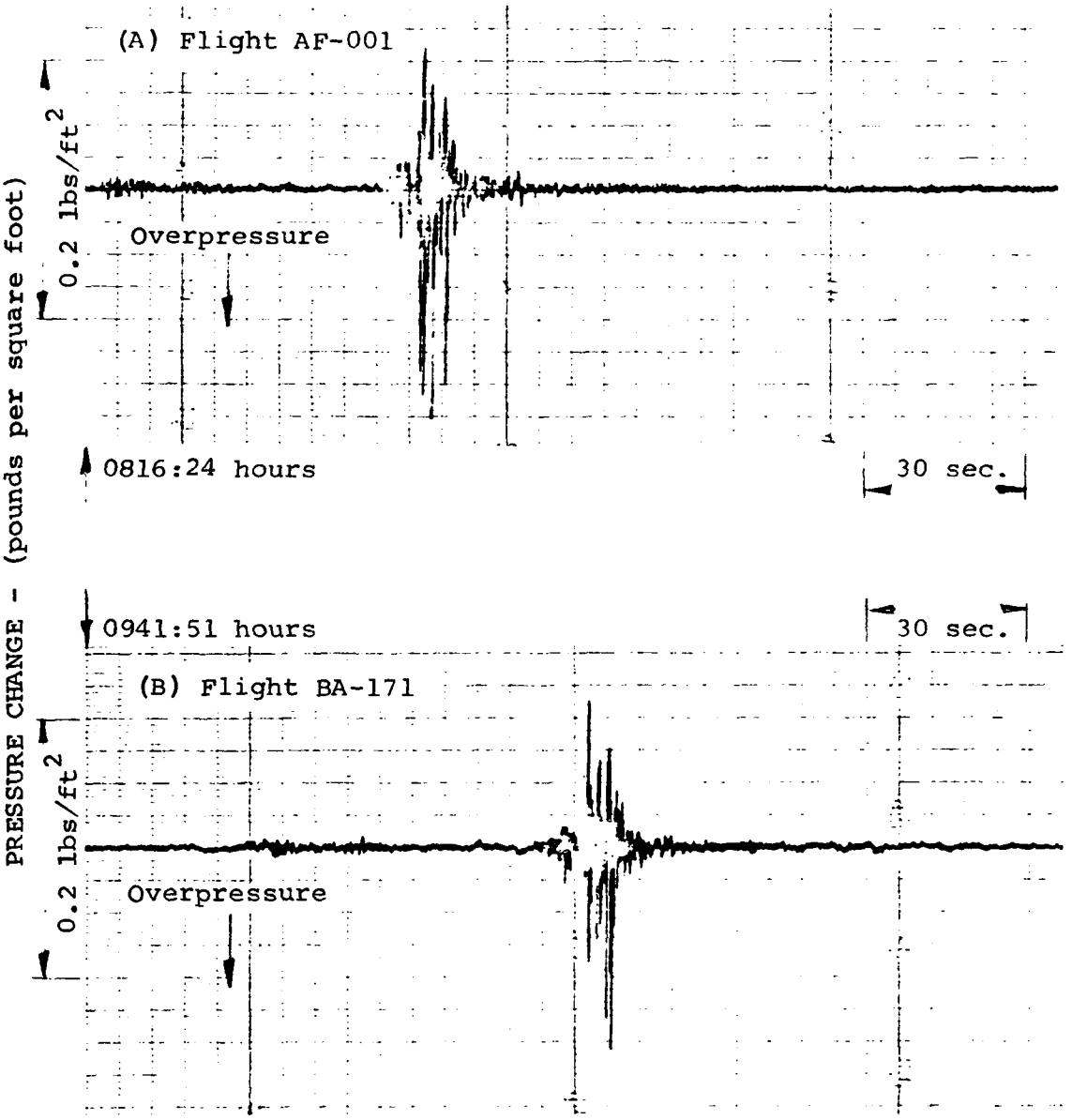

A) Source: Air France Flight AF-001
B) Source: British Airways Flight BA-171

FIGURE 13. PRESSURE TIME HISTORIES MALDEN MA - AUGUST 15, 1979

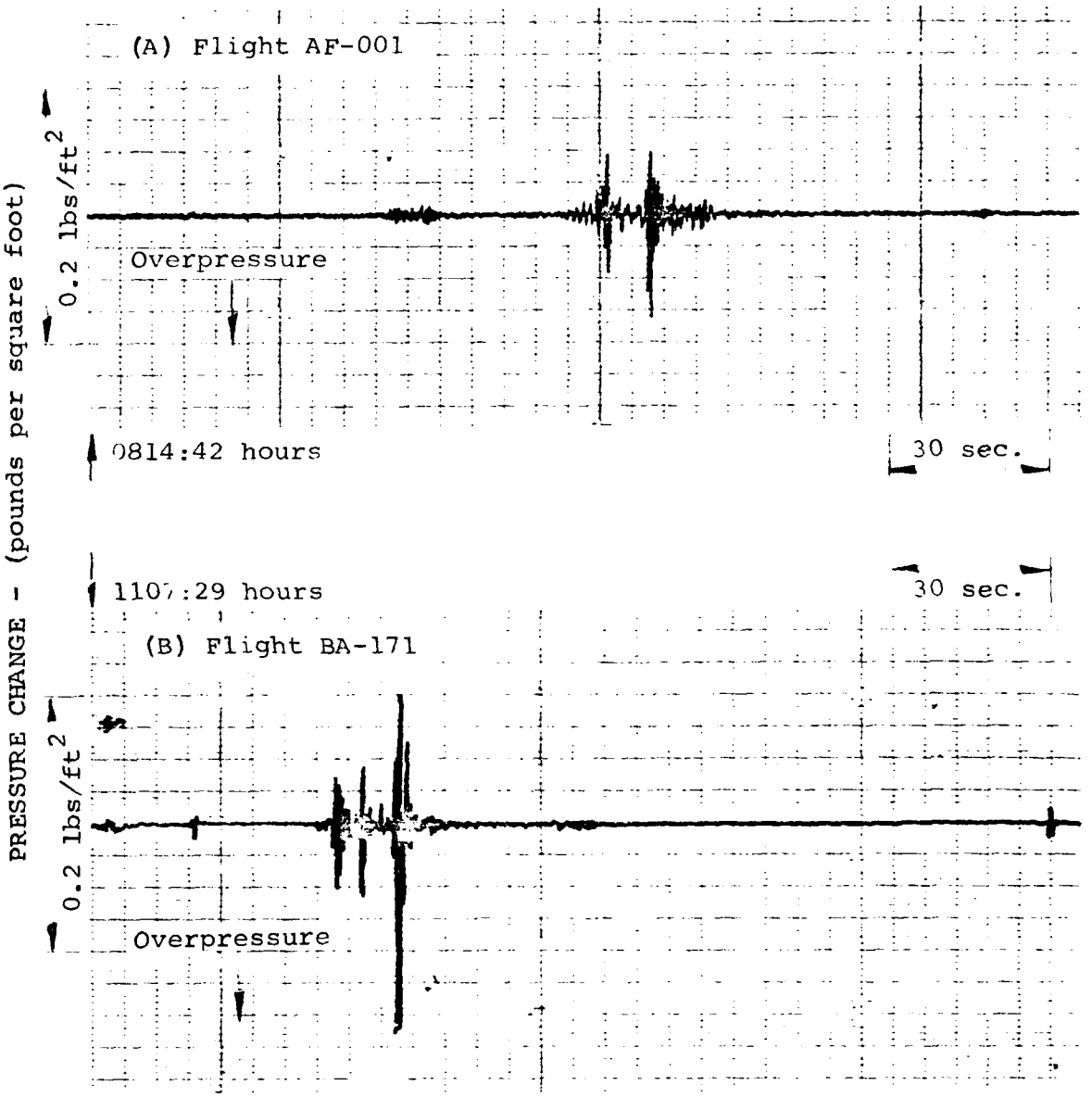

A) Source: Air France Flight AF-001
B) Source: British Airways Flight BA-171

FIGURE 14. PRESSURE TIME HISTORIES MALDEN MA - AUGUST 21, 1979

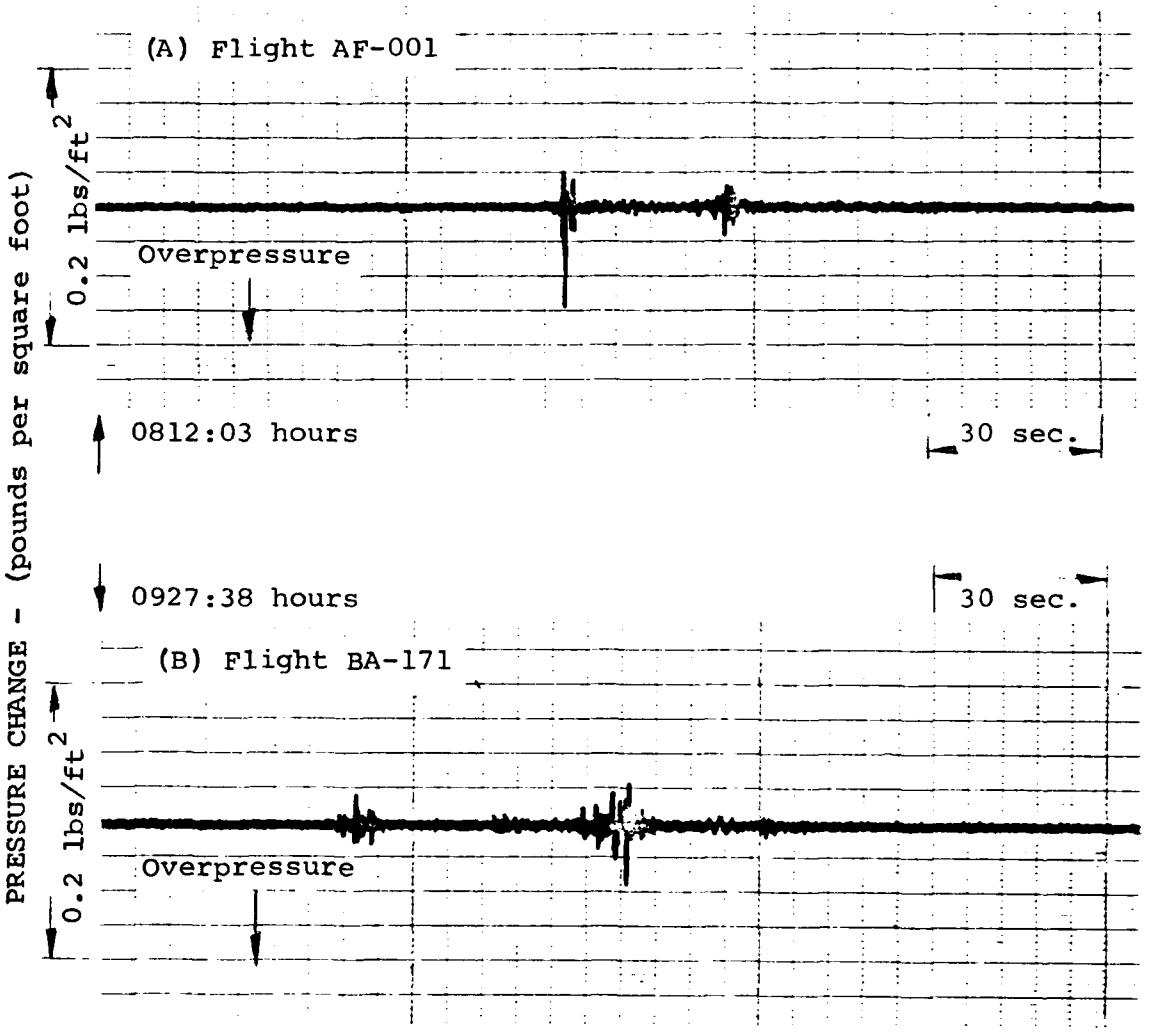

A) Source: Air France Flight AF-001
B) Source: British Airways Flight BA-171

FIGURE 15. PRESSURE TIME HISTORIES MALDEN MA - SEPTEMBER 5, 1979

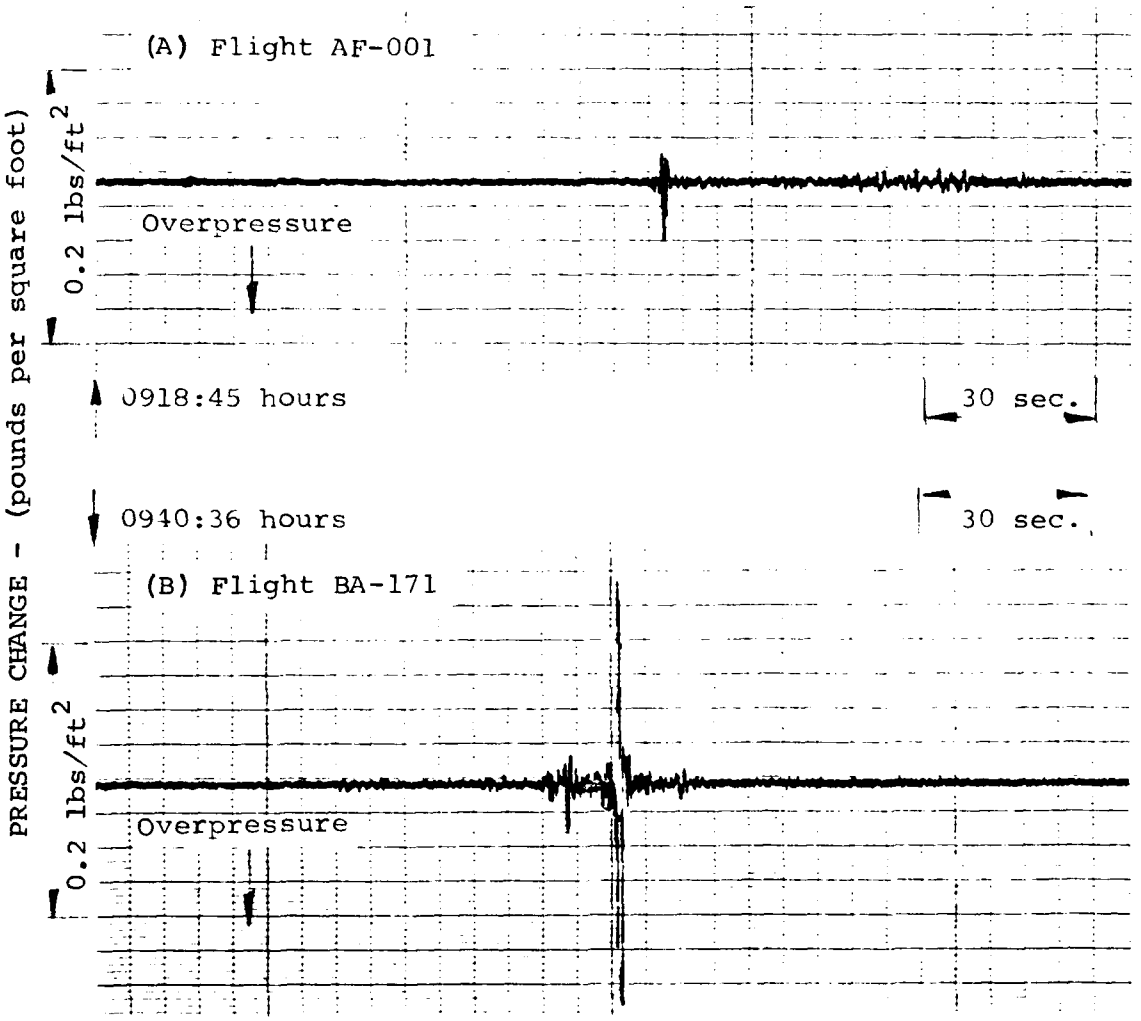

A) Source: Air France Flight AF-001
B) Source: British Airways Flight BA-171

FIGURE 16. PRESSURE TIME HISTORIES MALDEN MA - SEPTEMBER 12, 1979

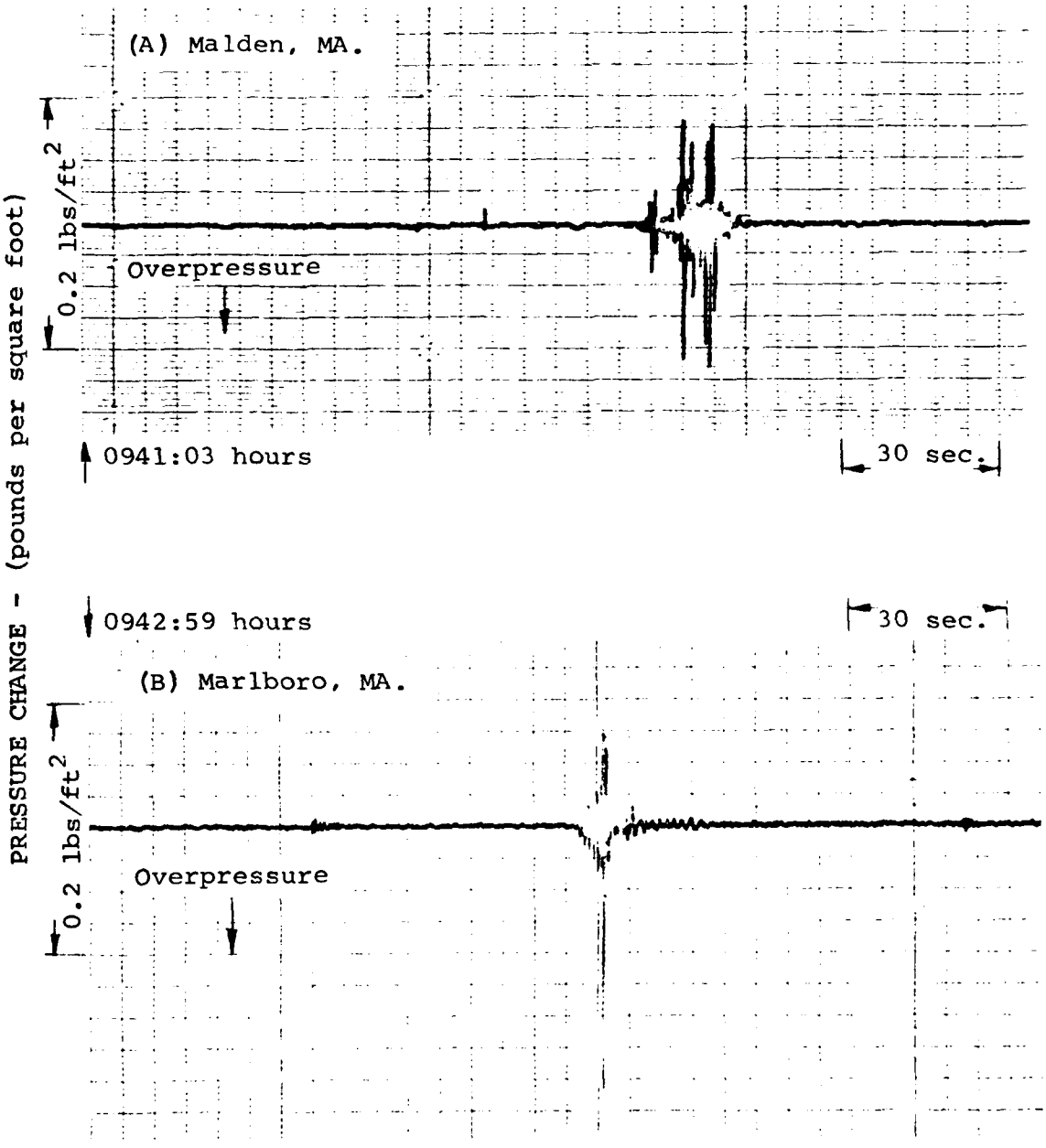

A) Malden, MA.
B) Marlboro, MA.

FIGURE 17. PRESSURE TIME HISTORIES SOURCE: BRITISH AIRWAYS FLIGHT NO. BA-171 JUNE 27, 1979

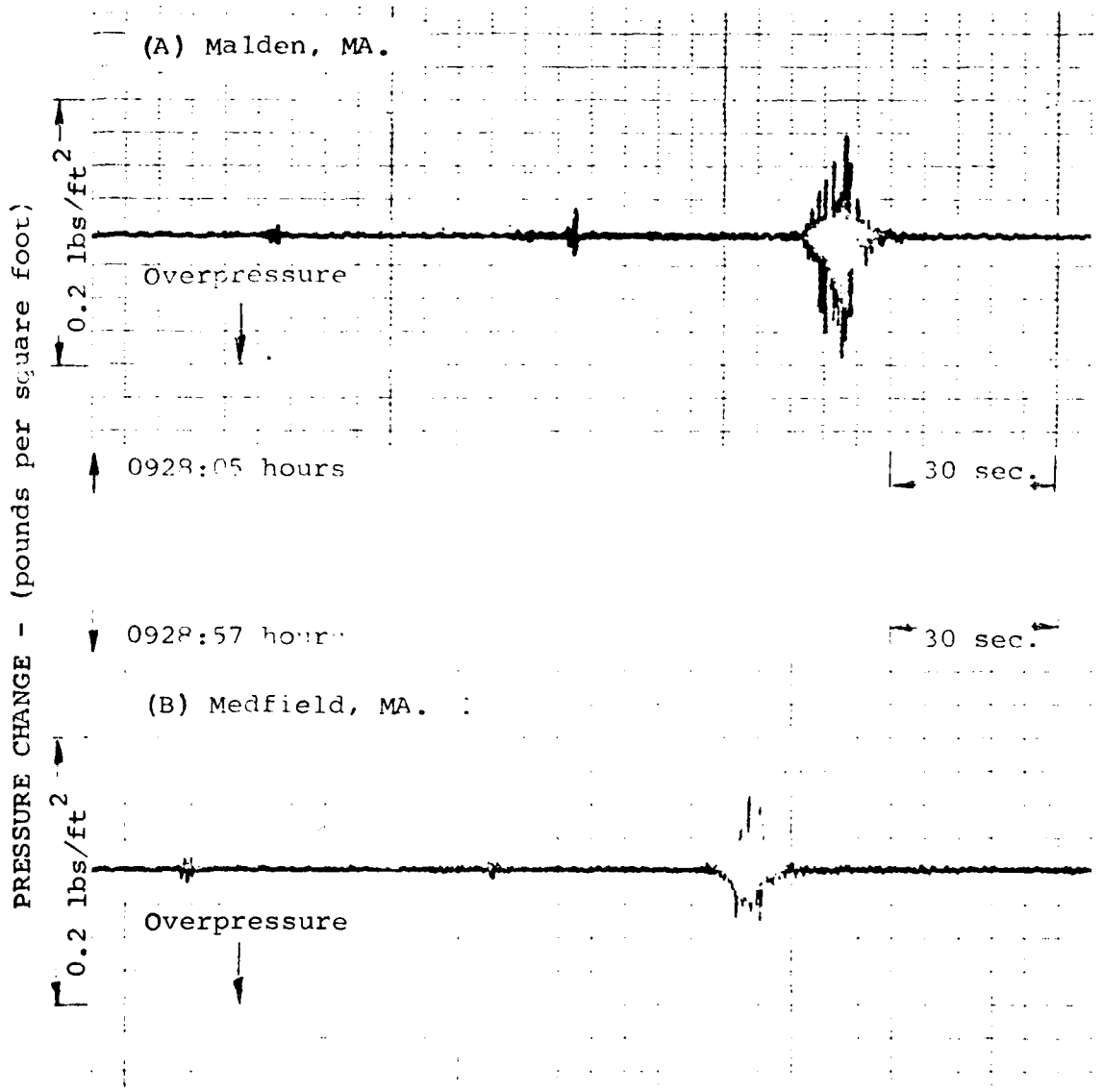

A) Malden, MA.
B) Medfield, MA.

FIGURE 18. PRESSURE TIME HISTORIES SOURCE: BRITISH AIRWAYS FLIGHT NO. BA-171 JUNE 28, 1979

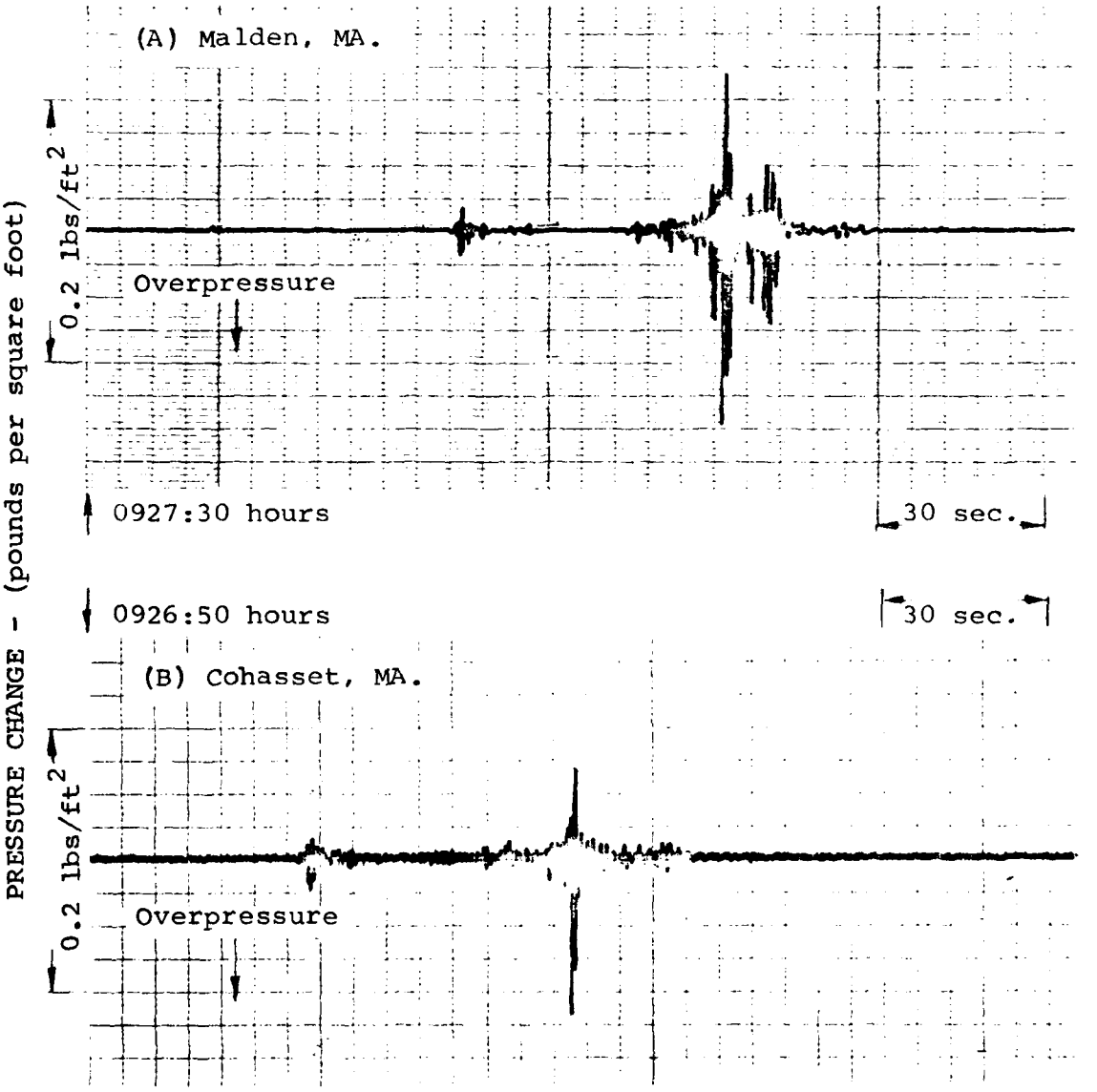

A) Malden, MA.
B) Cohasset, MA.

FIGURE 19. PRESSURE TIME HISTORIES SOURCE: BRITISH AIRWAYS FLIGHT NO. BA-171 JUNE 29, 1979

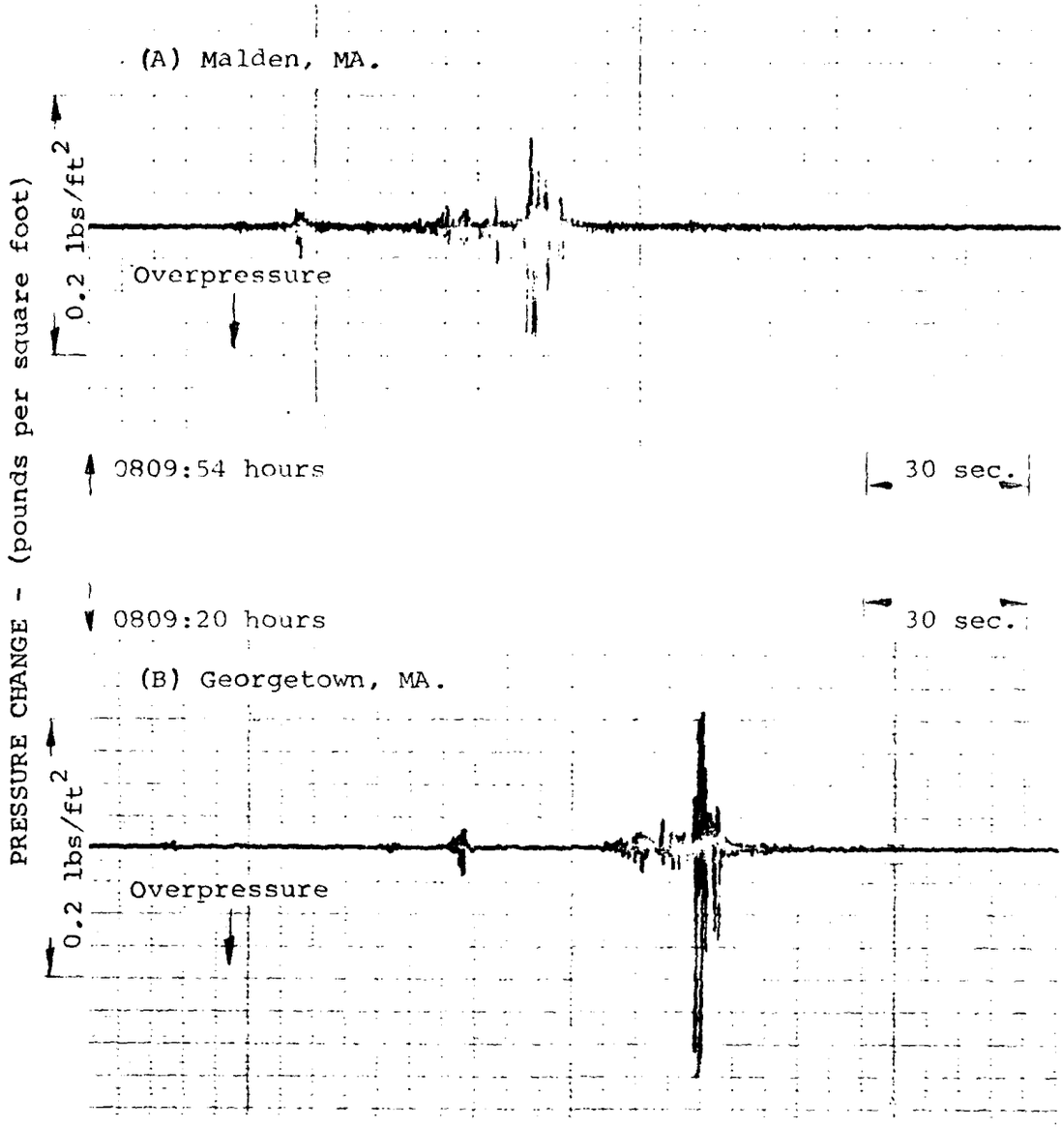

A) Malden, MA.
B) Georgetown, MA.

FIGURE 20. PRESSURE TIME HISTORIES SOURCE: AIR FRANCE FLIGHT NO. AF-001 JULY 9, 1979

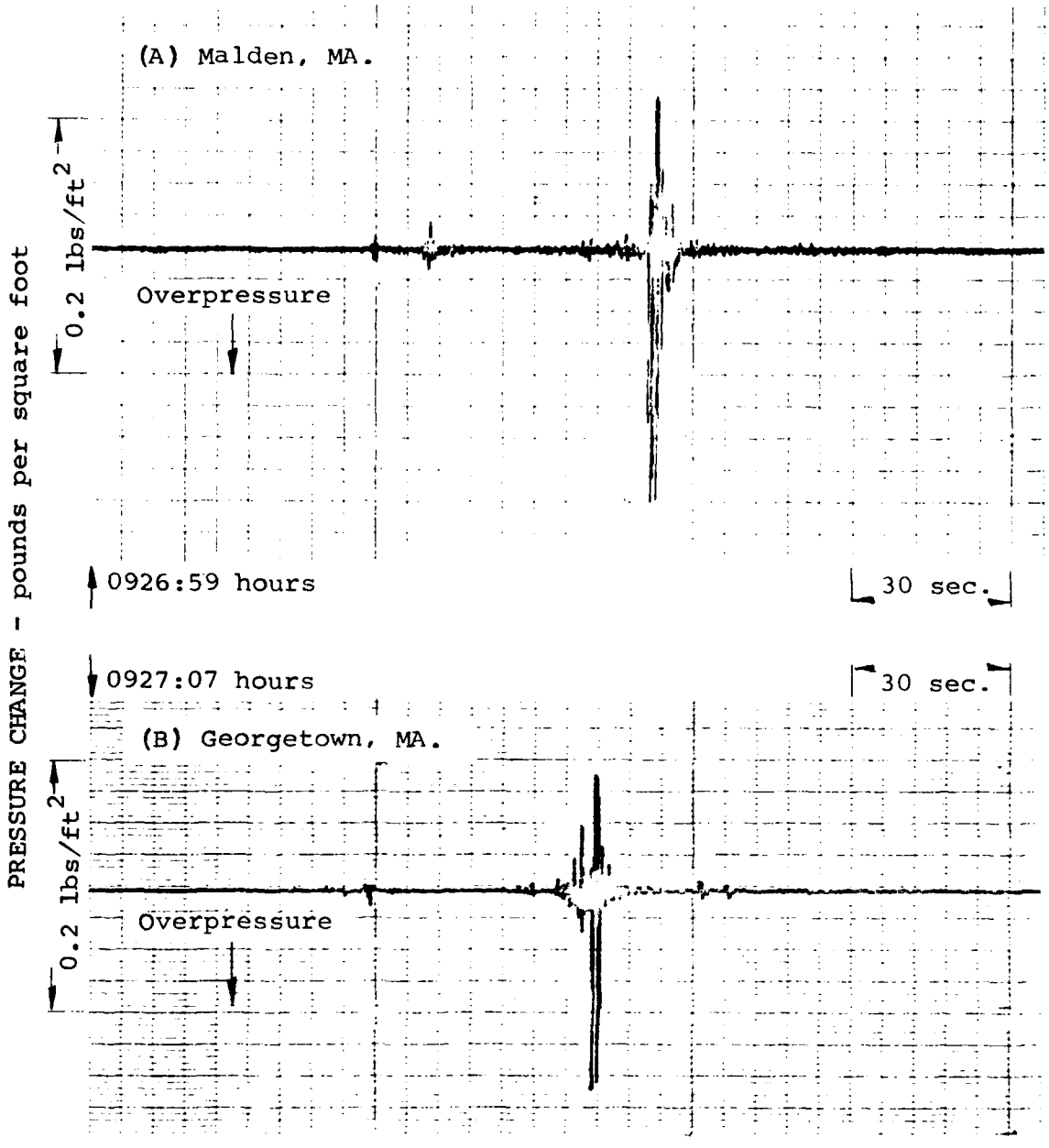

A) Malden, MA.
B) Georgetown, MA.

FIGURE 21. PRESSURE TIME HISTORIES SOURCE: BRITISH AIRWAYS FLIGHT NO. BA-171 JULY 9, 1979

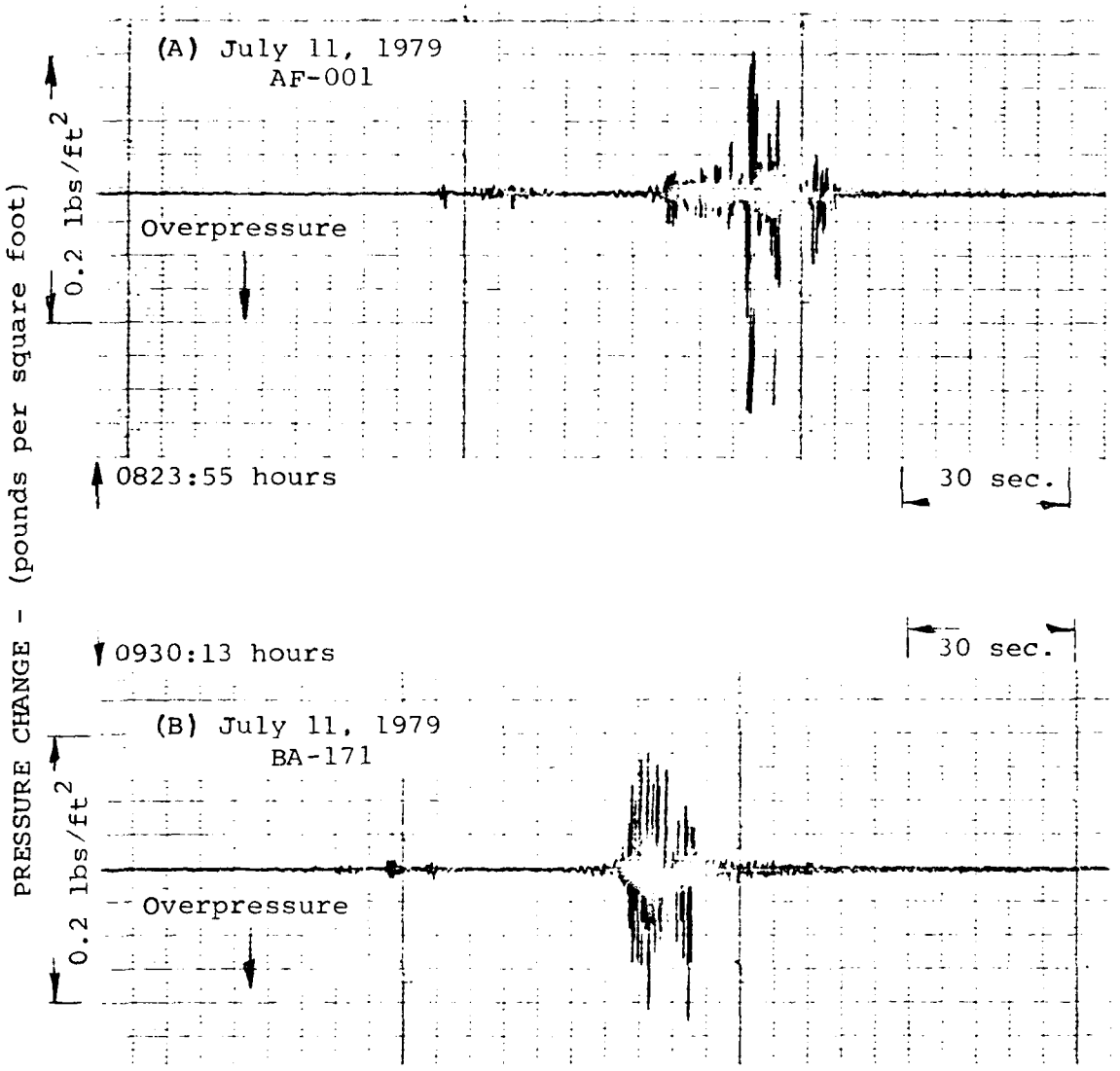

A) Source: Air France Flight AF 001
July 11, 1979
B) Source: British Airways Flight BA-171
July 11, 1979

FIGURE 22. PRESSURE TIME HISTORIES GEORGETOWN MA

(See Figure 9 for July 11, 1979 data at Malden MA)

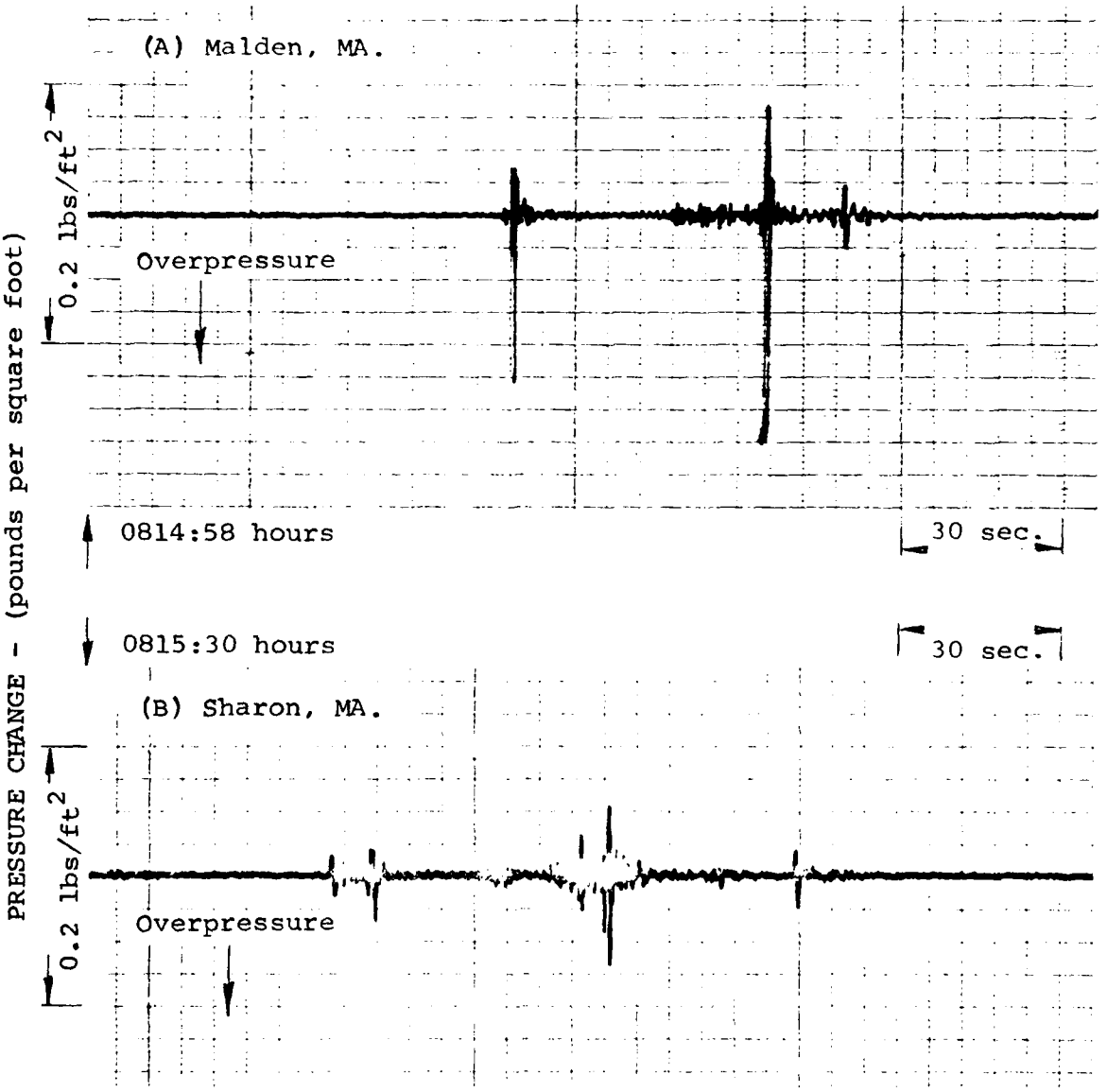

FIGURE 23. PRESSURE TIME HISTORIES SOURCE: AIR FRANCE FLIGHT NO. AF-001 AUGUST 2, 1979

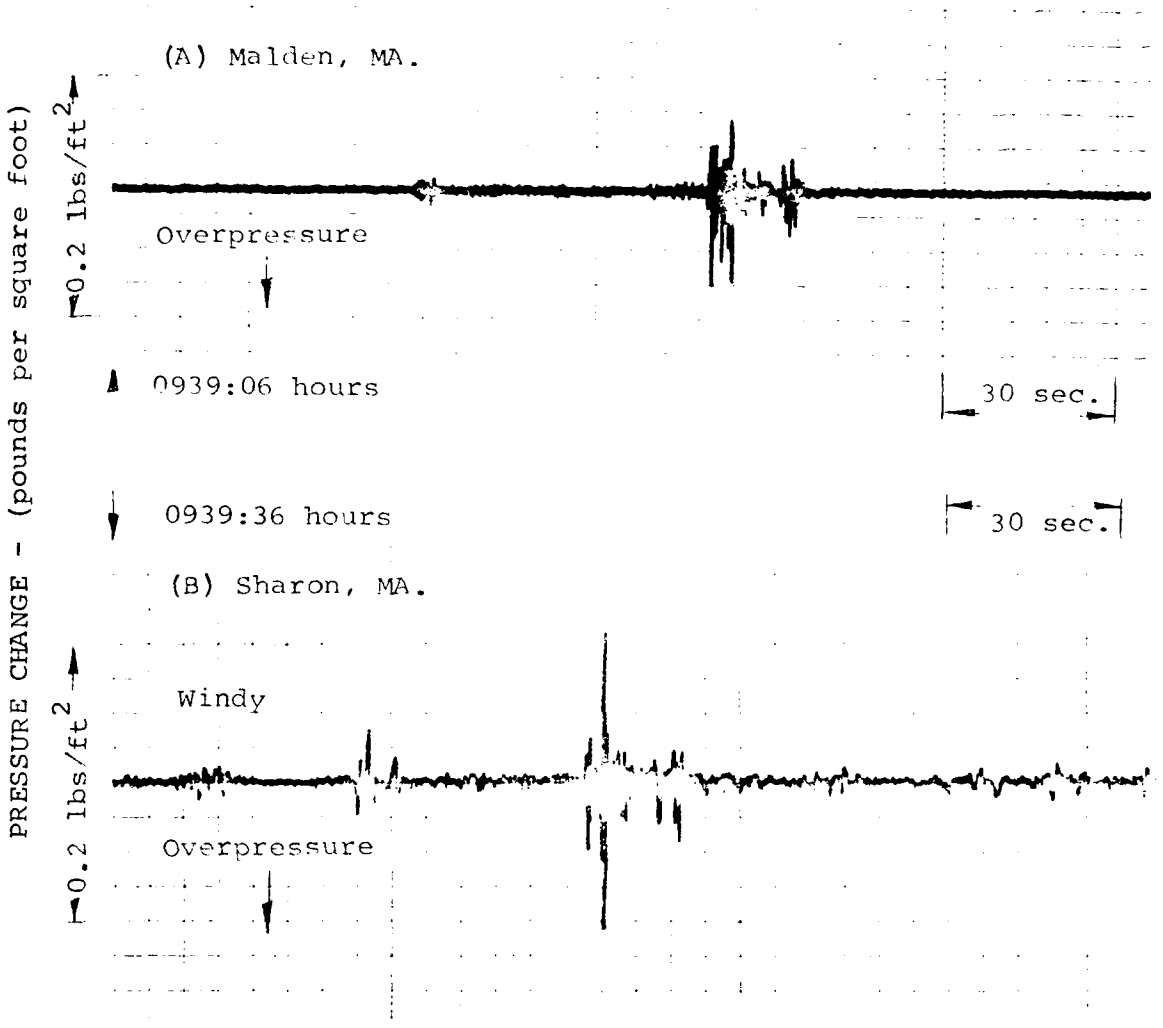

A) Malden, MA.
B) Sharon, MA.

FIGURE 24. PRESSURE TIME HISTORIES SOURCE: BRITISH AIRWAYS FLIGHT NO. BA-171 AUGUST 2, 1979

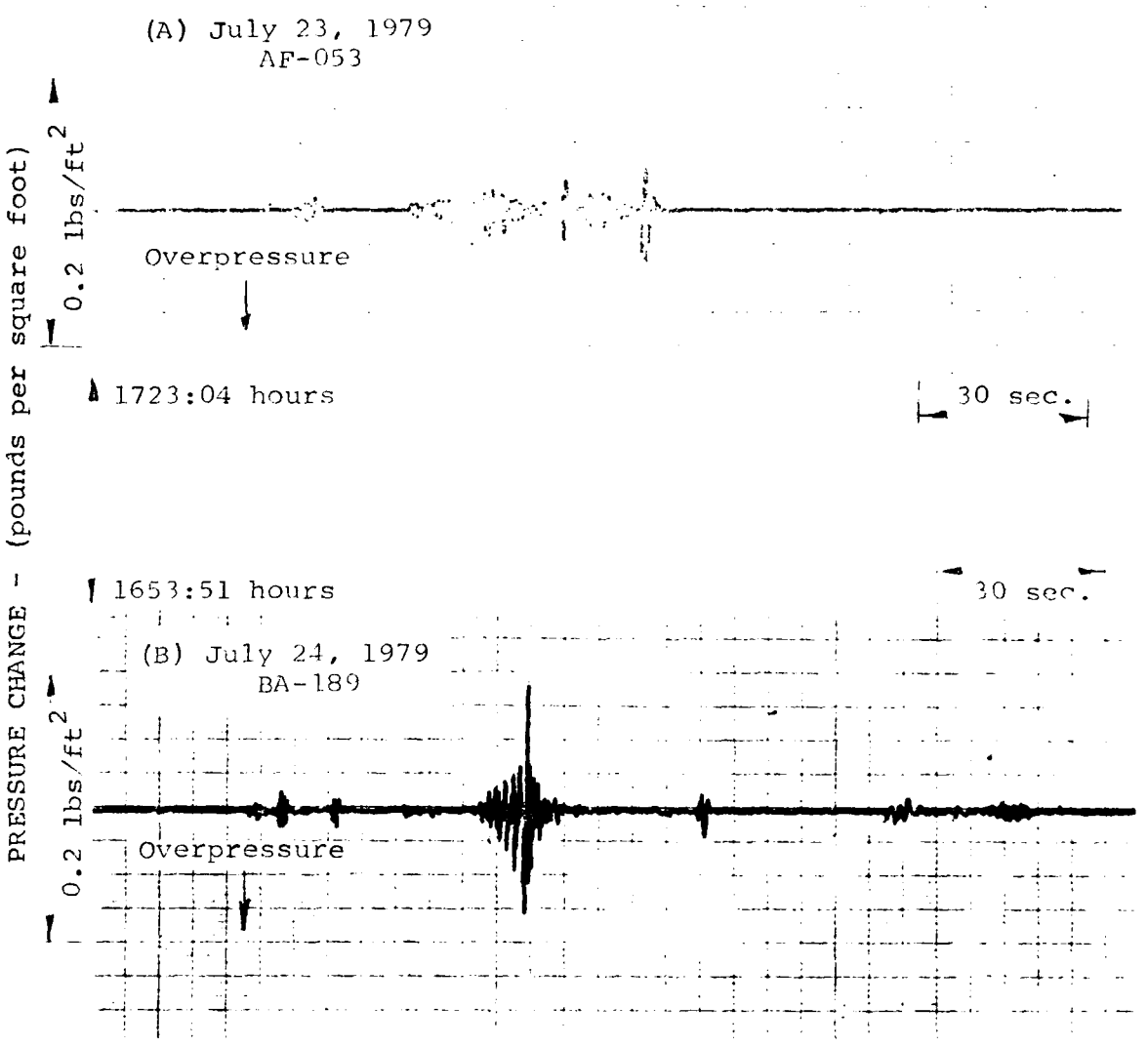

A) Source: Air France Flight AF-053
July 23, 1979
B) Source: British Airways Flight BA-189
July 24, 1979

FIGURE 25. PRESSURE TIME HISTORIFS APPLEBACHSVILLE PA

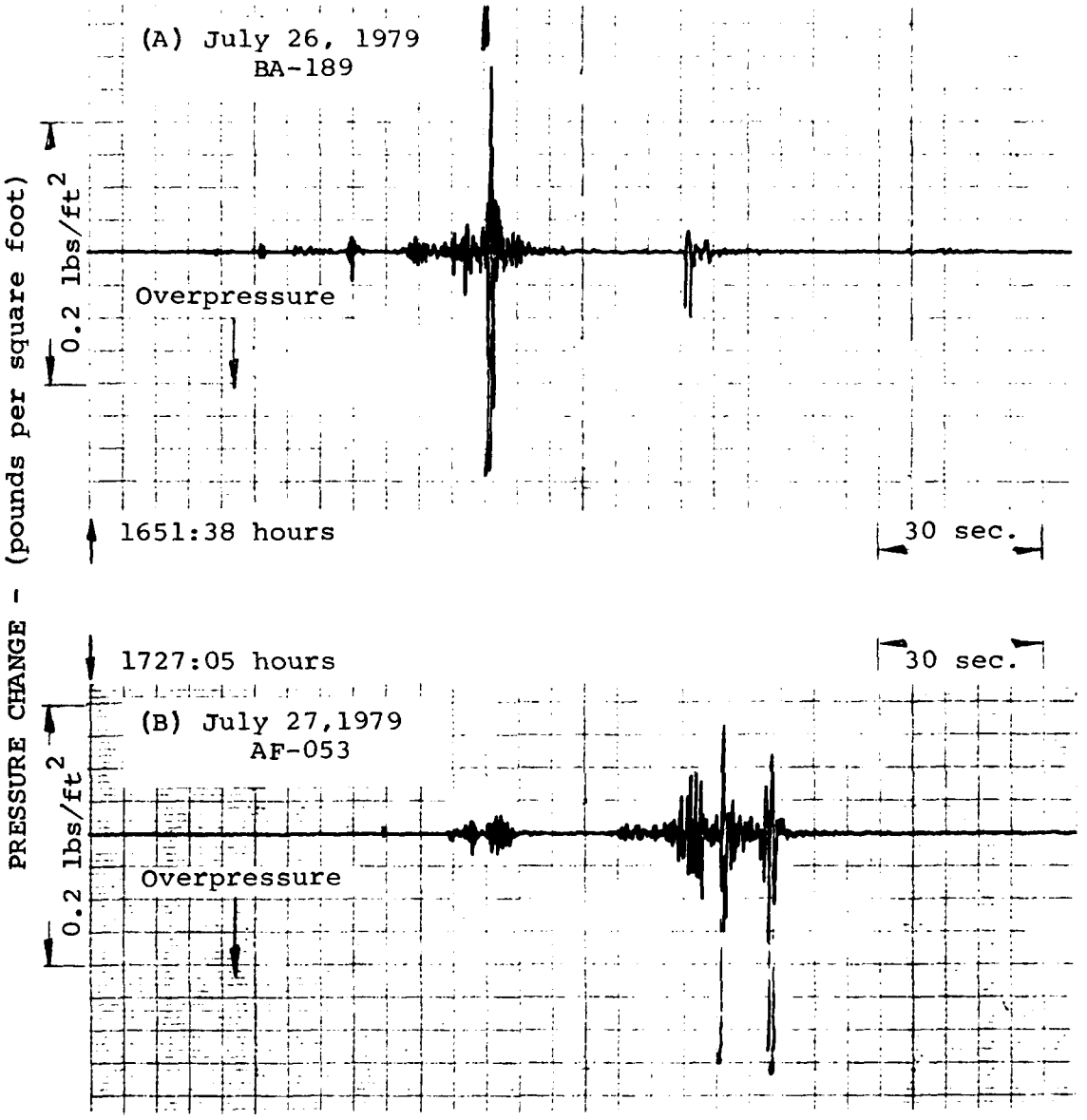

A) Source: British Airways Flight BA-189
July 26, 1979
B) Source: Air France Flight AF-053
July 27, 1979

FIGURE 26. PRESSURE TIME HISTORIES APPLEBACHSVILLE PA

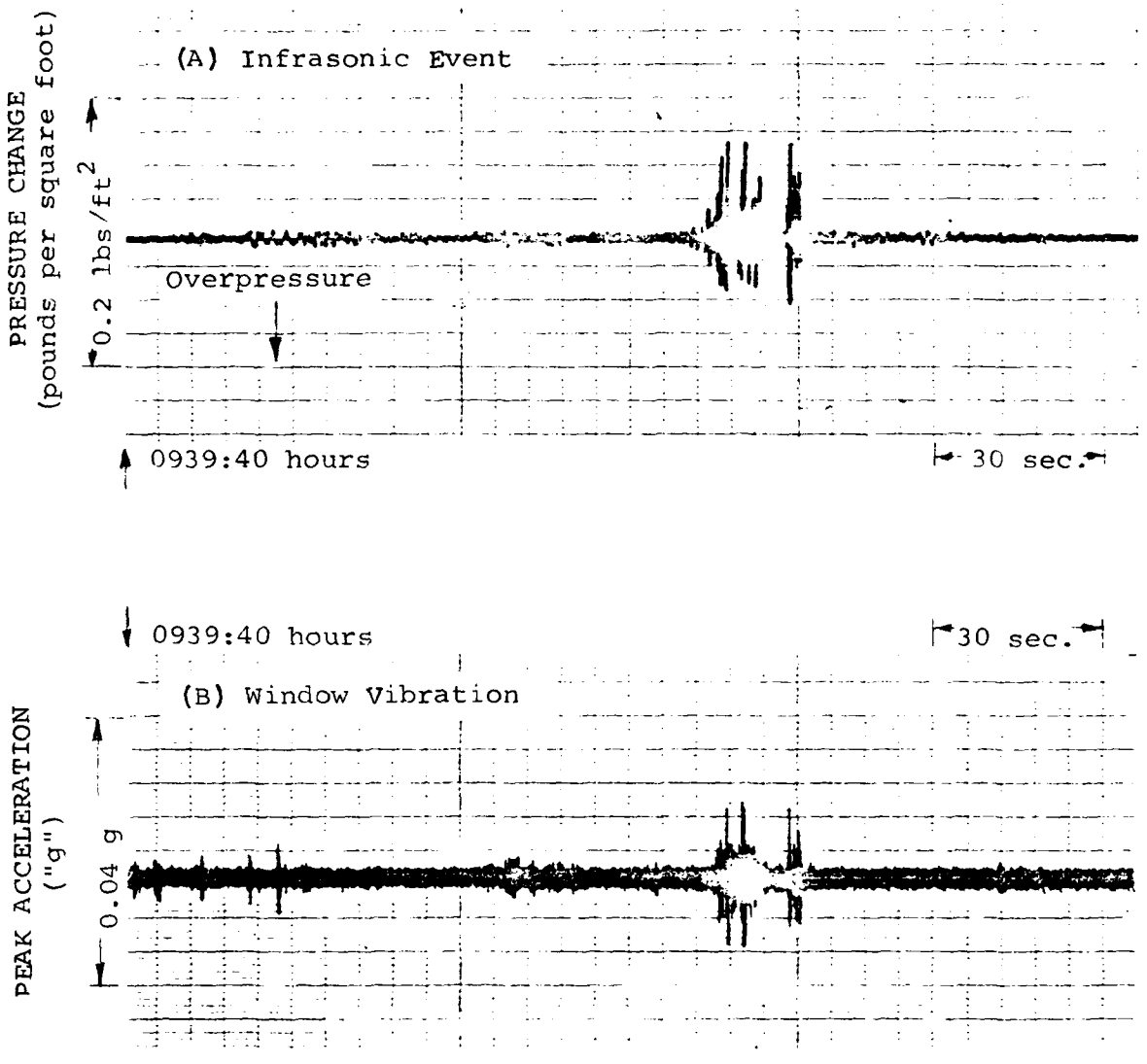

A) Infrasonic Exterior Pressure Change
B) Window Vibrational Acceleration

FIGURE 27. TIME HISTORIES WILMINGTON MA - JUNE 20, 1979
SOURCE: BRITISH AIRWAYS FLIGHT NO. BA-171

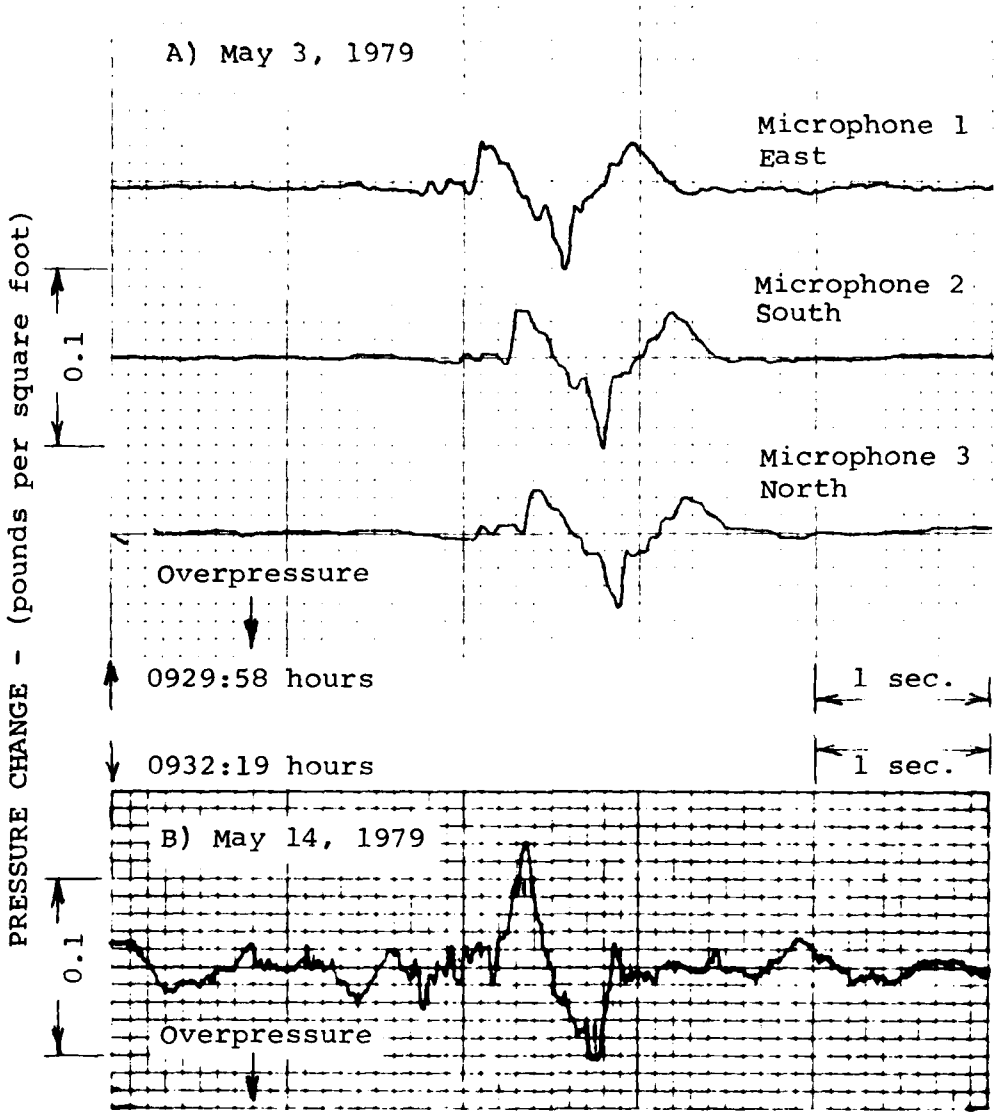

A) May 3, 1979
Time coincident data from 3-microphone triangular array
B) May 14, 1979

FIGURE 28. EXPANDED PRESSURE TIME HISTORIES SOURCE: BRITISH AIRWAYS FLIGHT BA-171 MALDEN MA

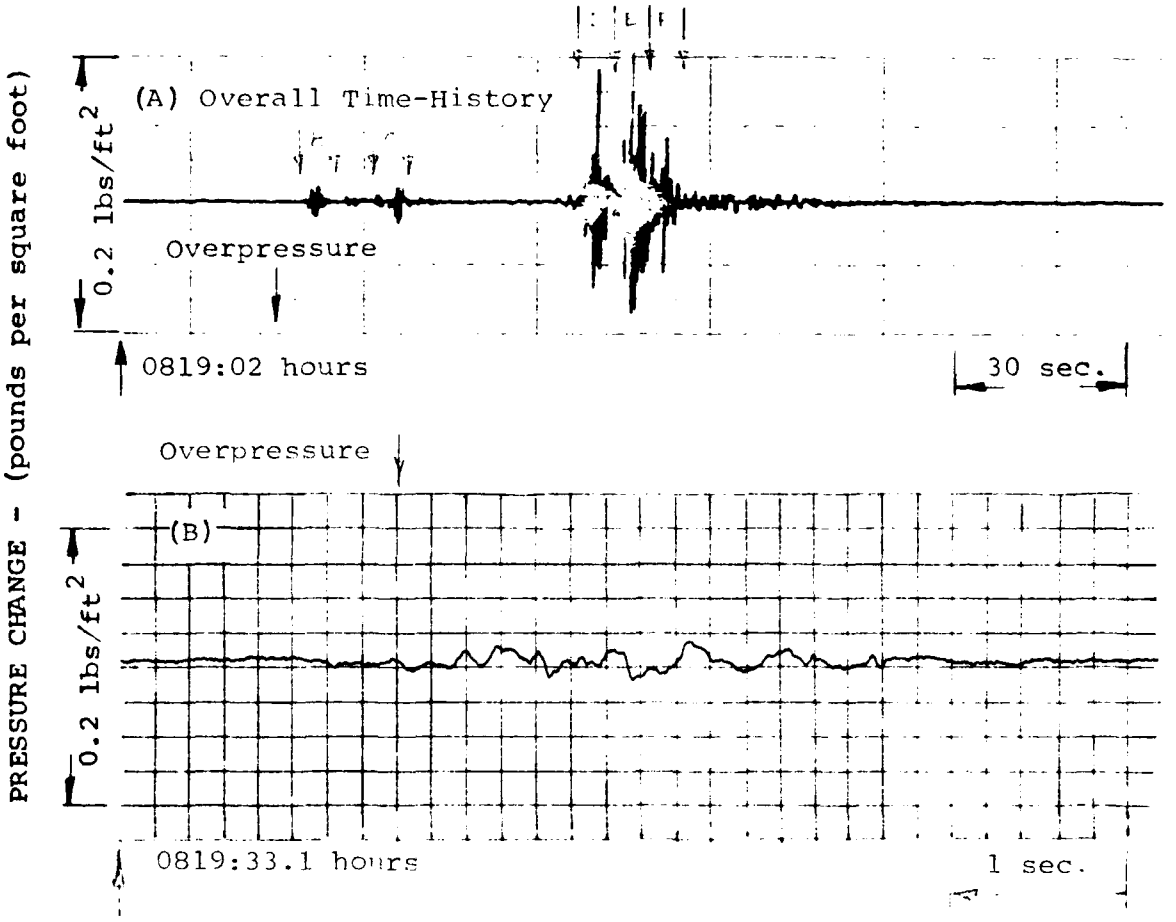

A) Overall Time-History

B-F) Expanded Time-History Segments
- B) 0819:33.1 - 0819:39.1
- C) 0819:46.3 - 0819:52.3
- D) 0820:21.1 - 0820:27.1
- E) 0820:27.1 - 0820:33.1
- F) 0820:33.1 - 0820:39.1

FIGURE 29. EXPANDED PRESSURE TIME HISTORY MALDEN MA - JUNE 13, 1979 SOURCE: AIR FRANCE FLIGHT AF-001

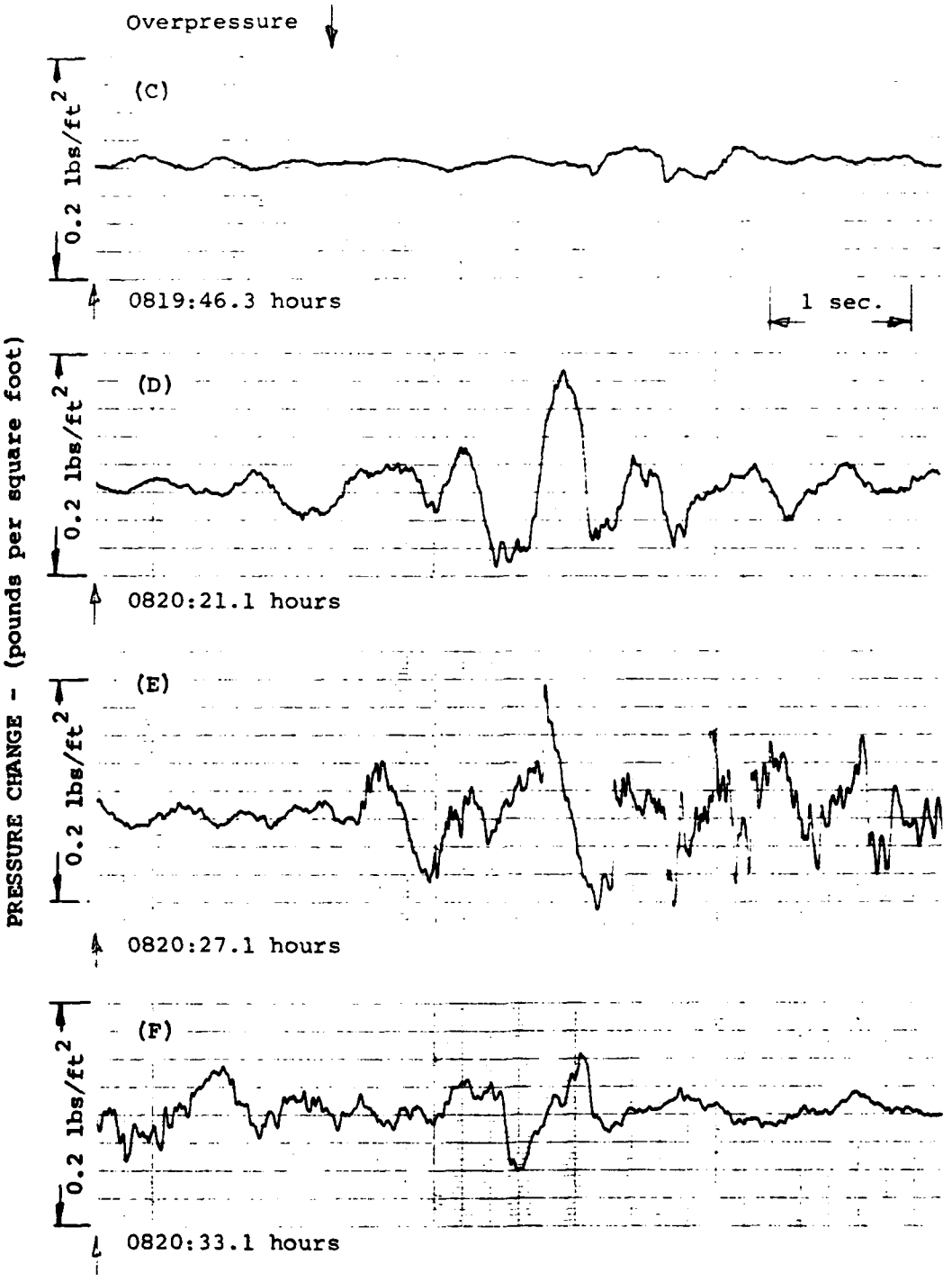

FIGURE 29. EXPANDED PRESSURE TIME HISTORY MALDEN MA - JUNE 13, 1979 SOURCE: AIR FRANCE FLIGHT AF-001 (CONT.)

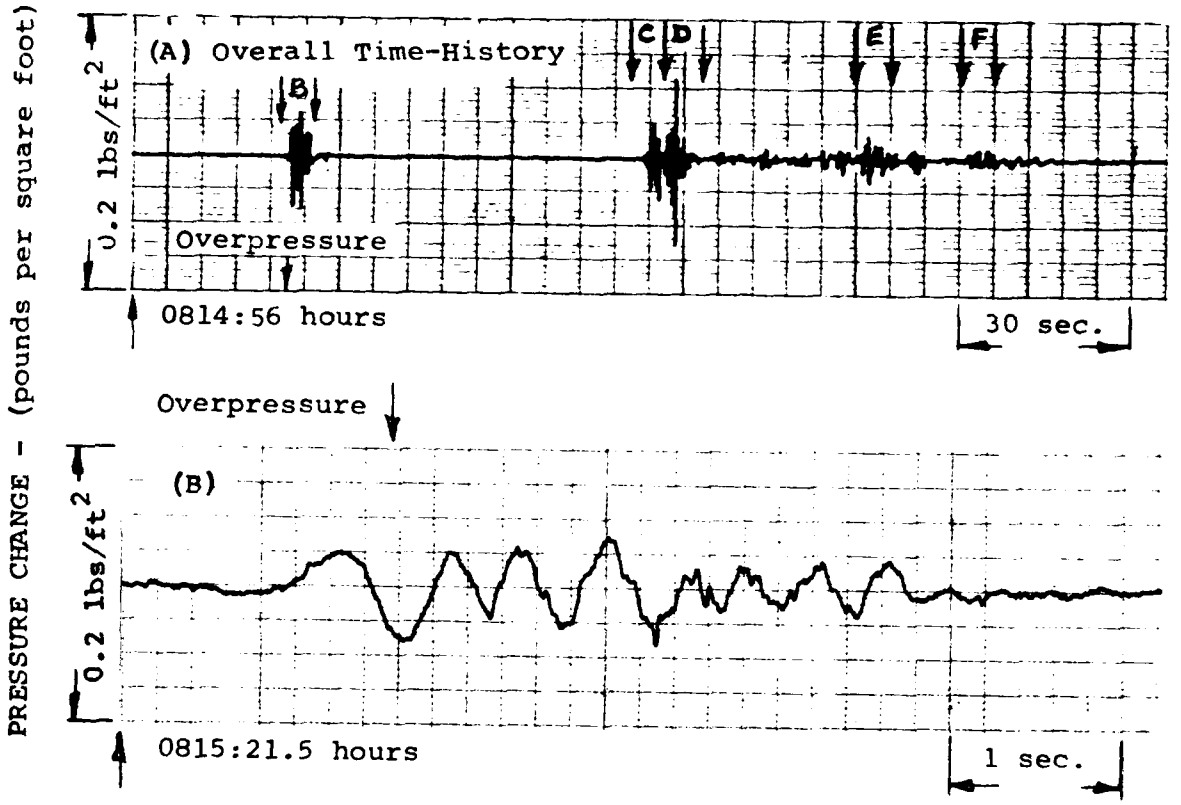

A) Overall Time-History

B-F) Expanded Time-History Segments
- B) 0815:21.5 - 0815:27.5
- C) 0816:22.7 - 0816:28.7
- D) 0816:28.7 - 0816:34.7
- E) 0817:01.1 - 0817:07.1
- F) 0817:19.3 - 0817:25.3

FIGURE 30. EXPANDED PRESSURE TIME HISTORY MALDEN MA - JUNE 20, 1979 SOURCE: AIR FRANCE FLIGHT AF-001

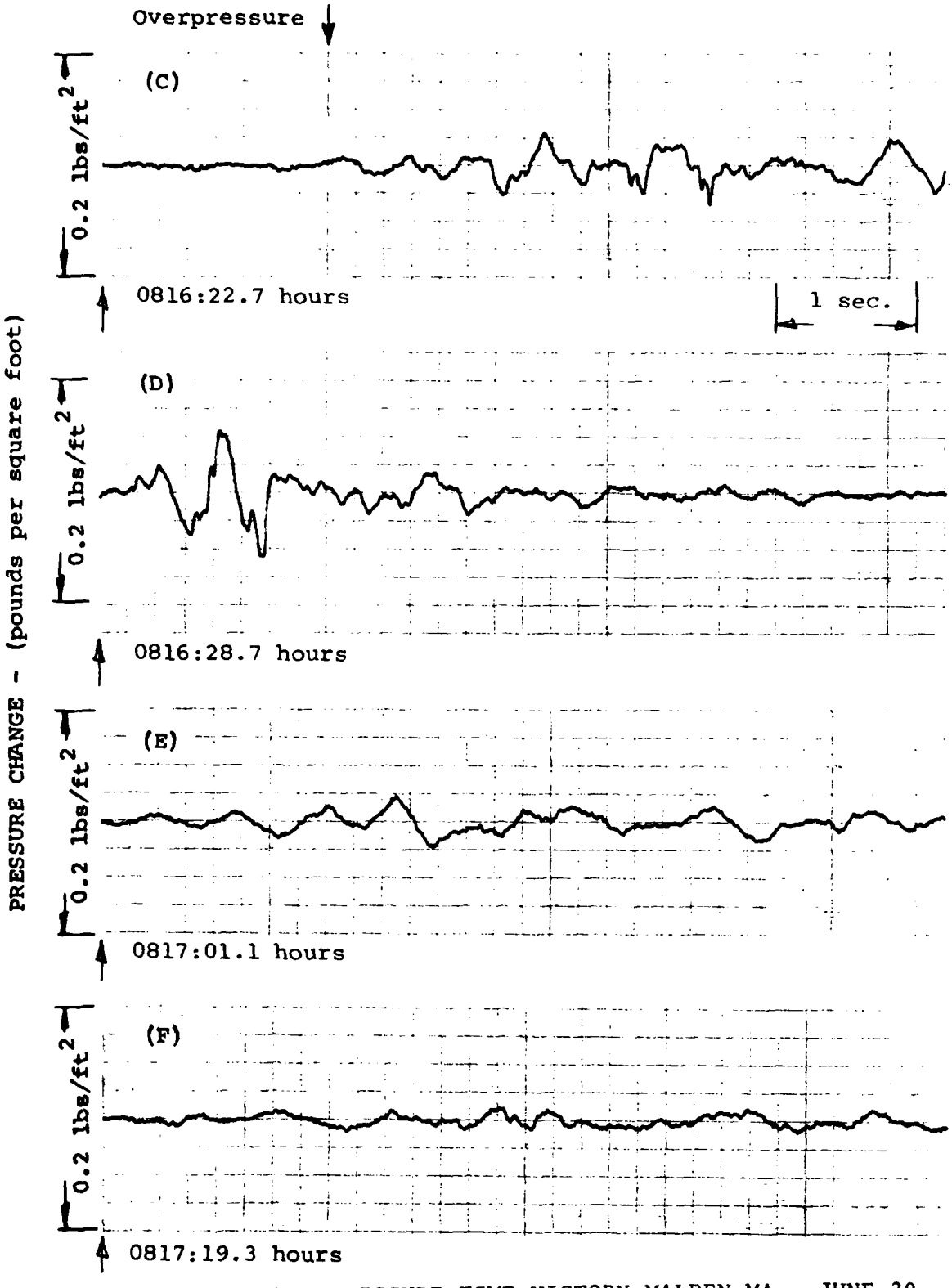

FIGURE 30. EXPANDED PRESSURE TIME HISTORY MALDEN MA - JUNE 20, 1979 SOURCE: AIR FRANCE FLIGHT AF-001 (CONT.)

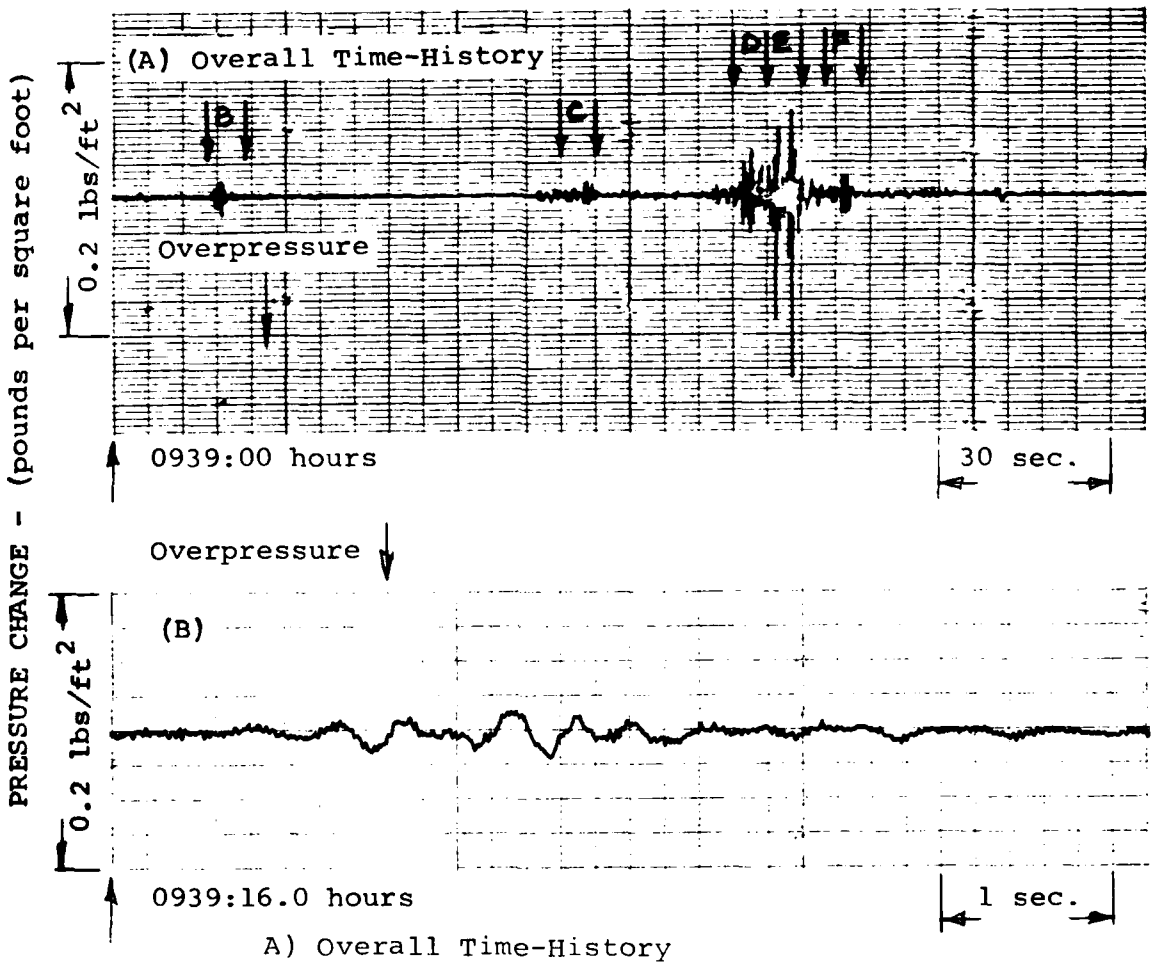

A) Overall Time-History

B-F) Expanded Time-History Segments
- B) 0939:16.0 - 0939:22.0
- C) 0940:18.0 - 0940:24.0
- D) 0940:48.2 - 0940:54.2
- E) 0940:54.2 - 0941:00.2
- F) 0941:04.0 - 0941:10.0

FIGURE 31. EXPANDED PRESSURE TIME HISTORY MALDEN, MA - JUNE 20, 1979 SOURCE: BRITISH AIRWAYS FLIGHT BA-171

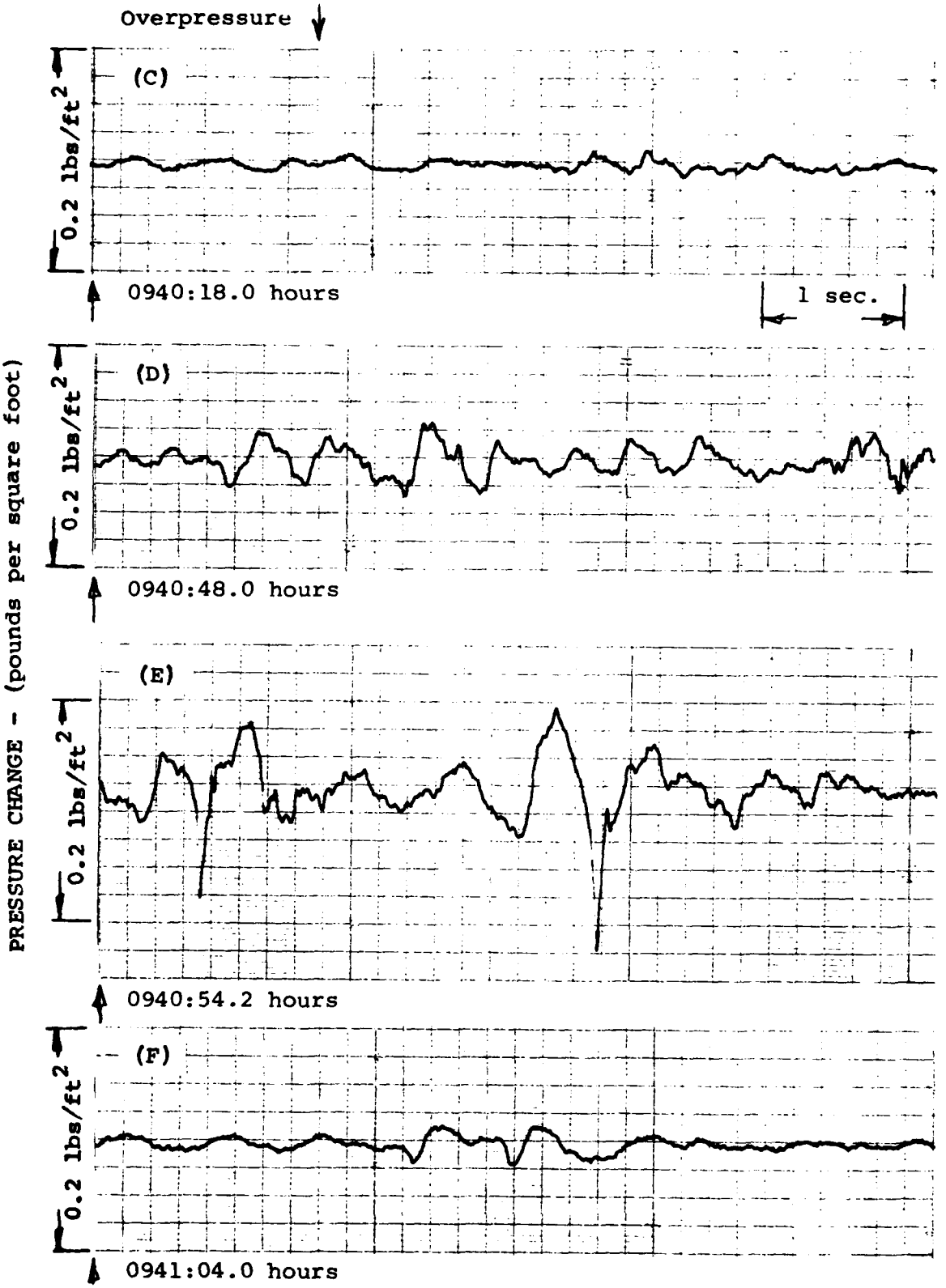

FIGURE 31. EXPANDED PRESSURE TIME HISTORY MALDEN MA - JUNE 20, 1979 SOURCE: BRITISH AIRWAYS FLIGHT BA-171 (CONT.)

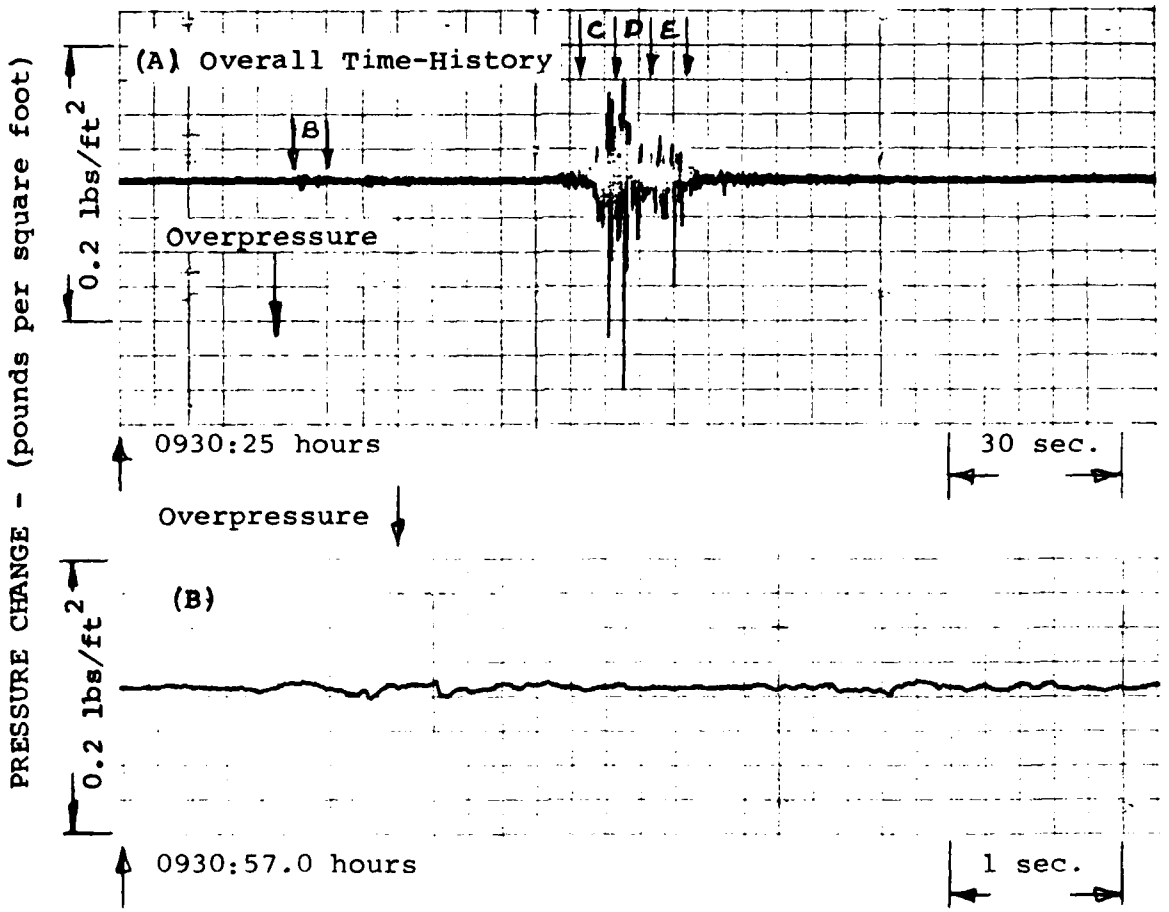

A) Overall Time-History

B-E) Expanded Time-History Segments
B) 0930:57.0 - 0931:03.0
C) 0931:48.4 - 0931:54.4
D) 0931:54.4 - 0932:00.4
E) 0932:00.4 - 0936:06.4

FIGURE 32. EXPANDED PRESSURE TIME HISTORY MALDEN, MA - JULY 11, 1979 SOURCE: BRITISH AIRWAYS FLIGHT BA-171

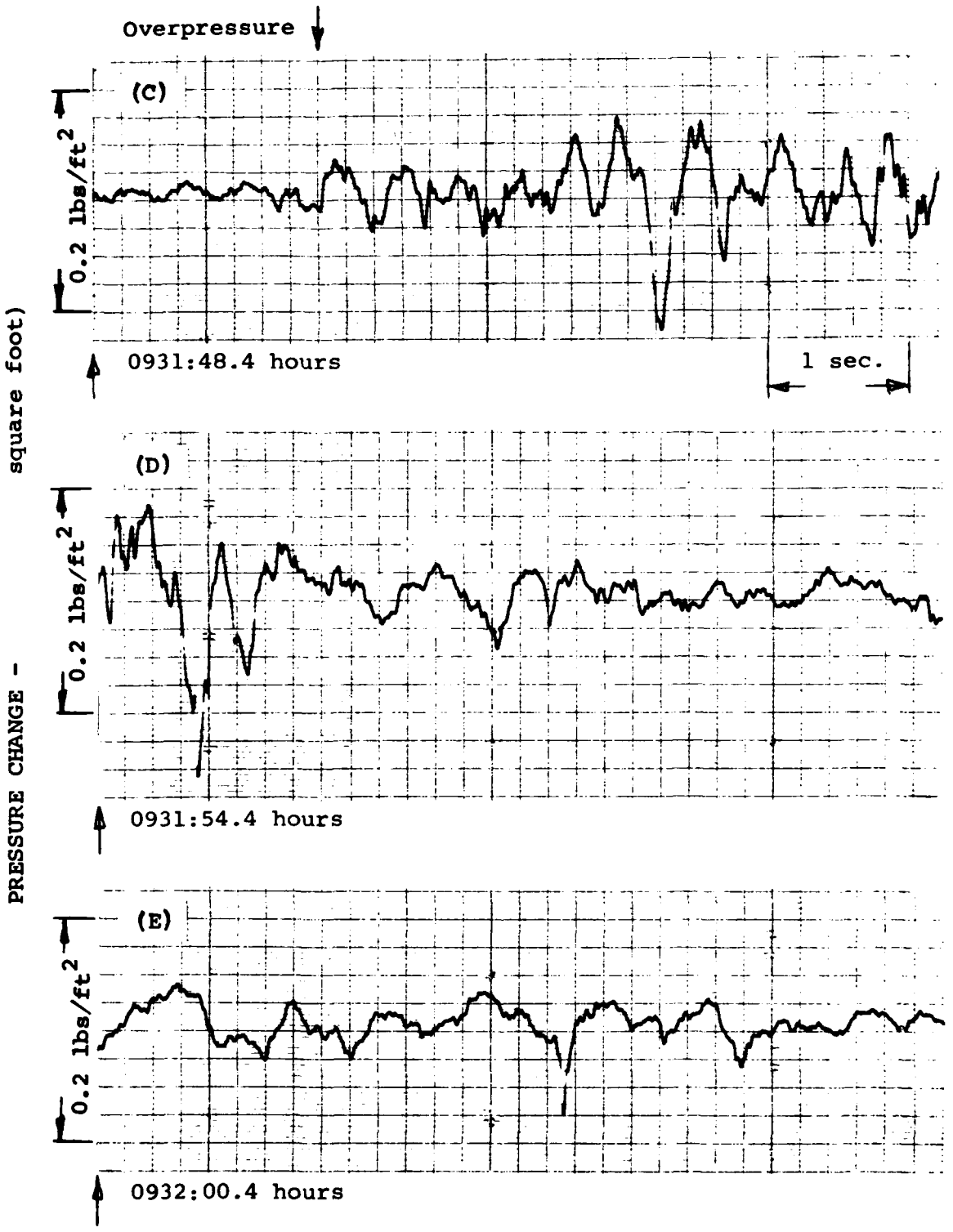

FIGURE 32. EXPANDED PRESSURE TIME HISTORY MALDEN, MA - JULY 11, 1979 SOURCE: BRITISH AIRWAYS FLIGHT BA-171 (CONT.)

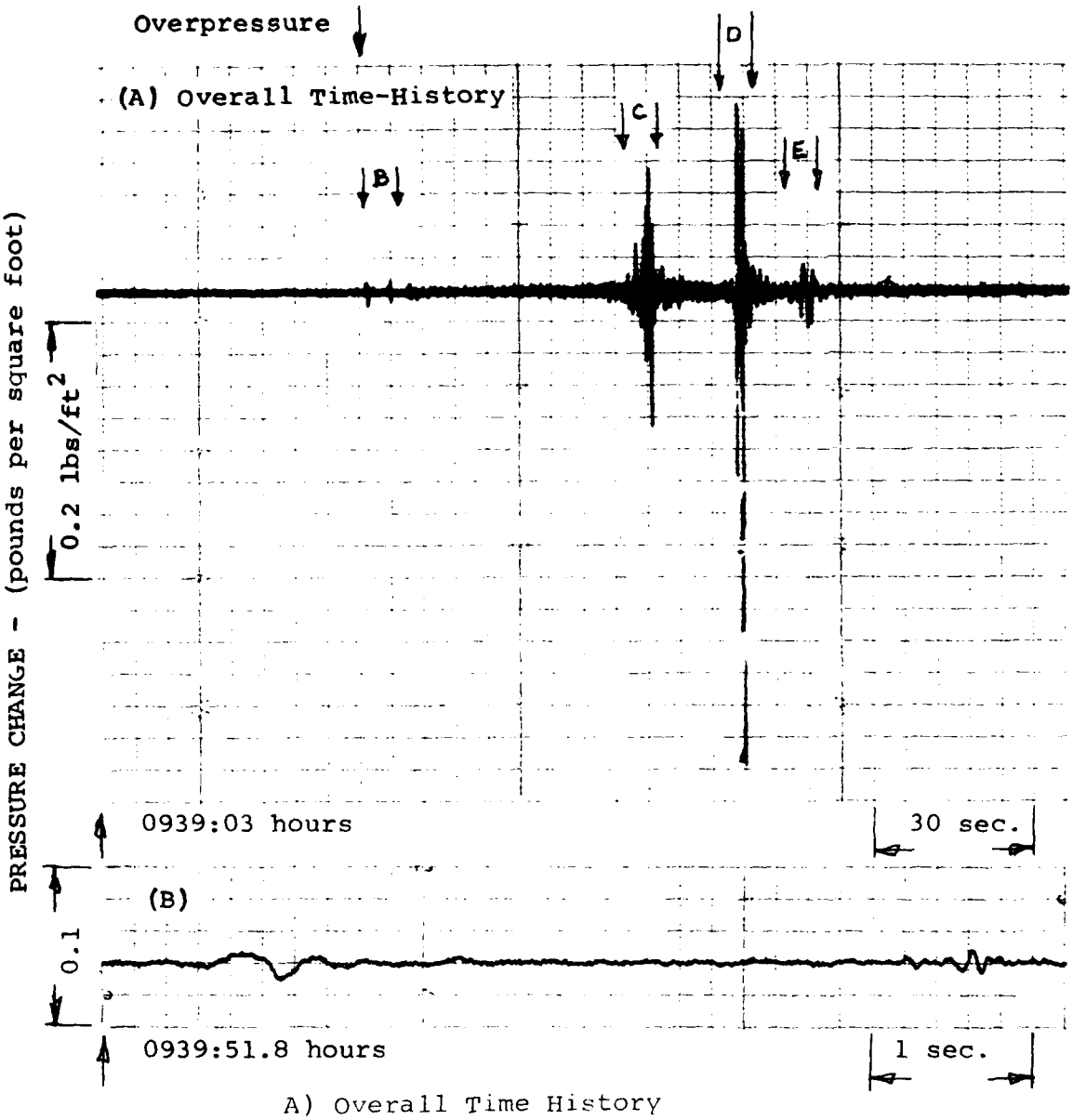

A) Overall Time History

B-E) Expanded Time-History Segments
B) 0939:51.8 - 0939:57.8
C) 0940:41.2 - 0940:47.2
D) 0940:59.6 - 0941:05.6
E) 0941:11.6 - 0941:17.6

FIGURE 33. EXPANDED PRESSURE TIME HISTORY MALDEN, MA - JULY 18, 1979 SOURCE: BRITISH AIRWAYS FLIGHT BA-171

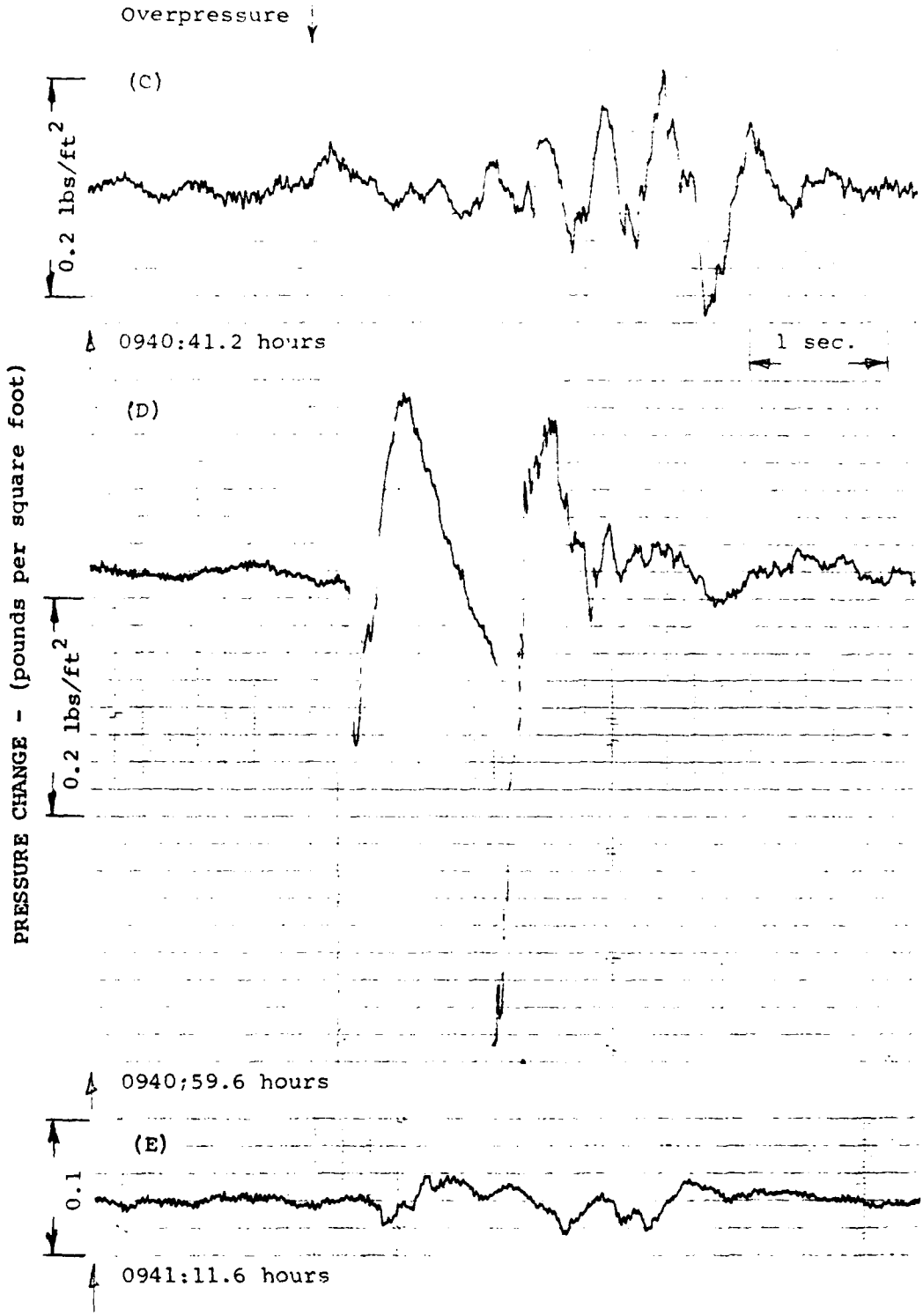

FIGURE 33. EXPANDED PRESSURE TIME HISTORY MALDEN, MA - JULY 18, 1979 SOURCE: BRITISH AIRWAYS FLIGHT BA-171 (CONT.)

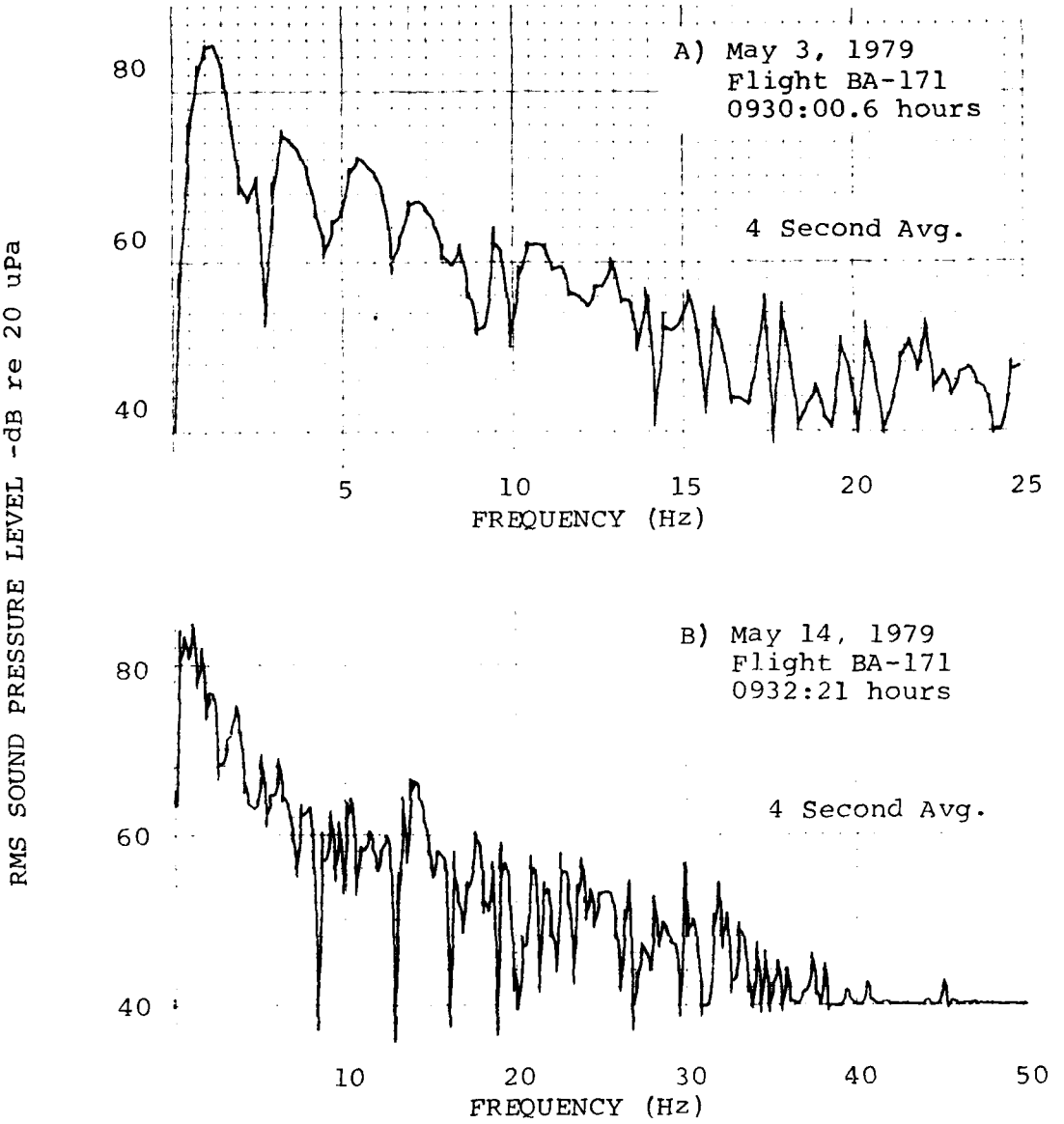

A) Source: British Airways Flight BA-171
May 3, 1979
B) Source: British Airways Flight BA-171
May 14, 1979

FIGURE 34. INFRASONIC FREQUENCY SPECTRA ACOUSTIC EVENT, MALDEN MA

(See Figure 28 for Pressure Time Histories)

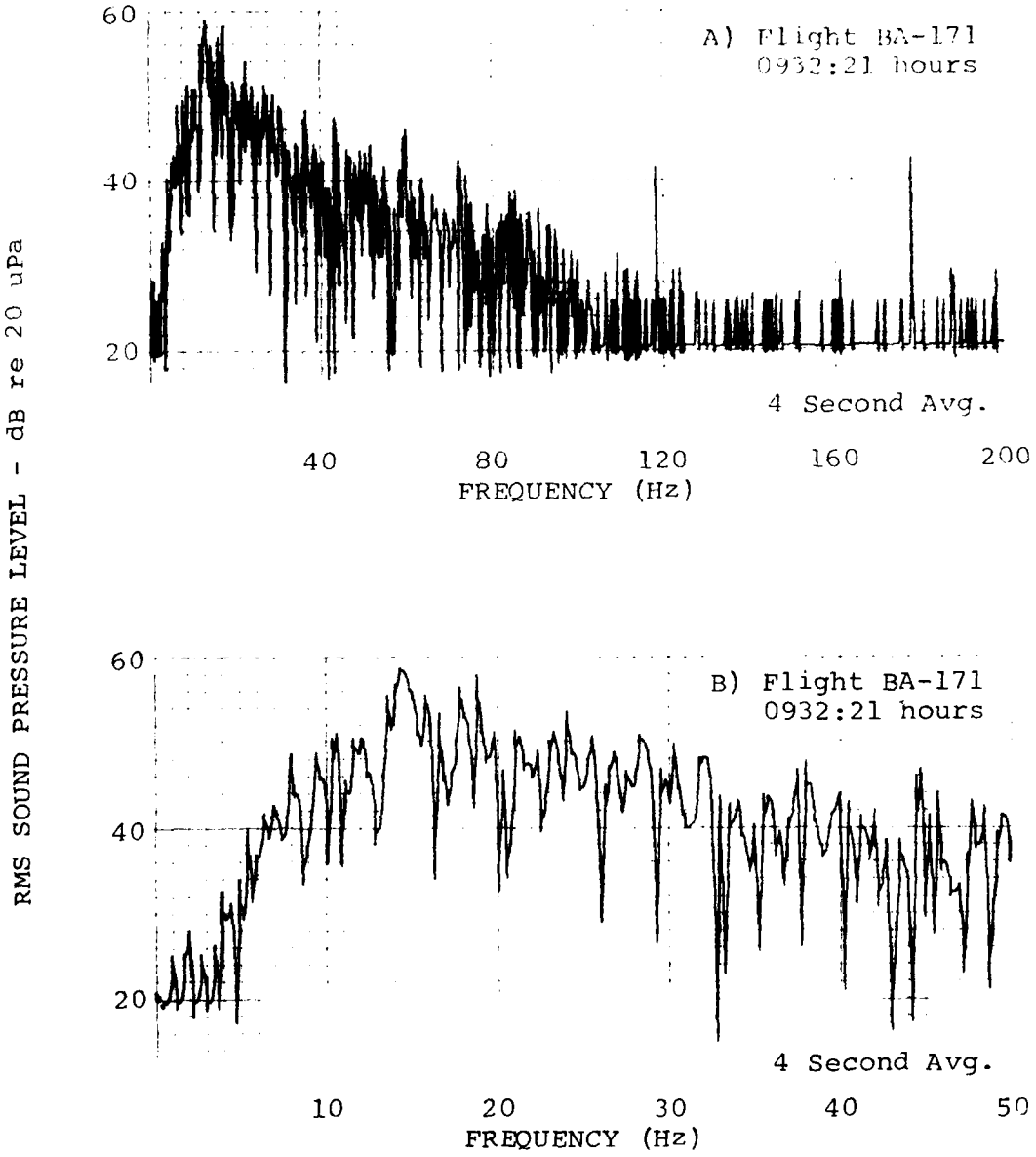

A) Source: British Airways Flight BA-171
B) Source: British Airways Flight BA-171

FIGURE 35. ACOUSTIC FREQUENCY SPECTRA ACOUSTIC EVENT, MALDEN MA MAY 14, 1979

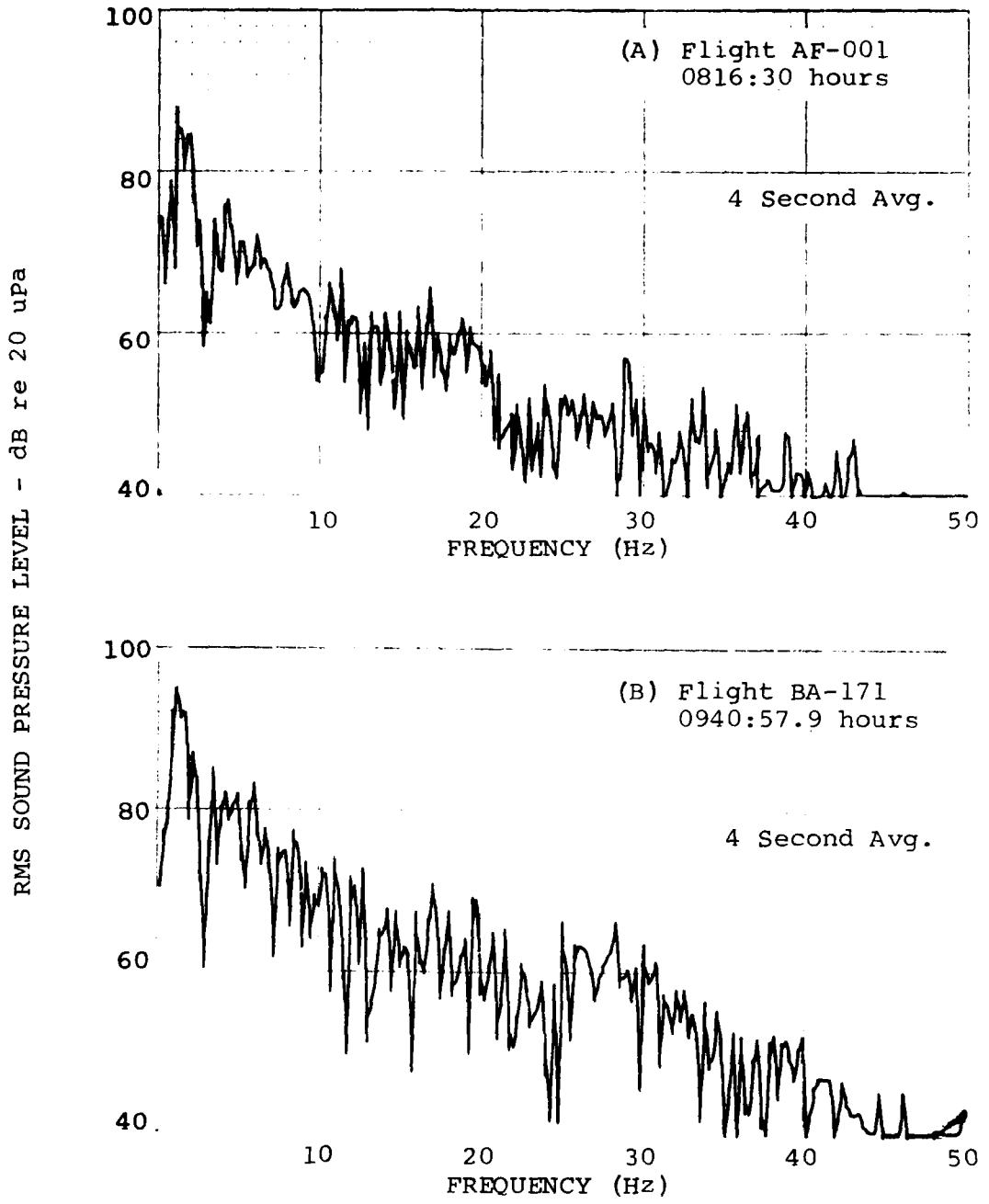

A) Source: Air France Flight AF-001
B) Source: British Airways Flight BA-171

FIGURE 36. INFRASONIC FREQUENCY SPECTRA ACOUSTIC EVENT, MALDEN MA JUNE 20, 1979

(See Figure 30 and 31 for Pressure Time Histories)

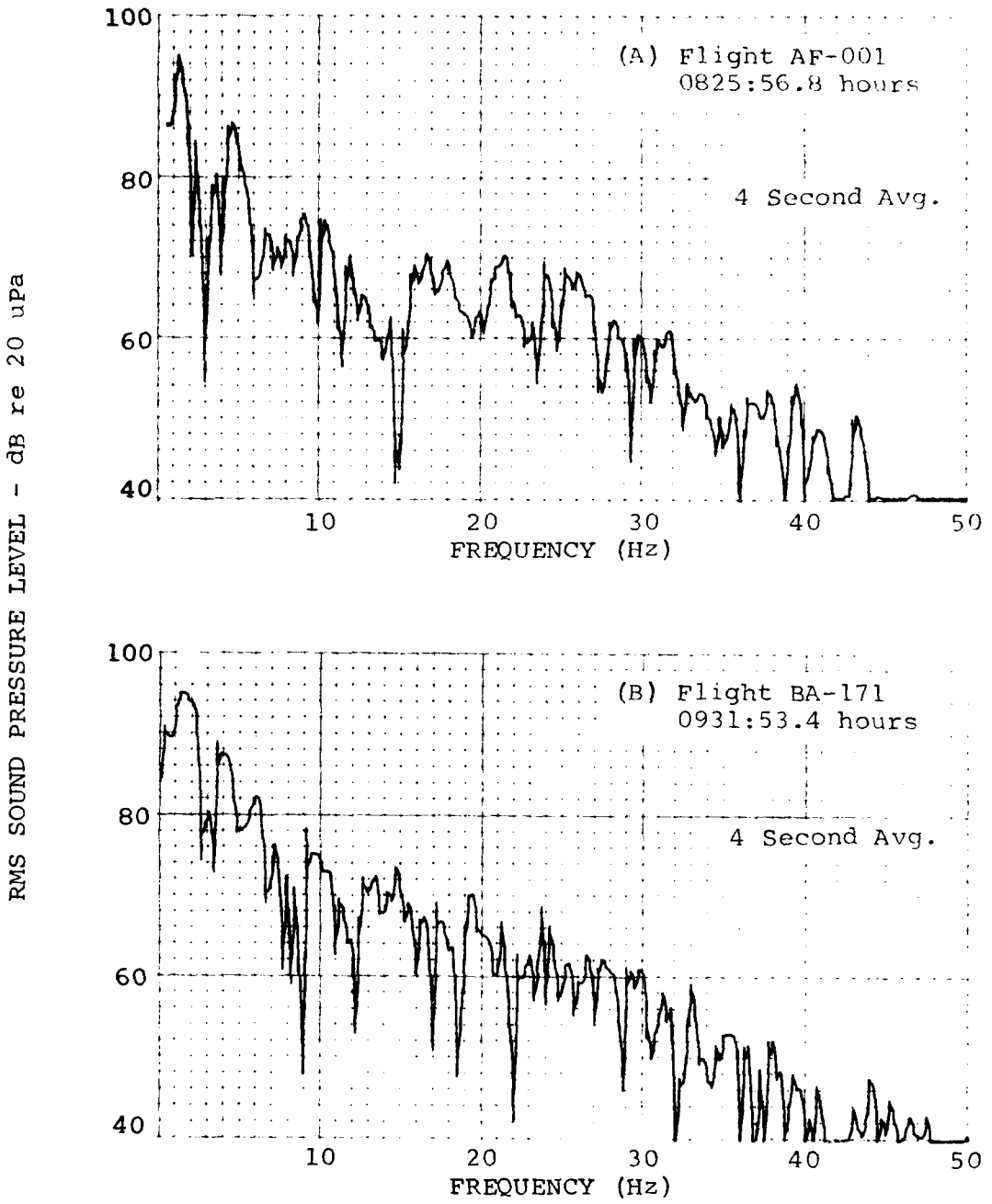

A) Source: Air France Flight AF-001
B) Source: British Airways Flight BA-171

FIGURE 37. INFRASONIC FREQUENCY SPECTRA ACOUSTIC EVENT, MALDEN MA JULY 11, 1979

(See Figure 9 for Pressure Time Histories)

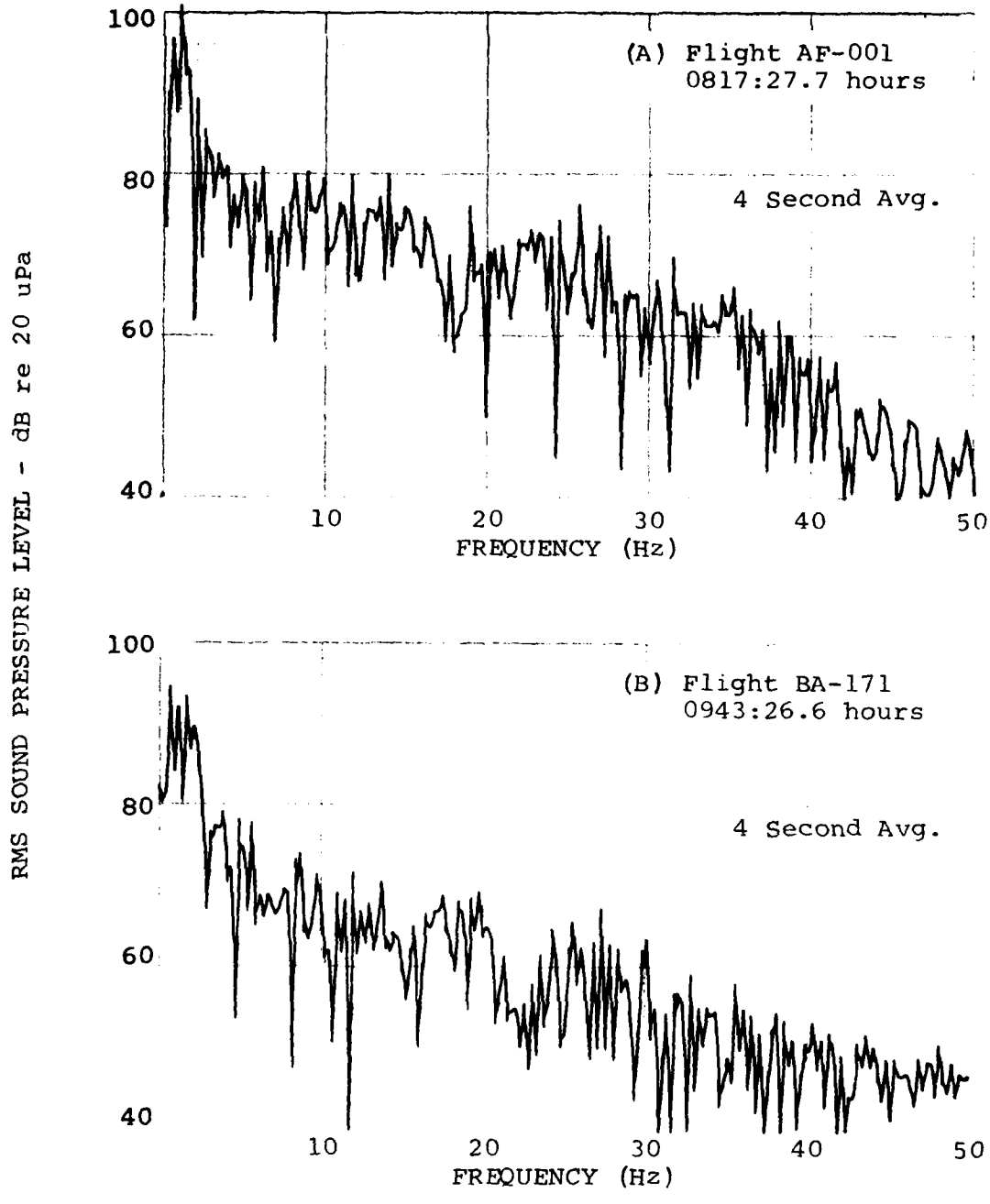

A) Source: Air France Flight AF-001
B) Source: British Airways BA-171

FIGURE 38. INFRASONIC FREQUENCY SPECTRA ACOUSTIC EVENT, MALDEN MA AUGUST 15, 1979

(See Figure 13 for Pressure Time Histories)

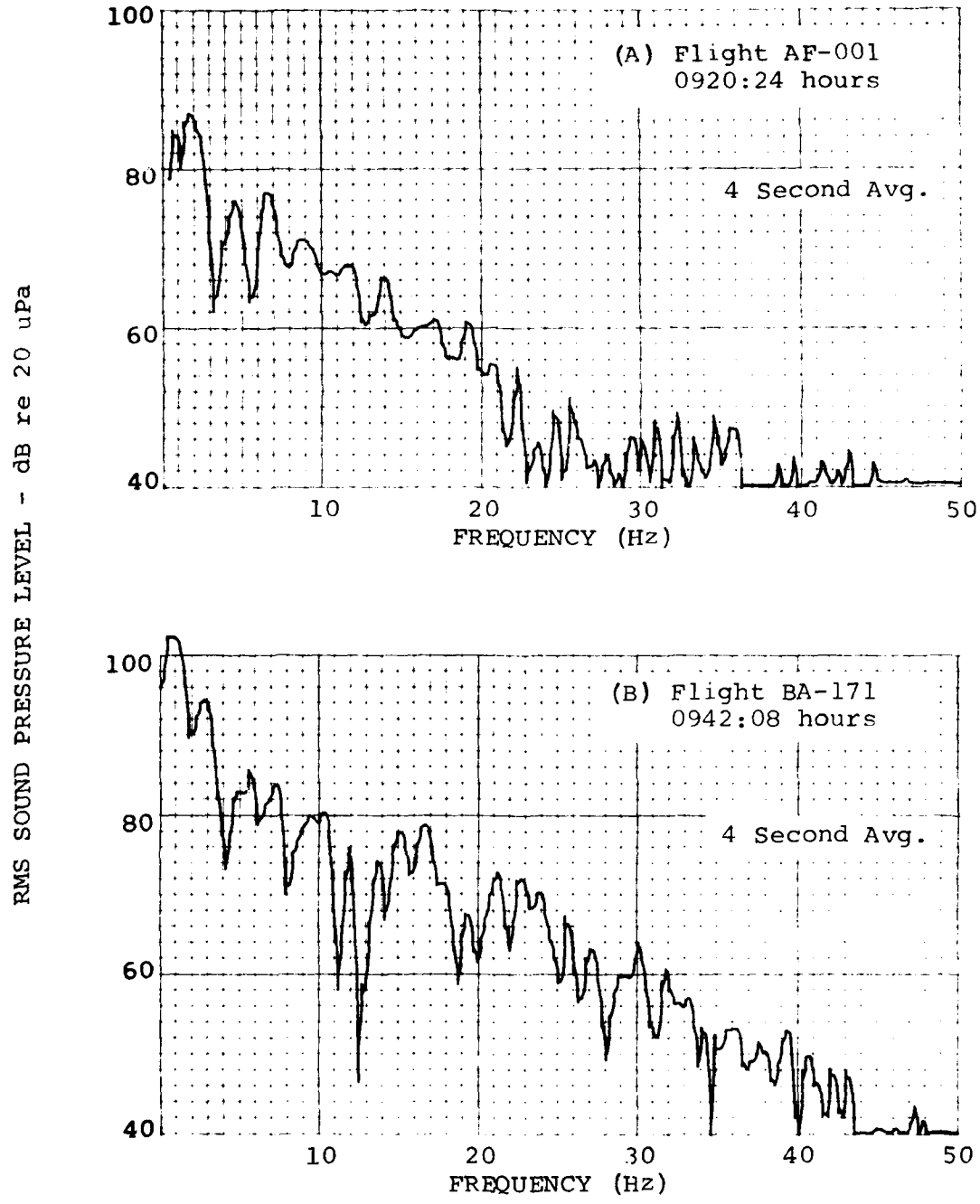

A) Source: Air France Flight AF-001
B) Source: British Airways Flight BA-171

FIGURE 39. INFRASONIC FREQUENCY SPECTRA ACOUSTIC EVENT, MALDEN MA SEPTEMBER 12, 1979

(See Figure 16 for Pressure Time Histories)

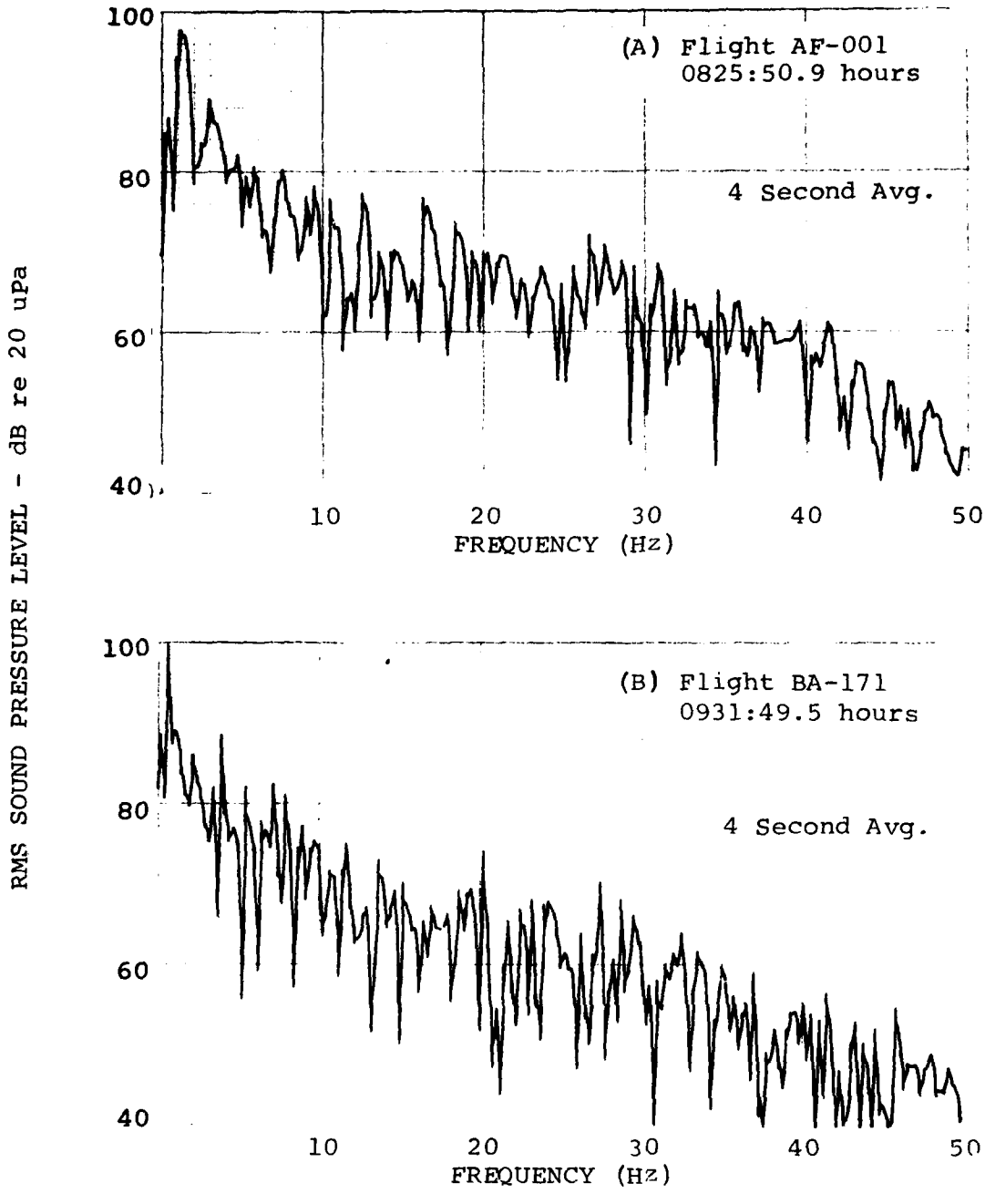

A) Source: Air France Flight AF-001
B) Source: British Airways Flight BA-171

FIGURE 40. INFRASONIC FREQUENCY SPECTRA ACOUSTIC EVENT, GEORGETOWN MA JULY 11, 1979

(See Figure 22 for Pressure Time Histories)

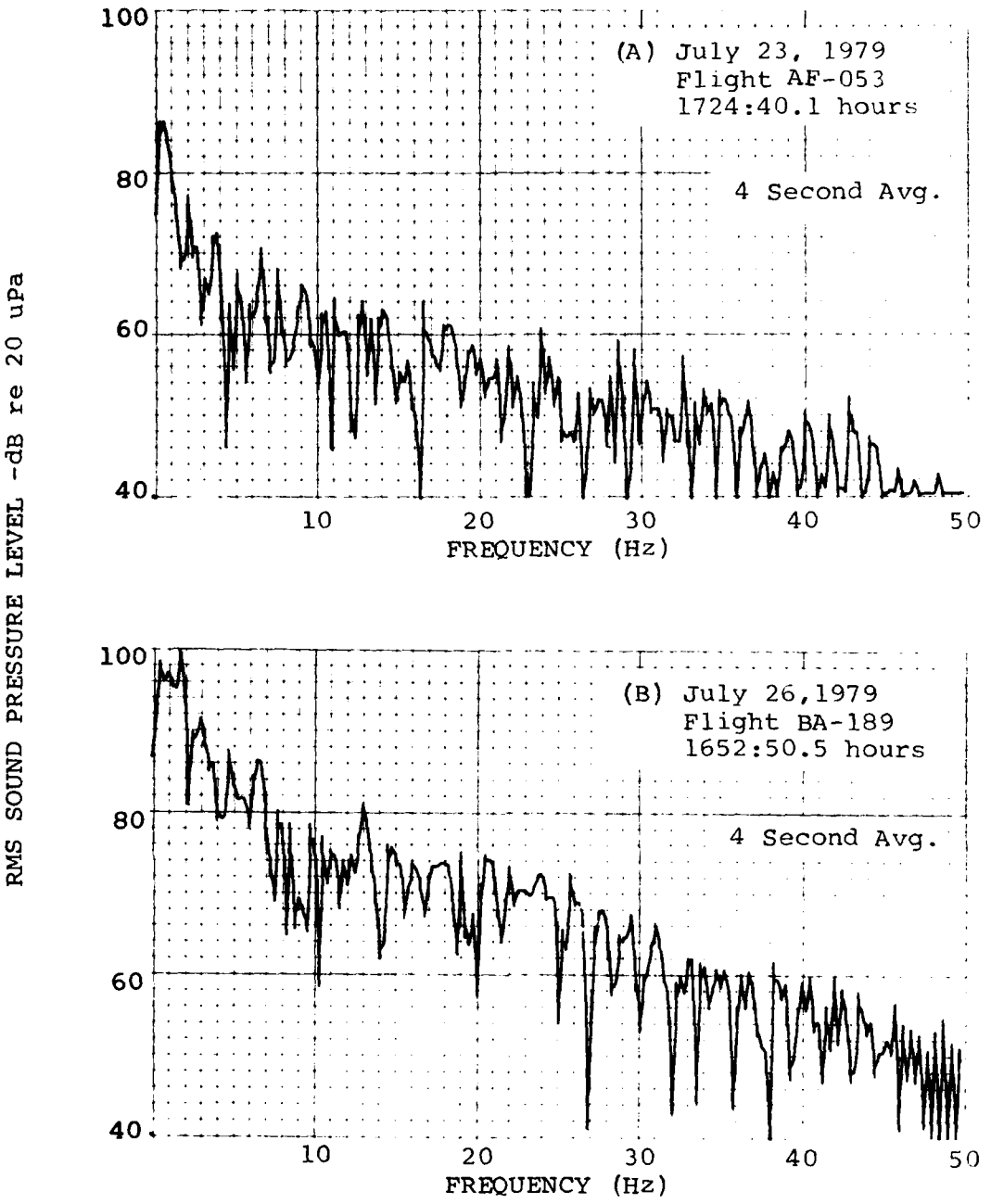

A) Source: Air France Flight AF-053
July 23, 1979

B) Source: British Airways Flight BA-189
July 26, 1979

FIGURE 41. INFRASONIC FREQUENCY SPECTRA ACOUSTIC EVENT, APPLEBACHSVILLE PA

(See Figures 25 and 26 for Pressure Time Histories

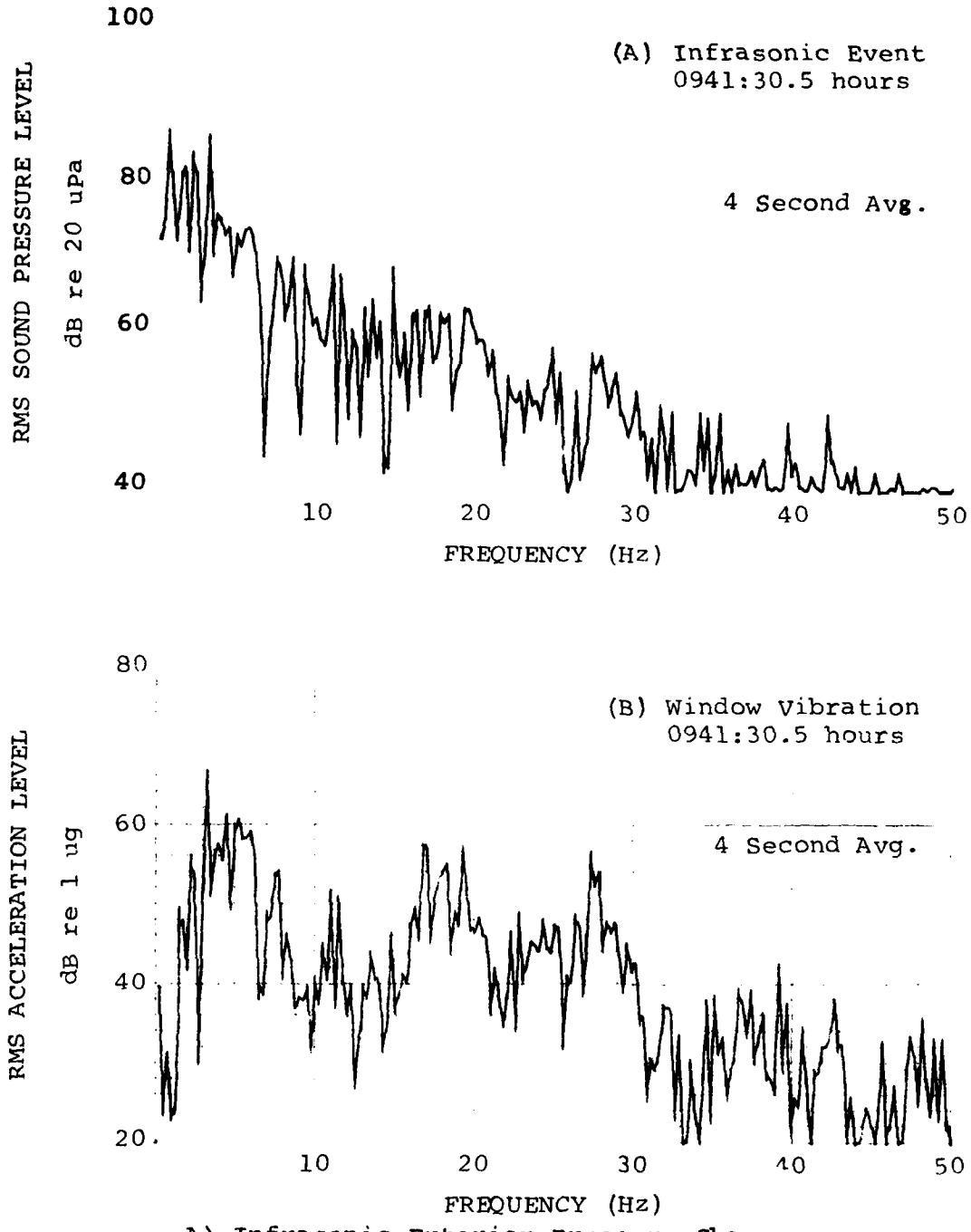

A) Infrasonic Exterior Pressure Change
B) Window Vibrational Acceleration

FIGURE 42. INFRASONIC FREQUENCY SPECTRA ACOUSTIC EVENT, WILMINGTON MA SOURCE: BRITISH AIRWAYS FLIGHT BA-171 JUNE 20, 1979

(See Figure 27 for Level Time Histories)

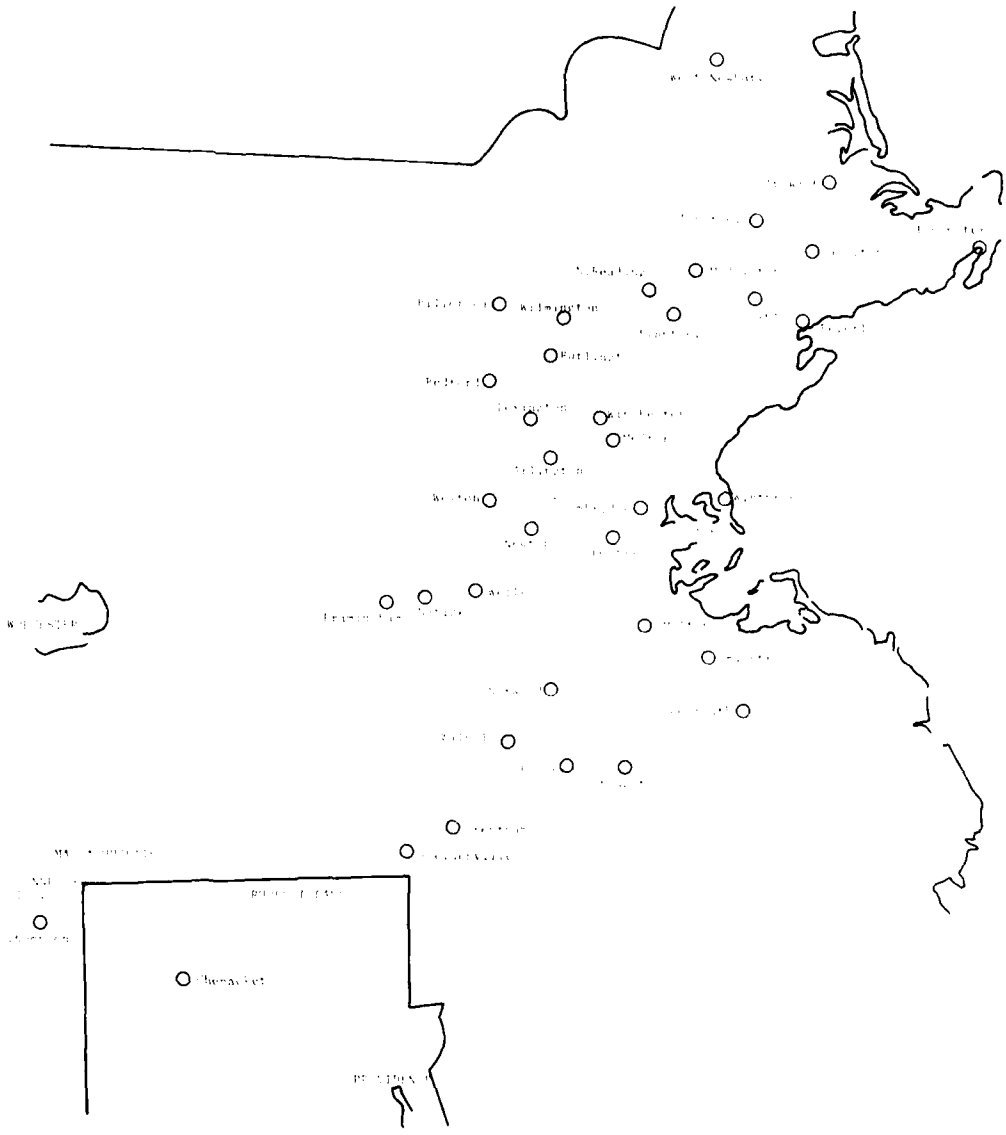

FIGURE 43. GEOGRAPHIC LOCATIONS OF SECONDARY SONIC BOOM REPORTS
Source: New England Region FAA

○ Reported events

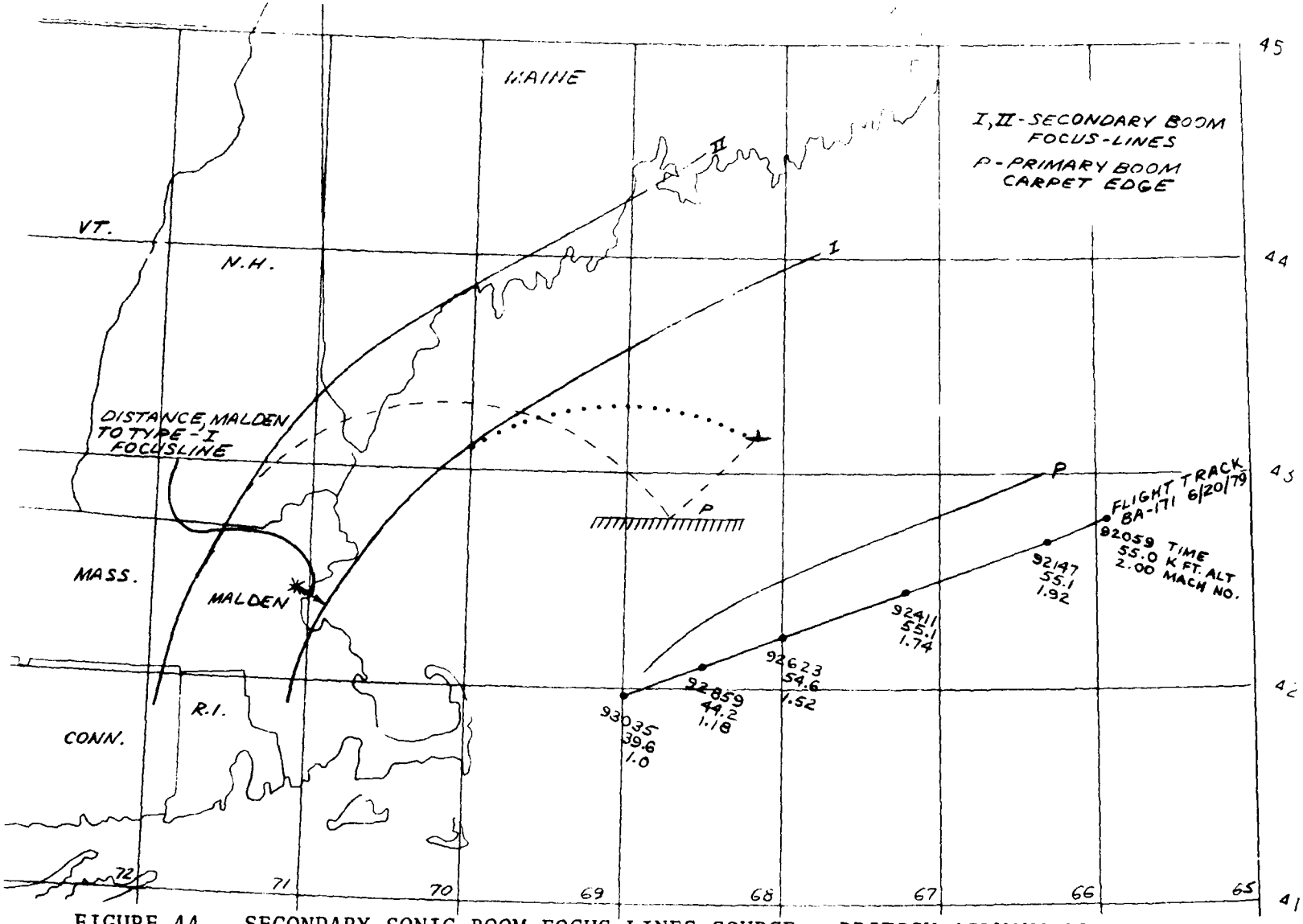

FIGURE 44. SECONDARY SONIC BOOM FOCUS-LINES SOURCE: BRITISH AIRWAYS FLIGHT BA-171 JUNE 20, 1979

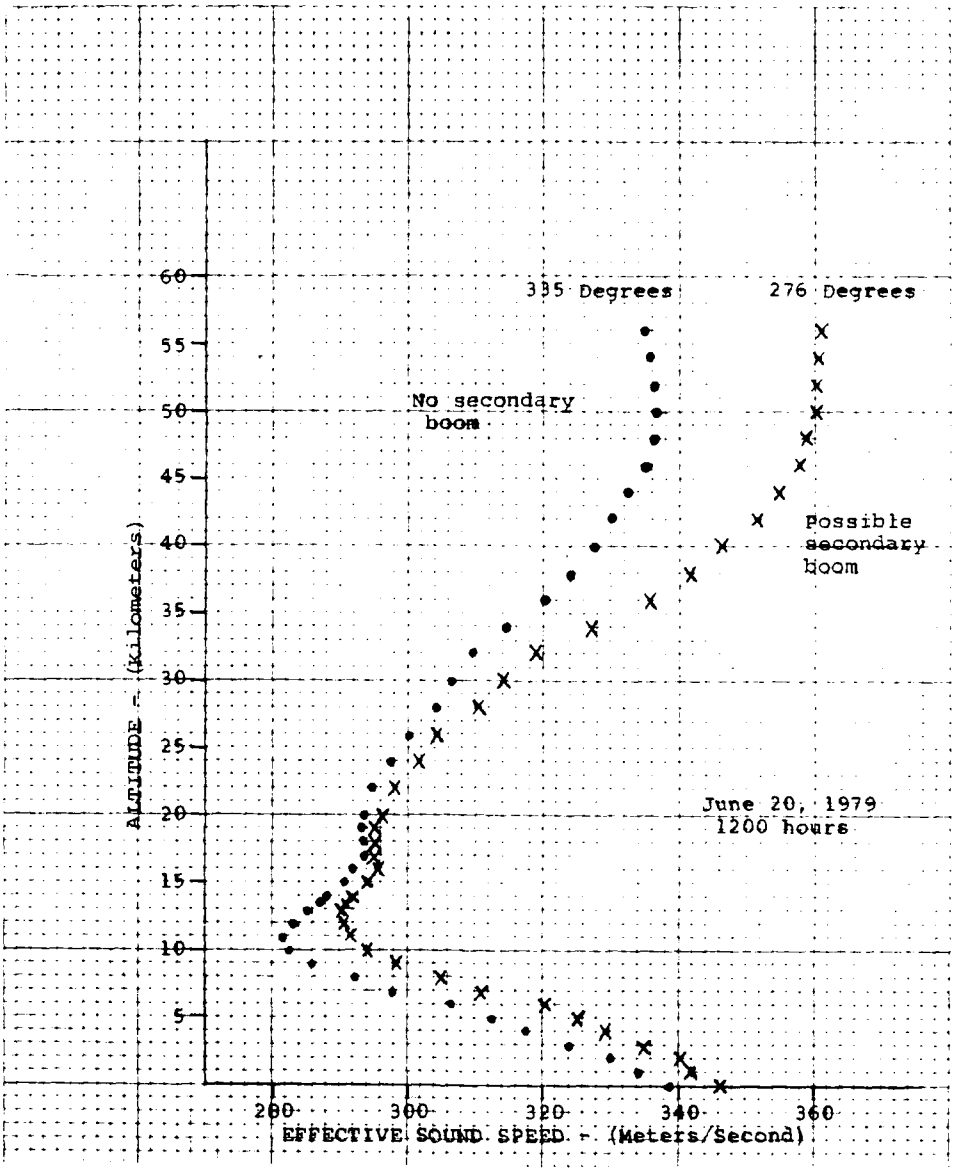

(x) Azimuth Angle 276 Degrees
(·) Azimuth Angle 335 Degrees

FIGURE 45. EFFECTIVE SOUND SPEED PROFILE BOSTON MA - JUNE 20, 1979
(See Figures 47, 48, and 49 for meteorological profiles)

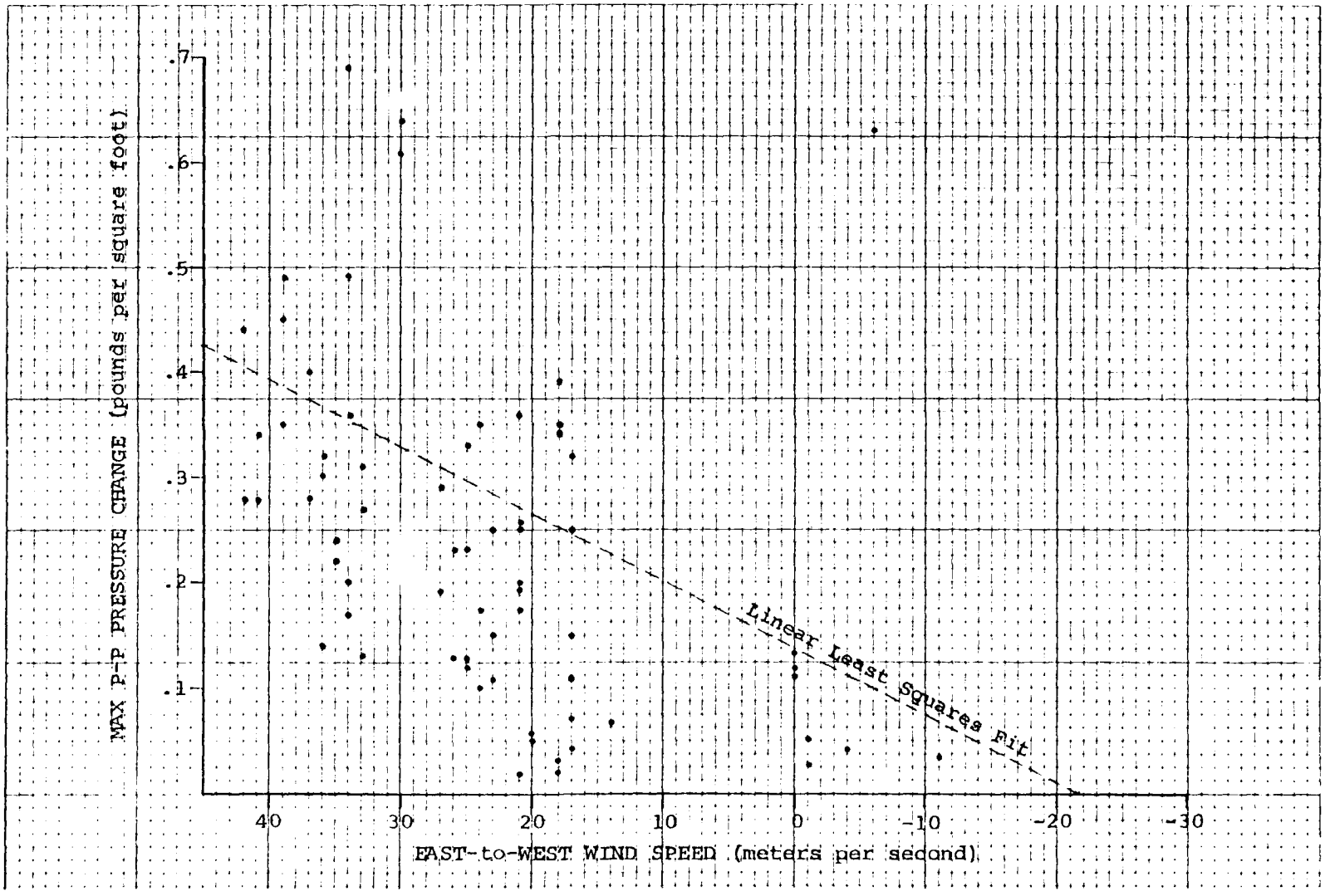

FIGURE 46. MAX PRESSURE CHANGE VERSUS E-W WIND SPEED ALTITUDE - 50 KILOMETERS MAY TO JUNE 1979

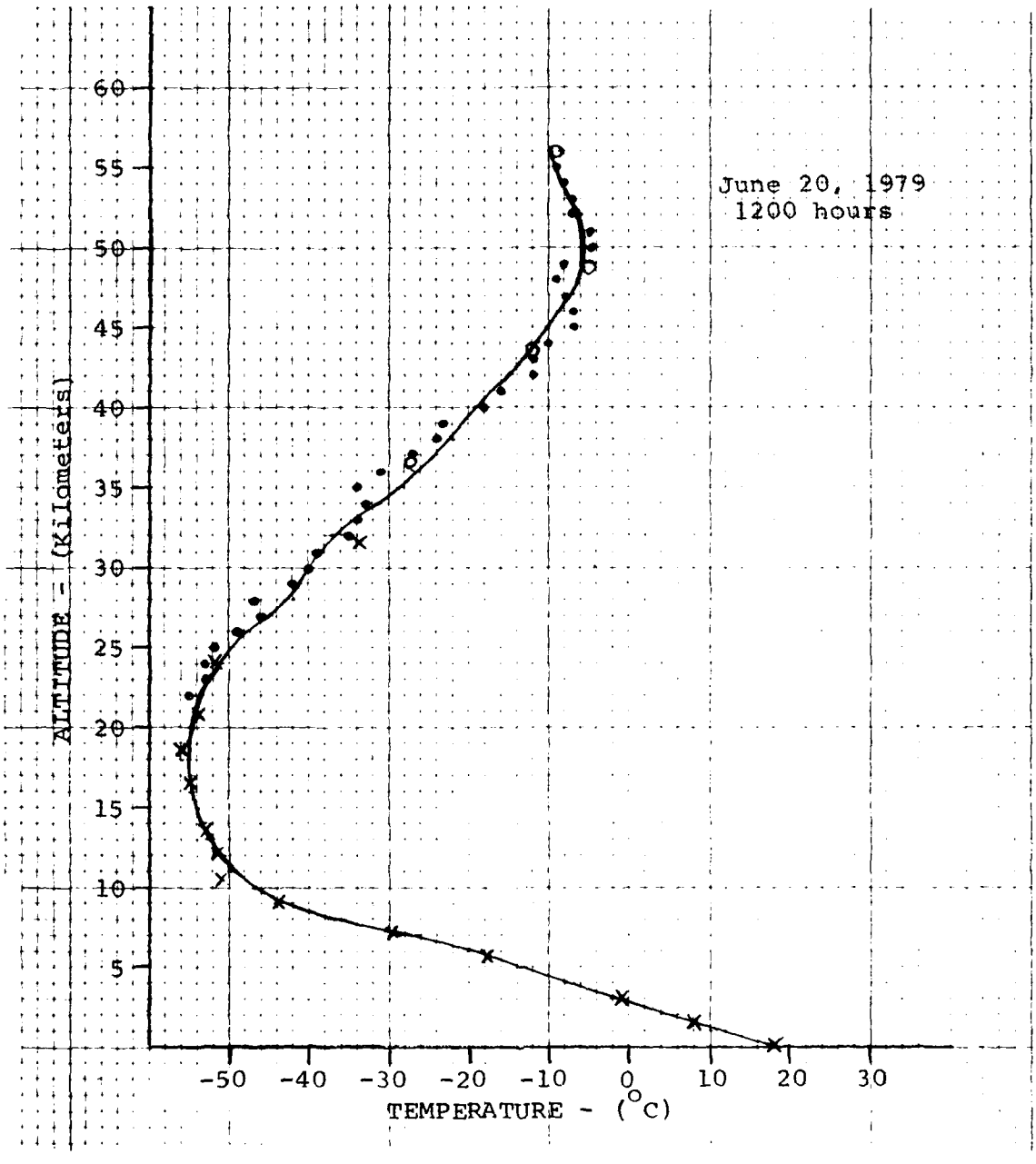

(•) Rocketsonde Data-Wallops Island, VA.
(x) Rawinsonde(Balloon borne) Data-Boston, MA.
(o) Satellite Radiance Data-Boston, MA.

FIGURE 47. TEMPERATURE PROFILE JUNE 20, 1979

AD-A088 160 TRANSPORTATION SYSTEMS CENTER CAMBRIDGE MA F/G 20/1
DETECTION AND ASSESSMENT OF SECONDARY SONIC BOOMS IN NEW ENGLAN--ETC(U)
MAY 80 E J RICKLEY, A D PIERCE
UNCLASSIFIED TSC-FAA-80-10 FAA-AEE-80-22 NL

2 OF 2
AD A088 160

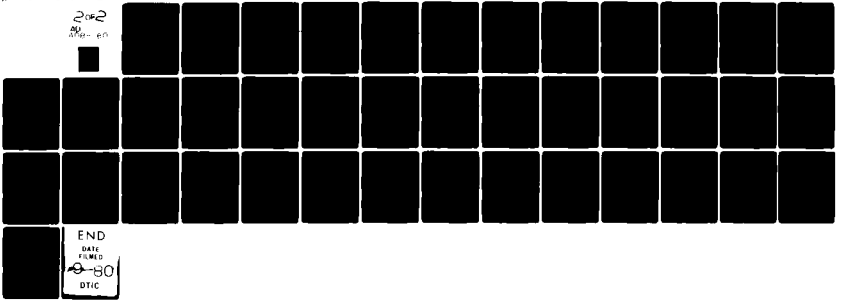

END
DATE FILMED
9-80
DTIC

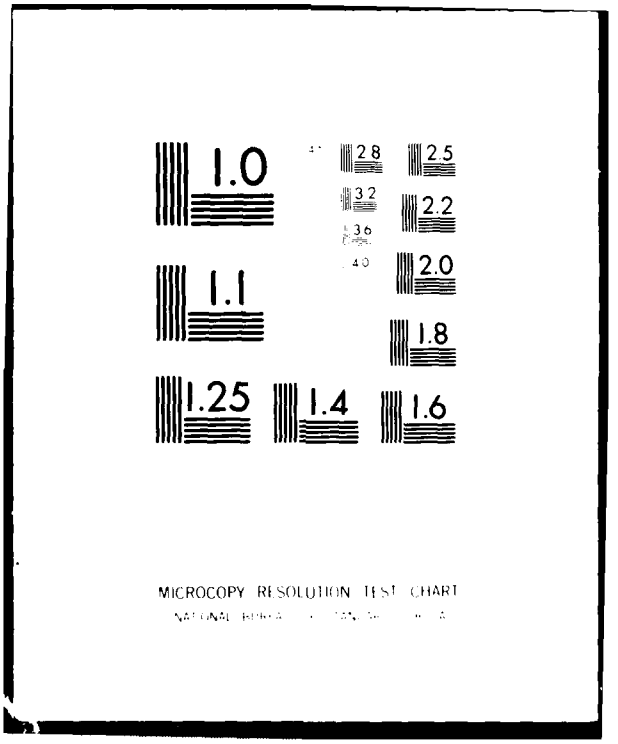
1.0
2.8
2.5
3.2
2.2
3.6
4.0
2.0
1.1
1.8
1.25
1.4
1.6
MICROCOPY RESOLUTION TEST CHART

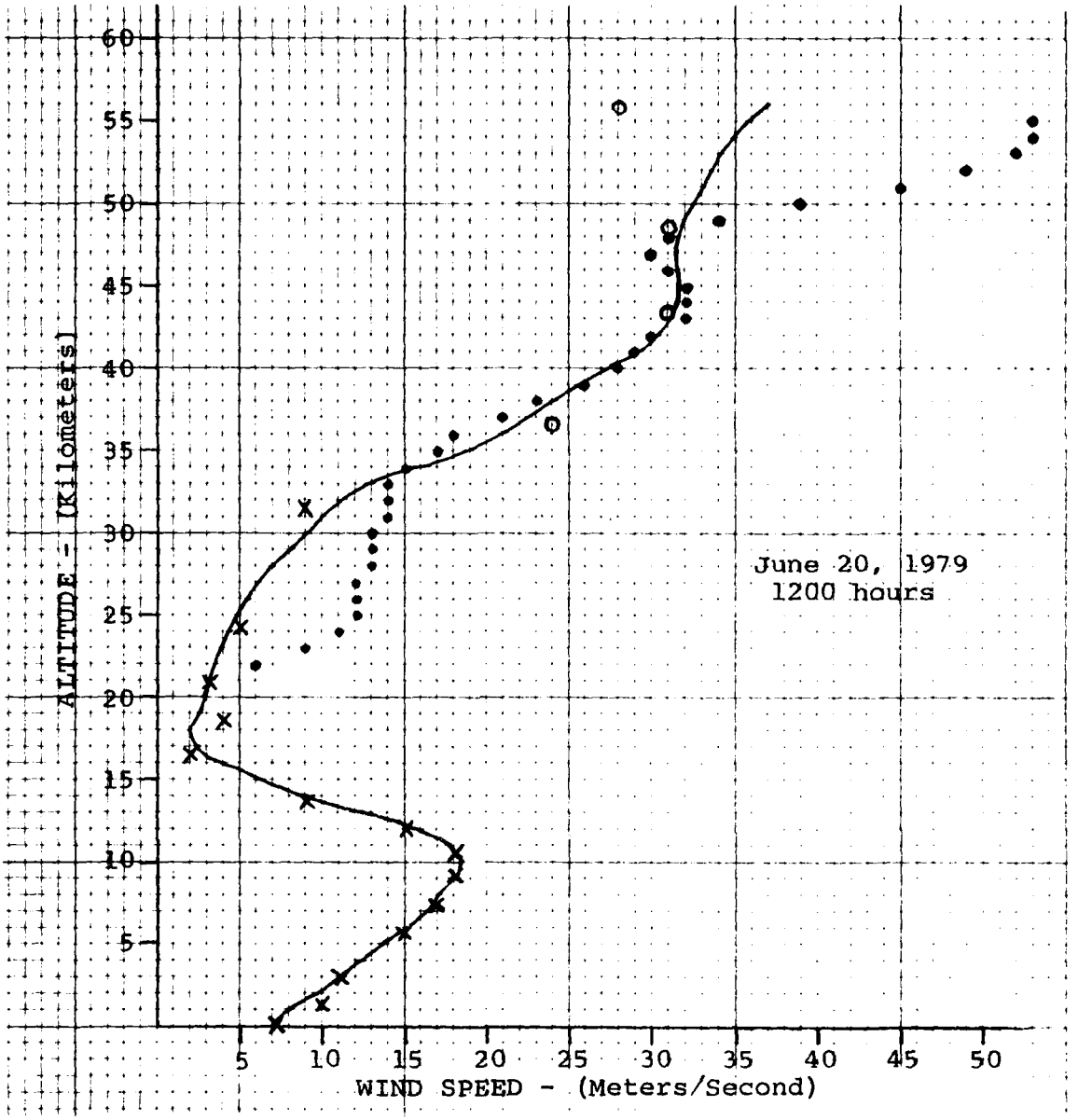

(•) Rocketsonde Data-Wallops Island, VA.
(x) Rawinsonde(Balloon borne)Data-Boston, MA.
(o) Satellite Radiance Data-Boston, MA.

FIGURE 48. WIND SPEED PROFILE JUNE 20, 1979

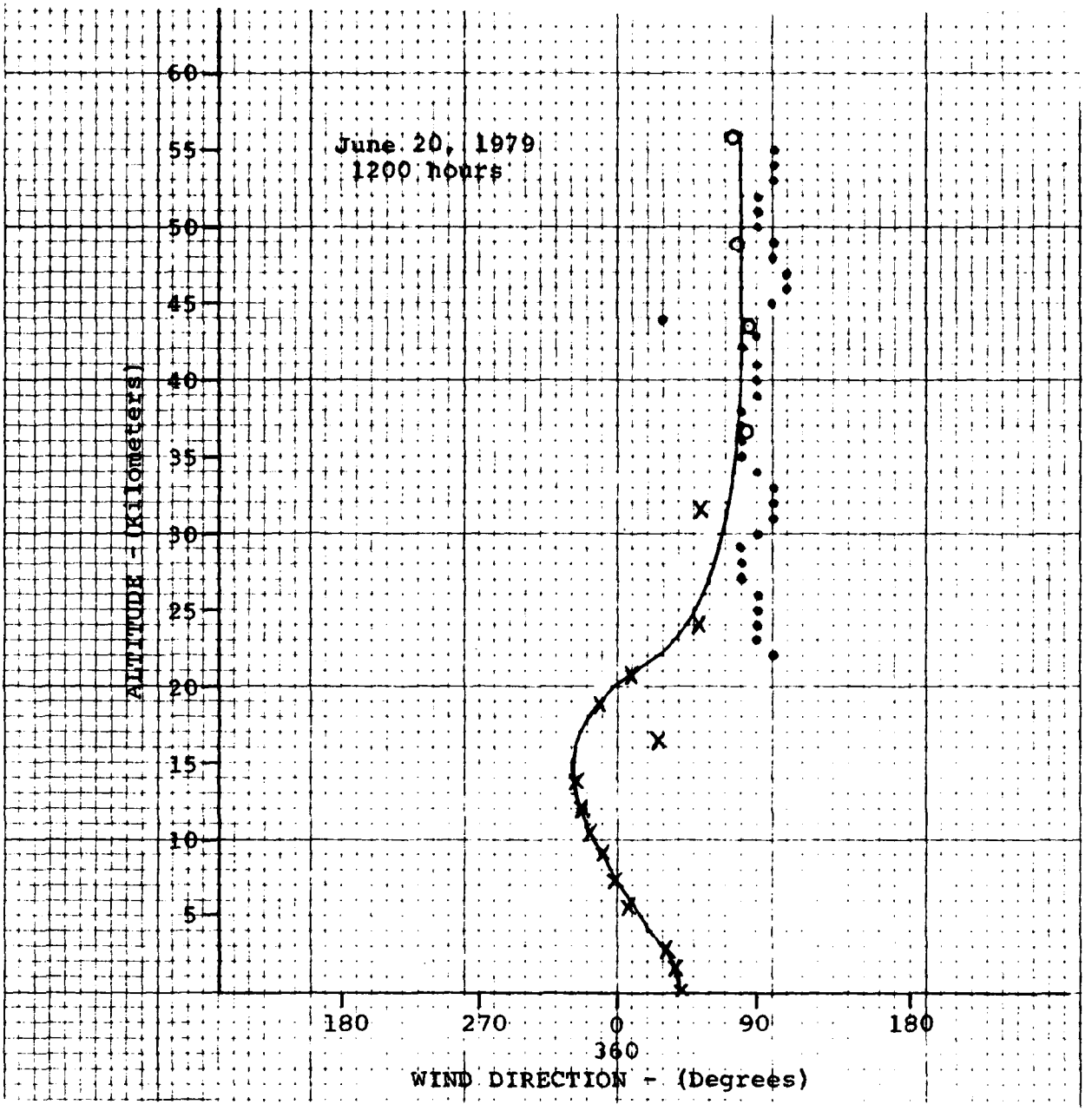

(•) Rocketsonde Data-Wallops Island, VA.
(x) Rawinsonde(Balloon borne)Data-Boston, MA.
(o) Satellite Radiance Data-Boston, MA.

FIGURE 49. WIND DIRECTION PROFILE JUNE 20, 1979

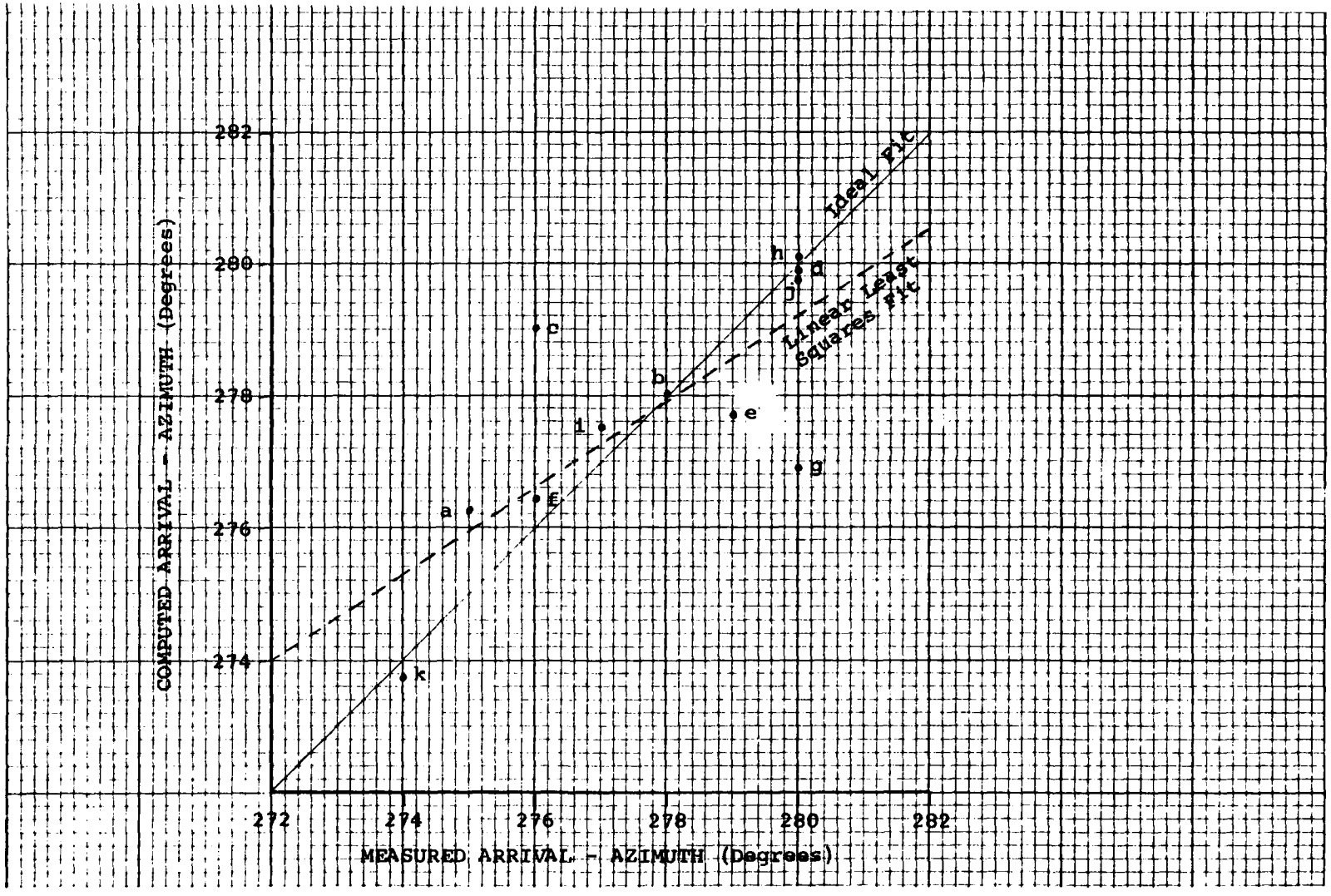

FIGURE 50. COMPUTED VERSUS MEASURED ARRIVAL RAY AZIMUTH ANGLES MALDEN MA (42°26'34"N, 71°05'07"W)
(See Table 4 for event a-m Identification)

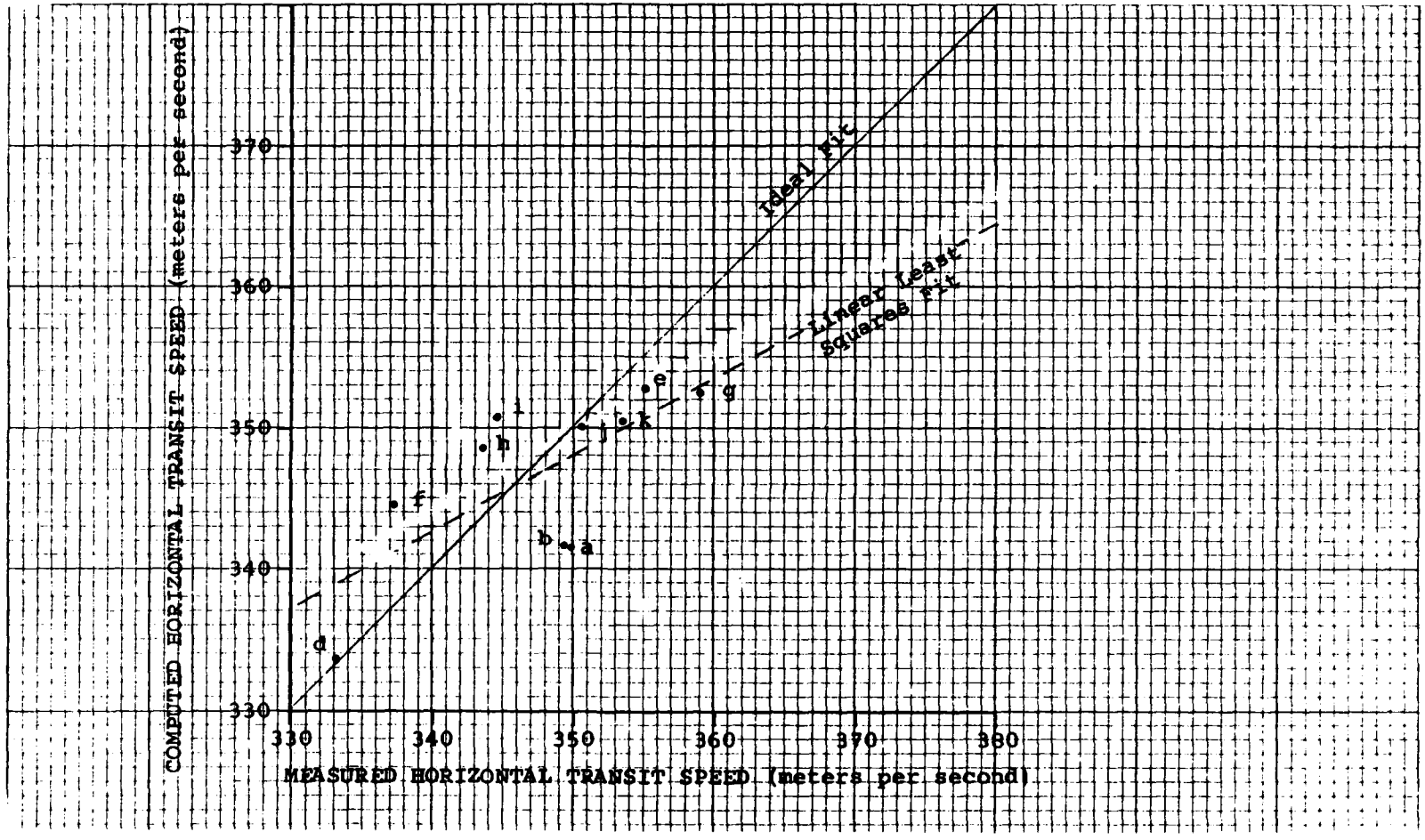

FIGURE 51. COMPUTED VERSUS MEASURED HORIZONTAL TRANSIT SPEED MALDEN MA

(See Table 4 for event a-m identification)

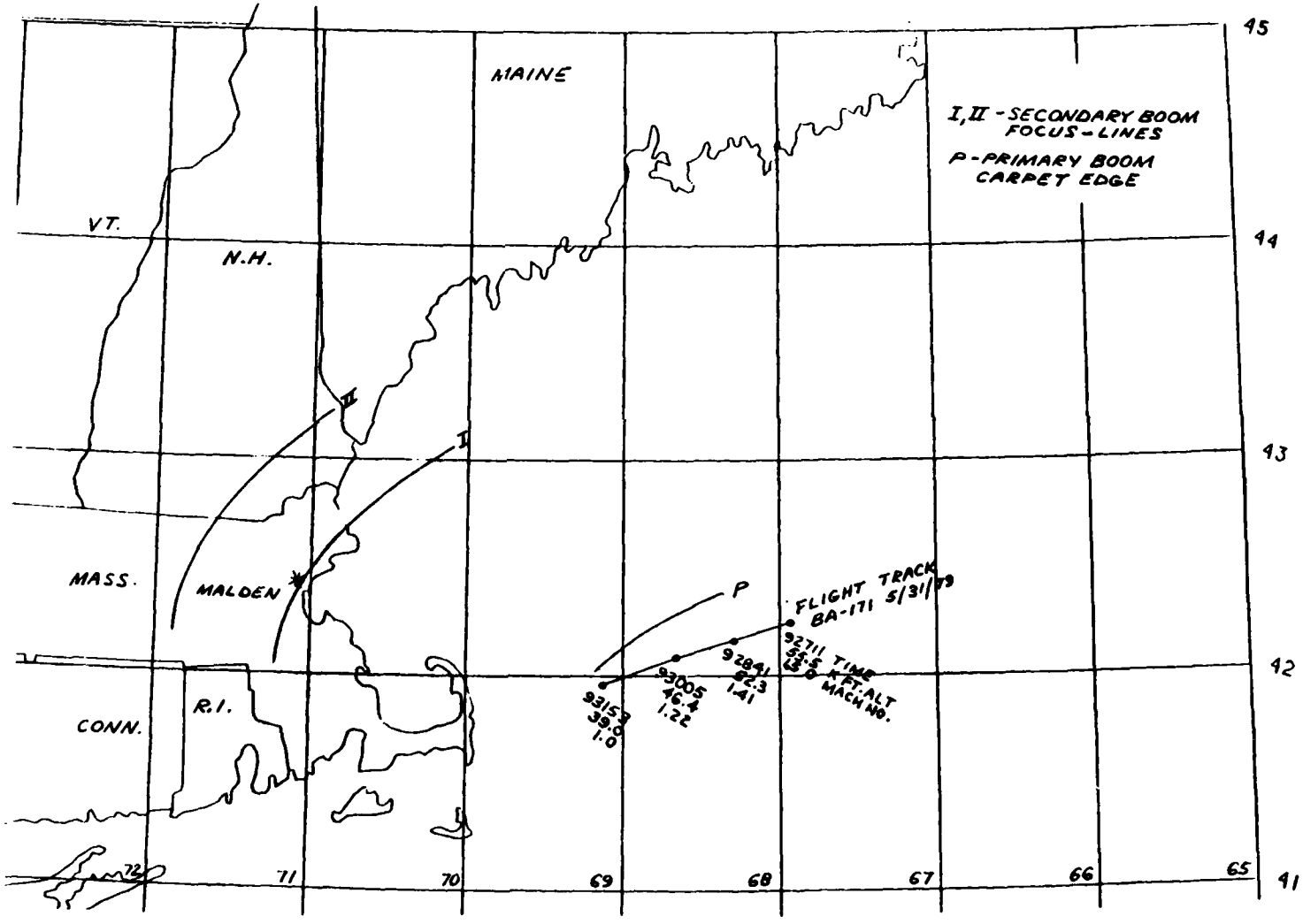

FIGURE 52. SECONDARY SONIC BOOM FOCUS-LINES SOURCE: BRITISH AIRWAYS FLIGHT BA-171 MAY 31, 1979

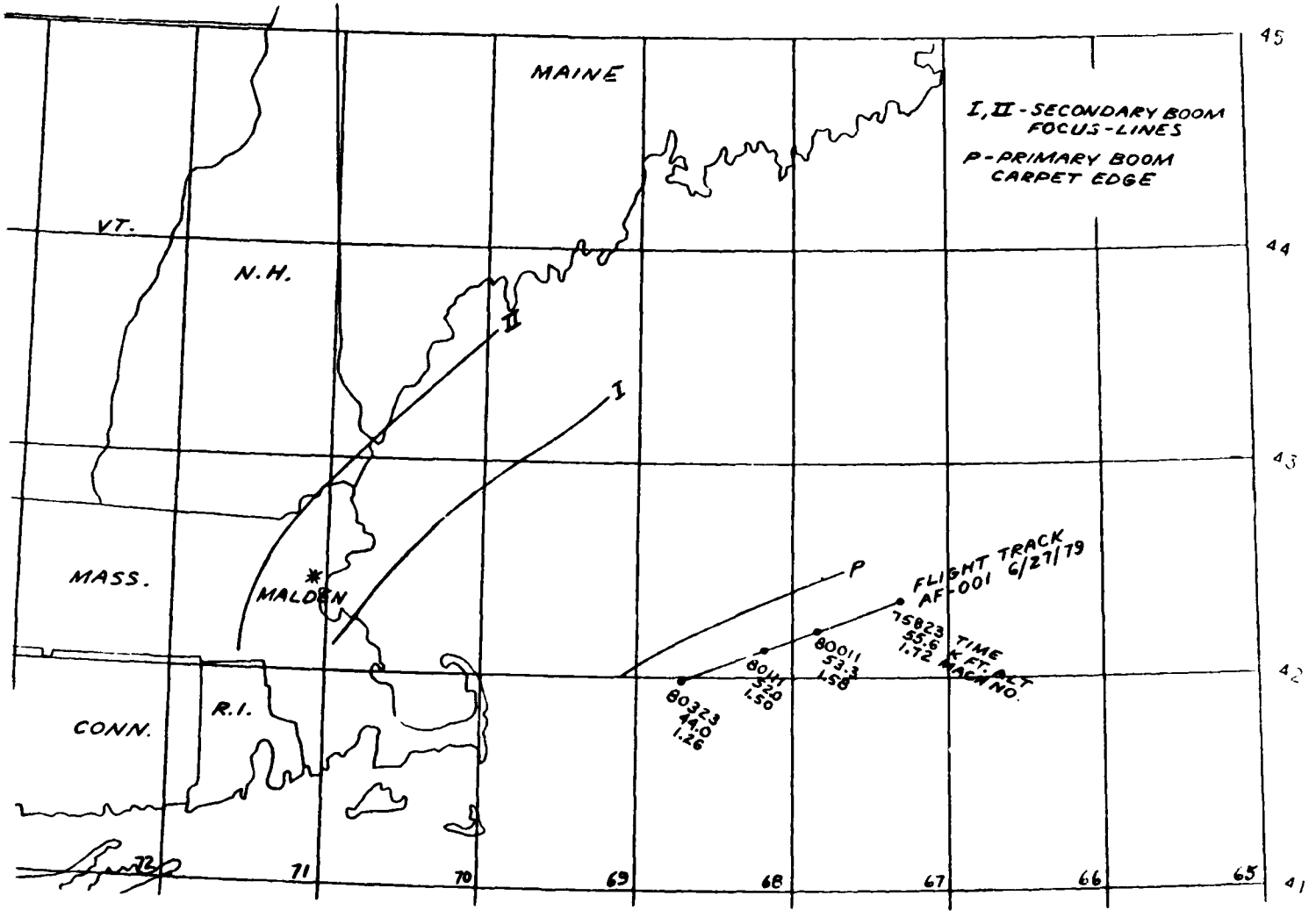

FIGURE 53. SECONDARY SONIC BOOM FOCUS-LINES SOURCE: AIR FRANCE FLIGHT AF-001 JUNE 27, 1979

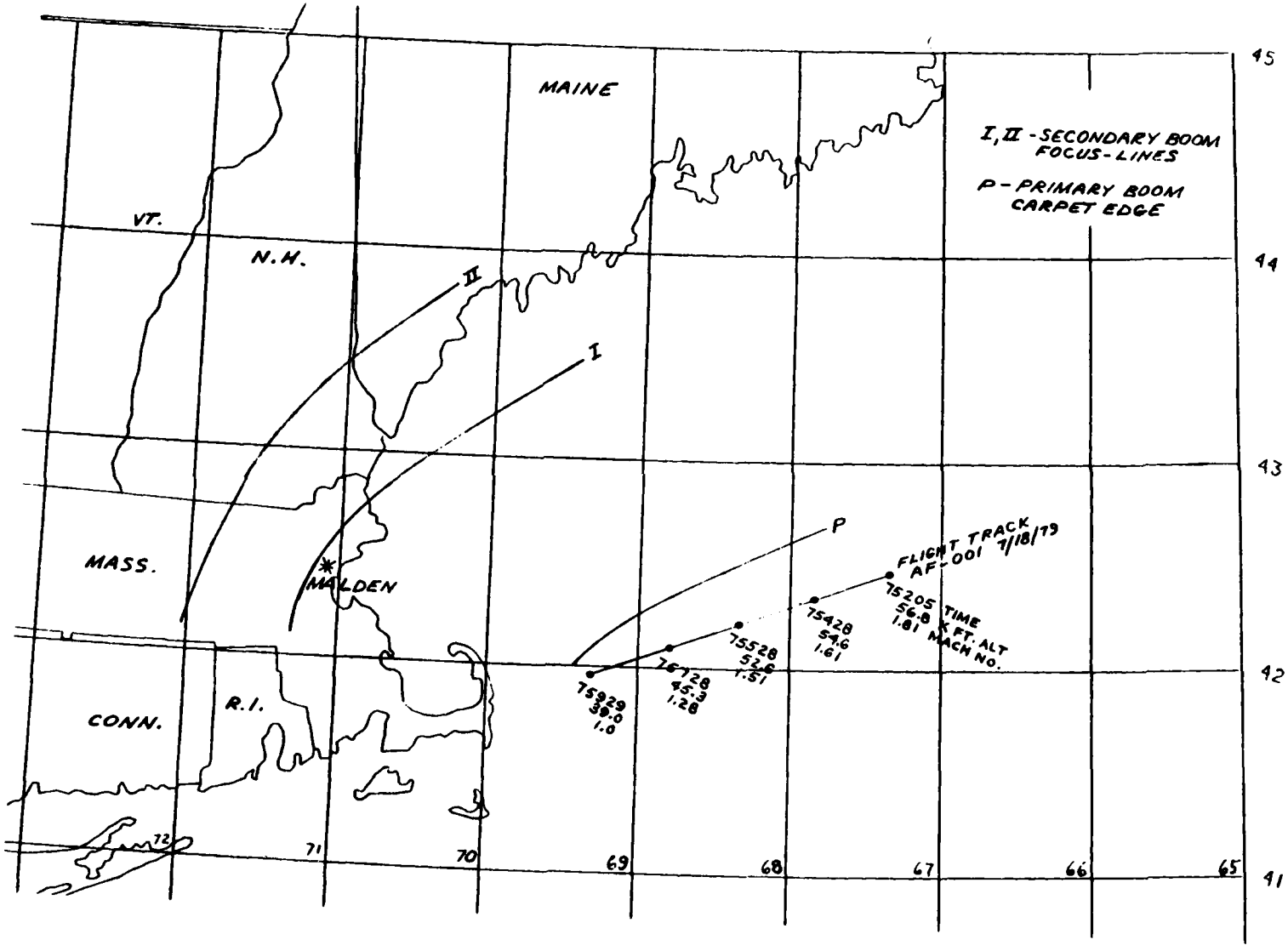

FIGURE 54. SECONDARY SONIC BOOM FOCUS-LINES SOURCE: AIR FRANCE FLIGHT AF-001 JULY 18, 1979

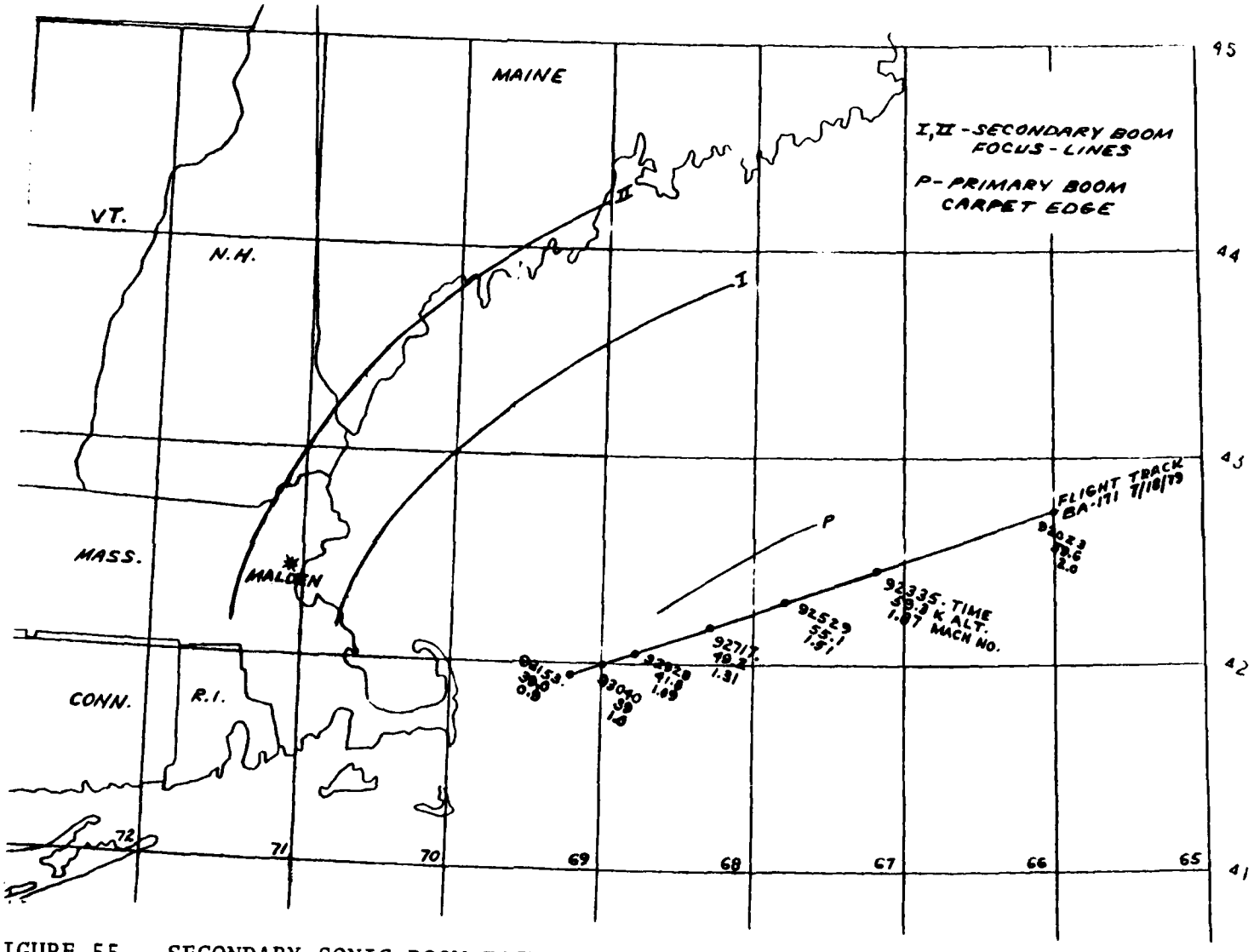

FIGURE 55. SECONDARY SONIC BOOM FOCUS-LINE SOURCE: BRITISH AIRWAYS FLIGHT BA-171 JULY 18, 1979

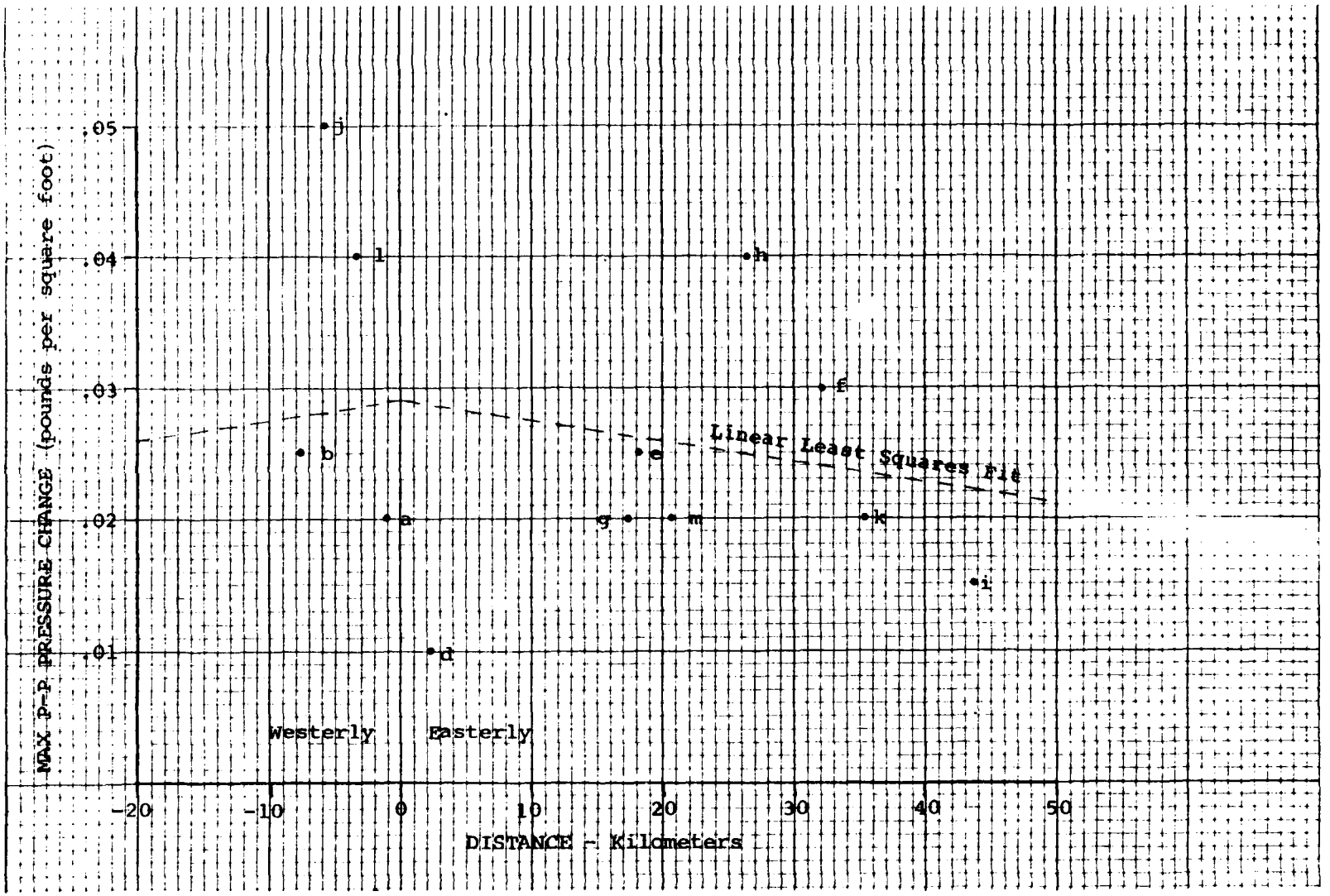

FIGURE 56. MAX PRESSURE CHANGE VERSUS DISTANCE MALDEN MA TO TYPE 1 SECONDARY BOOM FOCUS-LINE

(See Table 3 for event a-m identification)

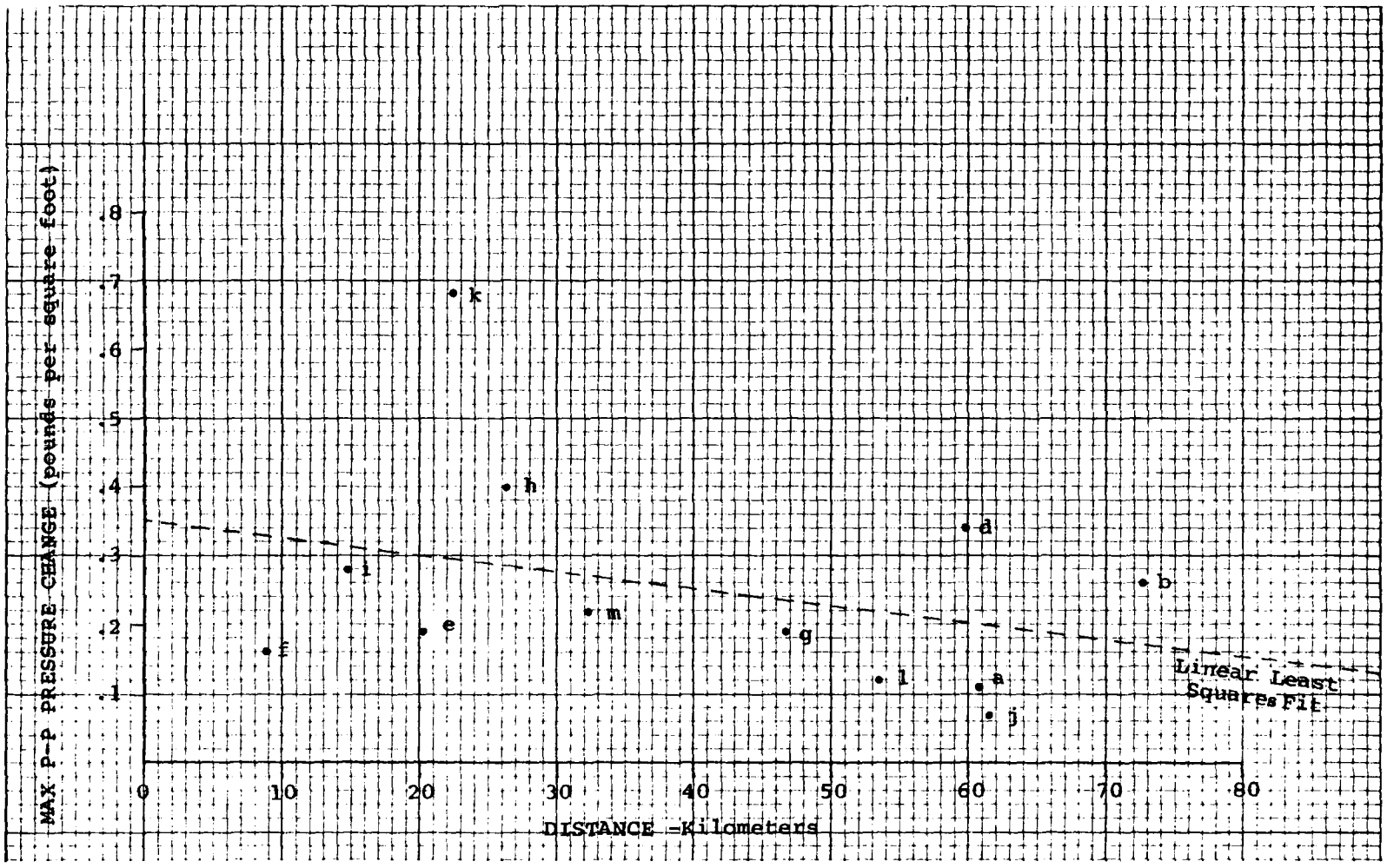

FIGURE 57. MAX PRESSURE CHANGE VERSUS DISTANCE MALDEN MA TO TYPE II SECONDARY BOOM FOCUS-LINE

(See Table 3 for event a-m identification)

TABLE 1
SECONDARY SONIC BOOM DETECTION
MALDEN MA (42°26'34"N, 71°05'07"W)

Date 1979	Time E.D.S.T.	Max. Pres. Change Peak to Peak lbs/ft^2	Arriving Ray Azimuth degrees(1)	Arriving Ray Elevation degrees	Elapsed Time(2) Seconds	Flight No.	Heard by Field Technicians	Meas. SPL dBA
May 3	0930:00.6	0.081	279	8	(3)	BA-171	No	
4	0938:37.7	0.033	281	10	(3)	BA-171	No	
7	0931:10.7	0.12	281	6	259.7	BA-171	Yes	
8	0933:31.3	0.13	279	7	256.3	BA-171	Yes	
9	0929:02.7	0.63	280	7	287.7	BA-171	Yes	
10	0931:21.5	0.13	278	10	255.0	BA-171	Yes	
11			No measurements made					
14	0932:21	0.12	278	16	253.0	BA-171	Yes	46
15	0937:57.5	0.041	278	28	314.5	BA-171	No	
16	0930		No measurable signal			BA-171	No	
17	0934:19	0.055	278	19	(3)	BA-171	No	
18	0813:55	0.027	280	29	(3)	AF-001	No	
18	0932:23	0.027	276	19	(3)	BA-171	No	
21	0753:30		Not recorded on tape		(3)	BA-173	Yes	
21	0823:09	0.072	281	17	(3)	AF-001	No	
21	0930:34.8	0.049	-	-	(3)	BA-171	No	
22	0743:55.5	0.25	278	10	241.5	BA-173	Yes	48
22	0819:44	0.19	278	11	240.0	AF-001	Yes	
22	0931:08.8	0.17	278	16	243.8	BA-171	Yes	
23	0820:43.6	0.10	279	19	283.6	AF-001	No	
23	0941:08.6	0.11	275	19	233.6	BA-171	Yes	52
24	0740:55.6	0.15	276	15	260.6	BA-173	Yes	
24	0821:05.3	0.07	280	14	(3)	AF-001	Yes	
24	0933:35	0.04	276	17	290.0	BA-171	No	
25	0819:56	0.02	271	24	(3)	AF-001	No	
25	0937:45	0.03	276	15	220.0	BA-171	No	
29	0830:55.1	0.36	282	10	265.1	AF-001	Yes	
29	0848:03.5	0.26	276	4	213.5	BA-173	Yes	
29	0931:56.7	0.02	75	-	-	Unidentified	No	
29	0936:15.6	0.20	278	11	230.6	BA-171	Yes	
30	0815:56	0.068	276	15	266.0	AF-001	No	
30			Flight 2 hours late, no measurements made					
31	0728:54	0.39	279	17	264.0	BA-173	Yes	48
31	0811:51.5	0.35	282	9	276.5	AF-001	Yes	48
31	0942:40	0.34	280	12	263.0	BA-171	Yes	46

(1) Degrees relative to True North.

(2) Elapsed Time from measured Event to Radar Track Time CPA Hyannis, MA.

(3) Telephone check, flights arrived on time at JFK.

Note: On May 18 measurement window expanded from 0900 to 1000 hours to 0730 to 1000 hours.

Note: Flight BA-173 does not operate on Wednesday and Friday.

TABLE 1A
SECONDARY SONIC BOOM DETECTION
MALDEN MA (42°26'34"N, 71°05'07"W)

Date 1979	Time E.D.S.T.	Max. Pres. Change Peak to Peak lbs/ft²	Arriving Ray Azimuth degrees(1)	Arriving Ray Elevation degrees	Elapsed Time(2) Seconds	Flight No.	Heard by Field Technicians	Meas. SPL dBA
June								
1	0812:08.5	0.25	282	15	344.5	AF-001	Yes	
1	1000:30.3	0.25	277	15	306.3	BA-171	Yes	
4	0732:57.8	0.15	274	17	186.8	BA-173	Yes	
4	0811:16.7	0.11	281	17	266.7	AF-001	Yes	
4	0934:37.5	0.25	277	11	217.5	BA-171	Yes	
5	0732:21	0.32	276	14	299.5	BA-173	Yes	
5	0810:26.5	0.11	279	18	312.5	AF-001	Yes	
5	No measurements made					BA-171		
6	0815:11.5	0.27	278	13	336.8	AF-001	Yes	
6	0951:45.3	0.16	276	20	344.6	BA-171	Yes	
7	0746:36.3	0.25	280	16	272.1	BA-173	Yes	
7	0816:00.7	0.19	281	16	296.2	AF-001	Yes	
7	0952:54	0.29	277	17	280.0	BA-171	Yes	
8	0812:53	0.33	282	19	286.0	AF-001	Yes	
8	0933:05.7	0.12	279	18	253.7	BA-171	Yes	
11	0737:25.3	0.35	280	23	291.8	BA-173	Yes	
11	0814:29	0.10	282	24	321.0	AF-001	Yes	
11	0952:28	0.17	275	15	258.0	BA-171	Yes	
12	0749:14.5	0.22	275	8	223.8	BA-173	Yes	
12	Flight 2 hours late, no measurements made					AF-001		
12	0937:01.6	0.24	276	17	229.6	BA-171	Yes	
13	0820:30.4	0.20	279	17	257.4	AF-001	Yes	
13	0935:30	0.17	276	10	218.5	BA-171	Yes	
14	0750:11	0.49	278	13	227.5	BA-173	Yes	
14	0821:03.4	0.36	280	13	285.5	AF-001	Yes	
14	0938:17.5	0.69	277	17	248.3	BA-171	Yes	
15	0819:04.8	0.61	282	12	297.8	AF-001	Yes	
15	0959:49.3	0.64	280	5	254.0	BA-171	Yes	
18	0736:35.6	0.31	277	14	250.0	BA-173	Yes	
18	0818:46	0.27	267	25	228.5	AF-001	Yes	
18	0941:56	0.13	278	17	241.8	BA-171	No	
19	0730:46.8	0.12	278	20	95.3	BA-173	No	
19	0815:17.8	0.13	284	10	111.1	AF-001	Yes	
19	0942:53.4	0.23	279	4	100.0	BA-171	Yes	
20	0816:41	0.13	279	16	(3)	AF-001	Yes	
20	0940:57.9	0.23	280	16	248.9	BA-171	Yes	
21	0737:44.7	0.36	279	18	268.4	BA-173	Yes	
21	0816:00	0.25	281	26	287.3	AF-001	Yes	
21	0947:25	0.31	277	15	265.9	BA-171	Yes	
22	0818:59	0.13	276	23	328.0	AF-001	Yes	
22	0935:51	0.21	277	28	(3)	BA-171	Yes	
25	0744:14	0.30	279	16	205.0	BA-173	Yes	
25	0814:44.8	0.14	280	22	262.5	AF-001	Yes	
25	0941:58.5	0.32	279	4	221.9	BA-171	Yes	
26	0750:54.3	0.34	279	15	238.0	BA-173	Yes	
26	0812:02.3	0.28	281	16	262.0	AF-001	Yes	
26	Flight 3 hours late, no measurements made					BA-171		
27	0815:01.7	0.40	280	6	262.6	AF-001	Yes	
27	0943:01.8	0.28	277	29	228.0	BA-171	Yes	
28	0736:56.2	0.35	277	9	192.9	BA-173	Yes	
28	0811:22.3	0.45	280	16	230.1	AF-001	Yes	
28	0930:21.3	0.19	278	26	242.3	BA-171	No	
29	0814:20.4	0.44	282	19	269.4	AF-001	Yes	
29	0929:26.2	0.28	277	8	251.2	BA-171	Yes	

(1) Degrees relative to True North.

(2) Elapsed Time from measured Event to Radar Track Time CPA Hyannis MA.

(3) Telephone check, flight landed on time at JFK.

TABLE 1B
SECONDARY SONIC BOOM DETECTION
MALDEN MA (42°26'34"N, 71°05'07"W)

Date 1979 July	Time E.D.S.T.	Max. Pres. Change Peak to Peak lbs/ft²	Arriving Ray Azimuth degrees(1)	Arriving Ray Elevation degrees	Elapsed Time(2) Seconds	Flight No.	Heard By Field Technicians	Meas. SPL dBA
2-6	No measurements made							
	No measurements made							
9	0724:21.5				287.5	BA-173	Yes	
9	0811:16.0	0.15	-	-	257.2	AF-001	Yes	
9	0928:46.3	0.25	-	-	252.3	BA-171	Yes	
10	Flight Late, no measurements					BA-173		
10	0813:10.2	0.12	-	-	254.2	AF-001	Yes	
10	0936:28.3	0.21	-	-	229.3	BA-171	Yes	
11	0825:56.8	0.11		-	240.1	AF-001	Yes	
11	0931:53.4	0.17	-	-	193.4	BA-171	Yes	
12	0733:37.8	0.33	-	-	-	BA-173	Yes	
12	0815:19.0	0.19	-	-	237.0	AF-001	Yes	
12	0941:53.0	0.20	-	-	221.2	BA-171	Yes	
13	0813:20.6	0.18	-	-	277.0	AF-001	Yes	
13	0932:33.6	0.12	-	-	246.9	BA-171	Yes	
16	0832:42.9	0.11	279	21	-	BA-173	Yes	
16	1036:29.5	0.09	285	20	272.3	AF-001	Yes	
16	1004:13.4	0.07	282	19	264.9	BA-171	Yes	
17	0726:04.7	0.17	278	14	233.3	BA-173	Yes	
17	0810:01.3	0.15	279	27	254.3	AF-001	Yes	
17	0952:39.0	0.11	280	17	225.6	BA-171	Yes	
18	0808:14.0	0.08	280	11	239.0	AF-001	Yes	48
18	0941:02.5	0.68	274	29	202.5	BA-171	Yes	<60
19	0726:47.2	0.17	280	25	245.7	BA-173	Yes	56
19	0809:24.8	0.33	277	21	190.3	AF-001	Yes	46
19	0945:29.0	0.21	276	23	187.0	BA-171	Yes	45
20	0808:30.4	0.65	278	12	204.1	AF-001	Yes	56
20	0923:20.0	0.31	278	20	203.9	BA-171	Yes	<45
23	No measurements made					BA-173		
23	0814:16.5	0.10	-	-	239.6	AF-001	Yes	
23	0935:22.3	0.11	-	-	222.8	BA-171	Yes	54
24	No measurements made					BA-173		
24	No measurements made					AF-001		
24	No measurements made					BA-171		
25	0809:33.5	0.12	-	-	266.9	AF-001	Yes	
25	0949:33.2	0.22	-	-	278.6	BA-171	Yes	
26	0726:36.5	0.47	-	-	268.7	BA-173	Yes	56
26	0818:32.3	0.04	-	-	304.6	AF-001	No	
26	0933:05.7	0.23	-	-	270.9	BA-171	Yes	50
27	0810:36.3	0.09	-	-	-	AF-001	Yes	
27	0934:57.7	0.23	-	-	248.5	BA-171	Yes	48
30	0733:14.3	0.21	278	18	236.5	BA-173	Yes	45
30	0814:01.7	0.19	-	-	254.0	AF-001	Yes	
30	0928:01.3	0.14	-	-	244.0	BA-171	Yes	45
31	No measurements made					BA-173		
31	No measurements made					AF-001		
31	No measurements made					BA-171		

(1) Degrees re True North

(2) Elasped Time from Measured Event to Radar Track Time CPA Hyannis Ma.

TABLE 1C
SECONDARY SONIC BOOM DETECTION
MALDEN MA (42°26'34"N, 71°05'07"W)

Date 1979	Time E.D.S.T.	Max. Pres. Change Peak to Peak lbs/ft²	Arriving Ray Azimuth degrees(1)	Arriving Ray Elevation degrees	Elapsed Time(2) Seconds	Flight No.	Heard by Field Technicians	Meas. SPL dBA
August								
1	0816:33.4	0.19	282	23	281.6	AF-001	Yes	55
1	0937:33.5	0.34	277	7	244.4	BA-171	Yes	
2		No measurement made				BA-173		
2	0817:03.4	0.34	277	16	243.7	AF-001	Yes	
2	0938:55.2	0.12	276	17	217.9	BA-171	Yes	
3		Flight late no measurements				AF-001		
3		Flight late no measurements				BA-171		
6		Flight cancelled				BA-173		
6	0814:15.3	0.18	277	20	247.1	AF-001	Yes	
6	0941:06.7	0.20	278	14	232.6	BA-171	Yes	45
7		Flight cancelled				BA-173		
7	0810:32.5	.24	280	24	259.0	AF-001	Yes	
7	0941:46.0	0.59	280	19	268.9	BA-171	Yes	
8	0815:18.0	0.14	281	15	260.5	AF-001	Yes	52
8	1004:01.7	0.24	279	12	232.2	BA-171	Yes	
9		Flight cancelled				BA-173		
9	0815:51.0	0.11	282	6	237.6	AF-001	Yes	52
9		Flight cancelled				BA-171		
10	0812:47.5	0.26	280	19	267.2	AF-001	Yes	49
10		Flight late no measurements				BA-171		
13		Flight cancelled				BA-173		
13	0812:19.5	0.18	278	11	209.5	AF-001	Yes	
13	0956:07.9	0.47	276	12	216.9	BA-171	Yes	
14		Flight cancelled				BA-173		
14	0822:20.1	0.12	280	22	254.1	AF-001	Yes	
14	0943:32.3	0.26	281	23	252.2	BA-171	Yes	56
15	0817:27.2	0.30	275	1	202.2	AF-001	Yes	54
15	0943:26.6	0.23	278	1	216.1	BA-171	Yes	
16		Flight cancelled			-	BA-173		
16	0818:24.4	0.17	284	9	288.9	AF-001	Yes	47
16	0942:30.2	0.21	276	10	249.2	BA-171	Yes	
17	0814:11.6	0.36	282	18	222.0	AF-001	Yes	50
17	0948:40.0	0.30	280	12	241.5	BA-111	Yes	57
20		Flight cancelled				BA-173		
20	0812:44.5	0.13	276	10	241.7	AF-001	Yes	
20	0936:11.9	0.19	279	16	260.0	BA-171	Yes	50
21		Flight cancelled				BA-173		
21	0816:26	0.12	281	16	246.1	AF-001	Yes	
21	1106:25.8	0.29	276	10	224.5	BA-171	Yes	46
22		Flight late no measurements				AF-001		
22	0937:54.4	0.15	283		99.1	BA-171	Yes	47
23		Flight cancelled				BA-173		
23	0816:22.4	0.07	281	13	233.3	AF-001	No	
23	0941:18.3	0.16	281	16	-	BA-171	Yes	45
24	0815:08.8	0.37	282	15	288.6	AF-001	Yes	48
24	0936:51.3	0.21	279	11	244.8	BA-171	Yes	50
27	0739:42.4	0.27	277	15	219.6	BA-173	Yes	
27	0812:20.5	0.19	283	23	225.5	AF-001	Yes	48
27	0932:16.2	0.12	275	8	206.8	BA-171	Yes	
28	0735:57.2	0.12	276	18	287.9	BA-173	Yes	50
28	0806:26.2	0.06	279	5	216.7	AF-001	No	
28		Flight late, no measurement				BA-171		
29	0818:01	0.07	-	-	242.0	AF-001	No	
29	0944:26	0.08	-	-	308.5	BA-171	No	
30	0744:01	0.13	-	-	248.1	BA-173	Yes	
30	0816:42	0.06	-	-	256.0	AF-001	No	
30	0942:10	0.14	-	-	236.9	BA-171	Yes	
31	0806:46	0.10	-	-	245.9	AF-001	No	
31	0945:50	0.15	-	-	256.8	BA-171	Yes	

(1) Degrees relative to True North

(2) Elapsed Time from measured Event to Radar Track Time CPA Hyannis MA

TABLE 1D
SECONDARY SONIC BOOM DETECTION
MALDEN MA (42°26'34"N, 71°05'07"W)

Date 1979	Time E.D.S.T.	Max. Pres. Change Peak to Peak lbs/ft^2	Arriving Ray Azimuth degrees(1)	Arriving Ray Elevation degrees	Elapsed Time(2) Seconds	Flight No.	Heard by Field Technicians	Meas. SPL dBA
September								
3		No measurements made						
4	0912:48.2	0.12	-	-	253.2	BA-173	Yes	
4	0810:57.0	0.04	-	-	239.2	AF-001	No	
4		Flight cancelled				BA-171		
5	0813:25.8	0.10	-	-	220.8	AF-001	Yes	
5	0929:10.5	0.07	-	-	246.1	BA-171	No	
6		Flight late, no measurements.				BA-173		
6	0811:09	<0.01(5)	-	-	189.0	AF-001	No	
6	0956:11.3	0.11	-	-	267.3	BA-171	Yes	
7	0814:50.3	0.10	-	-	244.6	AF-001	No	
7	0947:36.0	0.25	-	-	243.9	BA-171	Yes	
10	0812:50.0	0.19	-	-	314.8	AF-001	Yes	
10	0936:10.2	0.26	-	-	268.7	BA-171	Yes	
11		No measurements made				BA-173		
11	0808:32.0	0.07	-	-	275.3	AF-001	No	
11	0935:14.1	0.16	-	-	283.6	BA-171	Yes	
12	0920:23	0.06	-	-	249.4	AF-001	Yes	
12	0941:42	0.32	-	-	231.0	BA-171	Yes	
13	0739.09	0.07	-	-	130.0	BA-173	No	
13	0825:36	0.13	-	-	149.0	AF-001	Yes	
13	0929:31	0.03	-	-	138.0	BA-171	No	
14	0821:52	0.01	-	-	273.0	AF-001	No	
14	0926:50	0.01	-	-	237.0	BA-171	No	

(1) Degrees relative to True North.

(2) Elapsed time from measured Event to Radar Track Time CPA Hyannis MA.

(5) Flight Track Approx 40 miles south of the usual JFK bound flights

NOTE: On September 14, 1979 measurement were discontinued for the 1979 season.

TABLE 1E
SECONDARY SONIC BOOM DETECTION
MISCELLANEOUS SITES

Date 1979	Time E.D.S.T.	Max. Pres. Change Peak to Peak lbs/ft²	Arriving Ray Azimuth degrees(1)	Arriving Ray Elevation degrees	Elapsed Time(2) Seconds	Flight No.	Heard by Field Technicians	Meas. SPL dBA
	Georgetown MA. (42°42' 21"N, 70°58'58"W)							
July								
9	0724:19.9	0.41	290	35	285.9	BA-173	Yes	
9	0811:14.1	0.43	293	34	255.3	AF-001	Yes	
9	0928:42.1	0.30	288	35	248.1	BA-171	Yes	
10	1013:01.9	0.32	290	36	233.2	BA-173	Yes	
10	0813:08.8	0.35	296	37	252.8	AF-001	Yes	
10	0936:23.1	0.30	289	35	224.1	BA-171	Yes	
11	0825:50.9	0.40	294	36	234.2	AF-001	Yes	54
11	0931:49.5	0.20	289	35	189.5	BA-171	Yes	48
12		No measurements made.				BA-173	Yes	
12	0815:27.0	0.15	292	37	245.0	AF-001	Yes	
12	0941:55.0	0.25	285	38	223.2	BA-171	Yes	
13	0813:21.8	0.29	292	40	278.2	AF-001	Yes	
13	0932:36.8	0.27	288	39	250.1	BA-171	Yes	
	Wilmingron MA (42°33'14"N, 71°11'13"W							
June								
20	0941:38.3	0.09	-	-	306.0	BA-171	Yes	
	Marlboro MA (42°20'30"N, 71°30'45"W)							
June								
27	0944:36.8	0.25	-	-	323.0	BA-171	Yes	
	Medfield MA (42°12'51"N, 71°16'43"W)							
June								
28	0930:58.7	0.09	-	-	279.7	BA-171	Yes	
	Cohasset MA (42°51'45"N, 70°51'26"W)							
June								
29	0928:17.7	0.18	-	-	182.7	BA-171	Yes	
	Sharon MA (42 08'20"W, 71 10'00"W)							
August								
2	0817:07.4	0.11	-	-	247.7	AF-001	Yes	
2	0941:00.8	0.19	-	-	225.7	BA-171	Yes	
	Applebachsville PA (40°29'12"N, 75°15'56"W)							
July								
23	1724:40.1	0.07	274	30	407.3(4)	AF-053	No	
24	1655:08.3	0.18	-	-	373.3(4)	BA-189	Yes	47
25		Flight late, no measurements.				AF-053		
26	1652:50.5	0.36	-	-	369.2(4)	BA-189	Yes	57
27	1729:08.7	0.27	-	-	382.1(4)	AF-053	Yes	58

(1) Degrees relative to True North.

(2) Elapsed Time from measured Event to Radar Track Time CPA Hyannis, MA.

(4) Elapsed Time from measured Event to Radar Track Time CPA Asbury Park N J.

TABLE 2. SECONDARY SONIC BOOM REPORTS

Date	Observation Time	Location
April 23	4:00 p.m.	Thompson CT
April 24	3:55 p.m.	Thompson CT
May 11	5:17 p.m.	Thompson CT
May 22	8:20 a.m.	Milton MA
	5:15 p.m.	Thompson CT
May 23	8:23 a.m.	Wilmington MA
	9:41 a.m.	Wilmington MA
May 24	8:22 a.m.	Natick MA
May 27	7:45 a.m.	Natick MA
	8:23 a.m.	West Newton MA
	9:36 a.m.	West Newton MA
	9:40 a.m.	Natick MA
	9:40 a.m.	Walpole MA
	9:40 a.m.	Wilmington MA
May 28	8:16 a.m.	West Newton MA
May 29	8:35 a.m.	West Newton MA
	9:09 a.m.	Natick MA
	9:36 a.m.	Brookline MA
	9:37 a.m.	Wayland MA
May 30	9:08 a.m.	Walpole MA
	9:34 a.m.	Walpole MA
	9 to 10 a.m.	Medfield MA
	8:15 a.m.	Wilmington MA
May 31	7:30 a.m.	Natick MA
	8:12 a.m.	Brookline MA
	8:15 a.m.	Walpole MA

TABLE 3. MEASURED AND COMPUTED ARRIVAL TIMES OF SECONDARY SONIC BOOM SIGNATUTES AT MALDEN MA SITE

Plot ID	Flight,[1]	Date	Ground Wave		Secondary Boom Type I		Secondary Boom Type II	
			Measured	Computed	Measured	Computed	Measured	Computed
a	BA	5/23	9:38:58	9:38:35	9:39:45	9:40:27	9:41:09	9:40:53
b	BA	5/29	9:34:21	9:34:25	9:35:35	9:35:26	9:36:16	9:35:48
c	AF	5/30	8:13:48	8:13:23	8:15:10	NP[3]	8:15:56	NP[3]
d	BA	5/31	9:40:29	9:40:10	9:41:48	9:41:28	9:42:40	9:42:01
e	AF	6/13	8:18:54	8:18:40	8:19:49	8:20:12	8:20.30	8:20:47
f	BA	6/13	9:33:48	9:33:43	9:34:37	9:34:38	9:35:30	9:35:16
g	BA	6/20	9:39:18	9:39:17	9:40:22	9:40:38	9:40:58	9:40:55
h	AF	6/27	8:23:24	8:13:18	8:14:14	8:14:18	8:15:02	8:14:46
i	BA	6/27	9:41:29	9:41:12	9:42:19	9:41:48	9:43:02	9:42:17
j	AF	7/18	ND[2]	8:06:28	8:07:28	8:07:39	8:08:14	8:08:04
k	BA	7/18	9:38:58	9:38:57	9:39:53	9:39:14	9:41:03	9:39:40
l	AF	7/25	ND[2]	8:07:59	8:08:56	8:08:54	8:09:33	8:09:40
m	BA	7/25	ND[2]	9:47:46	9:48:47	9:49:00	9:49:33	9:49:26

[1]BA 171 and AF 001 flights

[2]Not discernible

[3]No secondary boom predicted

TABLE 4. MEASURED AND COMPUTED ELEVATION ANGLES OF INCIDENT SECONDARY SONIC BOOM ARRIVALS AT MALDEN MA SITE

Plot ID	Flight,[1] Date	Measured Elevation Angle (Degrees)	Computed Elevation Angle[2] (Degrees)
a	BA 5/23	19	7
b	BA 5/29	11	7
c	AF 5/30	5	NP[3]
d	BA 5/31	12	6
e	AF 6/13	17	23
f	BA 6/13	10	24
g	BA 6/20	16	12
h	AF 6/27	6	22
i	BA 6/27	29	23
j	AF 7/18	11	10
k	BA 7/18	29	17
l	AF 7/25	NM[4]	17
m	BA 7/25	NM	7

1 BA 171 and AF 001 flights

2 Based on ray path of Type I arrival

3 No secondary boom predicted

4 Not measured

(See Figure 50 for data plot.)

APPENDIX A

TSC SONIC BOOM COMPUTER PROGRAM

A.1 EVOLUTION OF THE PROGRAM

A program made available to TSC for the present study was a modification by E. B. Wright, dated April 1978, of an "Atmospheric Raytrace Program" from Sandia Laboratories, Albuquerque NM. References cited in the transmitted source program listing were a 1967 Sandia Laboratories report[12] by Dr. R. J. Thompson and a 1972 article[13] in the "Journal of the Acoustical Society of America," also by Thompson.

Both the program listed in Thompson's report and Wright's modification were evidently intended for analyses of acoustic arrivals from compact explosive sources in the atmosphere. A supersonic aircraft is a considerably different type of source, but the same propagation principles apply to both cases.

In Progress Report 2 of the present study,[14] some results were reported that were computed with a somewhat tedious application of the Wright version of the program and with relatively crude approximations. Since that time, a new program has been written that builds upon certain key subroutines in the Thompson-Wright program and that is specifically intended for the interpretation of secondary sonic boom arrivals from inbound flights to JFK.

A.2 INPUT DATA

The input data to the TSC version of the program consists of meteorological data and flight track data. The format in which such data was available to us determined the choice of input format for the program.

Meteorological Data. The Air Resources Laboratory (Silver Springs MD), of the National Oceanic and Atmospheric Administration (NOAA) furnished TSC with synthesized meteorological soundings

for the Boston area for the months of May, June, and July. The sources and procedures for the synthesized profiles, as explained in a letter of June 7, 1979 from Albion D. Taylor, are as follows.

The Upper Air Branch archive tape records, which constituted one source, gives heights and temperatures for each point of a grid (grid spacing approximately 381 km or 206 nautical miles) covering the Northern Hemisphere at each of a selected set of pressure levels. The levels ordinarily used are those of 1000, 850, 700, 500, 400, 300, 250, 150, and 100 mb. The corresponding grid values of temperatures and heights for such levels are derived from the fitting of smooth fields through all available rawinsonde (balloon borne) observations; this fitting is customarily carried out by the National Weather Service (NWS) as part of its day-to-day operations. Grid values for levels of 70, 50, 30, and 10 mb were obtained in nearly the same way, but had to be specially analyzed by the Upper Air Branch.

Data corresponding to pressure levels of 5, 2, 1, and 0.4 mb were obtained by an analysis of upper atmospheric temperatures as deduced from the remote sensing of infrared radiation. The sensing of the infrared radiation from the atmosphere was done by instrumentation carried on satellites.

The gridded data with suitable interpolations yields height and temperatures for each considered pressure level for the atmosphere above Boston (whose location was taken as 71°W, 42.3°N). It also yielded the corresponding values (with finite difference computations) for the two horizontal components of the pressure gradient for each pressure level. The horizontal pressure gradient in turn, via the "geostrophic wind assumption", yields the horizontal wind components at that same point.

The computer listing supplied to us by NOAA gives, for each day and for 1200 GMT (0800 EDST), the following quantities:

a) altitude, Y(I), in meters above mean sea level

b) temperature, T(I), in °C

c) wind speed magnitude, W(I), in m/s

d) direction, D(I), in degrees, reckoned clockwise from true north, from which the wind is blowing.

Here the index I, ranging typically from 1 to 18, corresponds to increasing altitude, Y(I + 1) > Y(I), and to decreasing pressure. The symbols used here are those that appear in the FORTRAN listing of the computer program.

Flight Track Data. Tabulated data obtained by the air traffic control radar system for inbound Concorde flights into JFK were supplied to TSC by the FAA Data Systems Office of Nashua NH. These data include aircraft flight number, speed in knots, altitude, position, and time of day. The numbers that the program ordinarily requires for input are

a) height, HS(I), in hundreds of feet

b) X-coordinate, XS(I), in nautical miles

c) Y-coordinate, YS(I), in nautical miles

d) aircraft ground speed, SMACH(I), in knots

e) time of day, TAU(I), generally expressed as hour (first two digits), minutes (next two digits), and seconds (next two digits, decimal point, digit). The FAA tabulation gives time GMT but, for the summer months, we ordinarily subtract 04 from the first two digits to obtain time EDST.

The program does not actually use the input ground speed but computes it internally from the X, Y position versus time. However, unless at least one ground speed larger than 100 is input, the program interprets input data differently than as discussed in this summary.

FAA personnel in Nashua say that the X and Y coordinates in the FAA printout correspond to a good approximation to distance increments in nautical miles in eastward and northward directions, respectively. The origin is such that a point in Hyannis with latitude and longitude 41.7125°N, 70.2156°W is at X = 365.6250 and

Y = 218.3750. The conversion suggested by these numbers is

LON = 70.2156 + (365.6250 - X)/44.790

LAT = 41.7125 + (Y - 218.3750)/60.000

such that 1 degree longitude corresponds to $\Delta X = -44.790$ nautical miles, 1 degree latitude corresponds to $\Delta Y = 60.000$ nautical miles. The coordinate origin would then be 78.38 W, 38.07 N, which is in the vicinity of Charlottesville VA.

Input Format. A typical input set includes the following (see Figure A-1):

Line 1: month (integer)

day of month (integer)

year (integer)

1 if airplane is flying into JFK
1 if airplane is British Airways, 2 if airplane is Air France
1 if airplane is BA, 2 if airplane is Air France

flight number (integer)

1 if NOAA-synthesized Boston meteorological data is used.

Line 2: integer NZ giving number of weather data altitudes

NZ Lines: height, temperature, wind direction, wind speed (lines in order of increasing height)

Next Line: integer NS giving number of aircraft positions along flight track

NS Lines: aircraft height, X-coordinate, Y-coordinate, 0.0, ground speed, and time of day. (The 0.0 is input if aircraft headings are to be computed from flight trajectory. Lines must be in order of increasing time.)

A.3 REDUCTION AND SMOOTHING OF INPUT DATA

The computations produced on a given input data set consist of (1) reduction and initial processing of the input data, (2) prediction of secondary boom impact areas, (3) prediction of event

arrival times at a specified reception site, and (4) prediction of extent of primary carpet region. The first such category is discussed below.

Reduced Meteorological Data. The initial steps in the program transform the input meteorological data to a tabulation that is generally longer (35 lines) and smoother than the probable atmospheric profile over Boston. Such a tabulation appears in the output (Figure A-2) and gives altitude in meters, height in meters, wind speed in meters per second, direction from which wind is blowing in degrees, and the sound speed in meters per second. The height is simply altitude, adjusted such that the initial height is zero. The sound speed is computed from the input temperature (after smoothing) using the standard theoretical relation for the sound speed in air.

The reasons for the smoothing of the input data are (1) the accuracy of the NOAA predictions for the time of the event is probably far less than any roughness implied by the input; (2) details of such roughness even if real would not be expected to be the same all along the acoustic propagation path; (3) non-physical roughness in the meteorological profile will lead to spurious predictions of acoustical propagation that would confuse the interpretation of the calculations.

Reduced Flight Trajectory Data. The input X(t) and Y(t) tabulations are smoothed to eliminate random errors in the radar tracking. The ground speed vector is then computed by numerical differentiation, yielding dX/dt and dY/dt for each of the considered times along the flight trajectory. Subtraction of the wind velocity at the corresponding flight altitude produces the airplane's velocity relative to that of the air. The direction of that vector gives the *aircraft heading* HDG(I); division of its magnitude (air-speed) by the flight altitude sound speed gives the *Mach number*, which thereafter is referred to by the program as SMACH(I). The X and Y coordinates are converted to longitude and latitude using the equation given in Section A.2.

The present version of the program is written for inbound flights and computes the aircraft heading, assuming it is between 180° (southward) and 270° (westward). Also, the program assumes

that the initial flight track point corresponds to supersonic flight and disregards all flight track data after the speed first goes subsonic (if ever).

Another weeding-out process eliminates the first point (and then all subsequent ones) for which the Mach number and aircraft heading are such that none of the sound rays generated toward the right of the airplane reach the ground. The theoretical model is such that a ray leaving the airplane with a bearing angle θ_B in the horizontal direction must have an initial elevation angle consistent with the local geometry of the Mach cone relative to the wind. This requires in particular that the horizontal phase velocity V_p of the ray is $V_p = u_f + Mc_f \cos(\theta_B - \theta_H)$, where u_f is the wind velocity component (positive if blowing towards listener) in direction θ_B at the altitude of flight, c_f is the sound speed, θ_H is the aircraft heading, and M is the Mach number.

The acoustical model predicts that V_p is constant along any given ray path. A ray with horizontal phase velocity V_p can reach the ground only if $V_p > u_g + c_g$, where u_g and c_g are the wind velocity component (direction θ_B) and sound speed at the ground. A flight trajectory data point is considered a potential source of ground level sonic booms only if this inequality is satisfied for at least one bearing angle θ_B.

With the application of the criteria just described, the number of source points NS is in general reduced. The program prints out a listing (Figure A-3) of aircraft height in meters, longitude and latitude of airplane, heading angle of airplane, and Mach number, versus increasing time (hours, minutes, seconds format) for each input flight trajectory point that survives this scrutiny.

A.4 SECONDARY SONIC BOOM FOOTPRINTS

From each source point along the aircraft trajectory, the program traces up to 21 rays that carry secondary sonic booms from the aircraft to the ground. Two types of rays are distinguished: (1) rays that go from the airplane upwards to mesosphere and then

back to the ground and (2) rays that go from the airplane downwards to ground (as a primary boom), that are then ground-reflected, propagate up to the mesosphere, then return to the ground.

Neither type of ray is possible unless the profile of sound speed and wind succeeds in refracting the ray downward in the atmosphere. The criterion for this to occur for a given ray bearing angle θ_B is that

$$V_p < (u + c)_{max}$$

where $(u + c)_{max}$ is the maximum value of sum, wind velocity component in direction θ_B plus sound speed, that occurs among heights exceeding the height of the aircraft. Here V_p is the phase velocity defined in the preceding subsection. Combining the relations given there with that above yields.

$$u_g + c_g < u_f + Mc_f \cos(\theta_B - \theta_H) < (u + c)_{max}$$

It should be noted that ug, uf and $(u + c)_{max}$ depend on the bearing angle.

In general, there is only a narrow range (if any at all) of bearing angles for which the above criteria are satisfied, this range being typically of the order of 5°. What the program does is to trace out up to 21 rays from the aircraft that have bearing angles within this range. For each ray of a given type (I or II as defined above), the computation yields a horizontal distance over which the ray propagates from aircraft to ground and a time of transit. Results for each type of ray and for each source location are printed out in the manner indicated in Figure A-4.

The title on the printout indicates the considered secondary ray type, (I) airplane to stratosphere (mesosphere) to ground or (II) airplane to ground to stratosphere (mesosphere) to ground. Then source location (airplane altitude, longitude, and latitude) is identified, along with the airplane heading, Mach number, and the time (hours, minutes, and seconds) at which the airplane

passed through this location. Two other parameters indicate where the Malden monitoring site is with respect to this source location. The bearing of the vector pointing from source to Malden is in degree clockwise from true north. The distance to Malden is printed in kilometers, where 1 km = 0.54 nautical miles.

In the accompanying ray tabulation, the computed rays are numbered in the order of increasing bearing angle. For each such ray, the ray range (horizontal distance travelled) is given in kilometers. This range typically begins large, decreases to a minimum, then increases to a slightly higher value, when the bearing angle runs through the range of possible values. The reason for this behavior is well understood in terms of the overall ray paths. The minimum coincides with where the *ray caustic* (surface where adjacent rays intersect) touches the ground.

The tabulation also gives the longitude and latitude of the point at which each ray touches the ground and the time (hours, minutes, and seconds) at which this occurs. (Such computations of course depend on the location of the source and the time of ray launching.) The transit time of the ray along the path is in a minutes and seconds format. The miss distance printed is the distance of the ray arrival point from the Malden site.

The line traced out on the earth's surface by the ray arrival points from any one such tabulation gives what is here termed a "footprint." The airplane generates one such footprint of each type from each point along its flight trajectory. The set of all footprints of a given ray type (I or II) covers an area of the map which roughly coincides with where the secondary booms of that type are expected to impact. The density of rays (rays per unit area of ground surface) gives a rough indication of how intense the arrivals may be expected to be. Since the density is higher for portions of the impacted region that are closer to the flight track, the quantities of greatest interest are the focus lines. The focus line for type I rays is always closer to the flight track than that for type II rays. The program does not actually determine and plot these inner envelope lines, but such are easily derived by hand-plotting a sequence of ray footprints on a map.

A.5 RECEPTION TIME COMPUTATIONS

For each secondary boom ray type, the program endeavors to find the ray that comes closest to the Malden site. All the rays successively computed are compared according to their "miss distances" and detailed intermediate results are kept stored for the closest ray found. Successive iterations give progressively closer rays.

Figure A-5 shows typical output regarding such a "closest" ray. The listing gives that ray's miss distance and detailed information concerning the point on the aircraft trajectory from which the ray was launched. Also listed is the closest ray's range (horizontal distance traveled), transit time and bearing angle.

The interpretation of such output depends on whether the Malden site falls on the near side or far side of the corresponding inner envelope line. If it falls on the far side (typical for the type I secondary boom carpet), then further narrowing of the intervals between successively considered points along the aircraft trajectory and an interpolation will in principle yield a ray (possibly more than one) that connects the trajectory with the Malden site. In such a case, the information of most interest include (1) the time the ray arrives at Malden, (2) the direction the ray appears to be heading when it reaches Malden, and (3) the elevation angle which the incoming ray makes with the ground. These are parameters that can be compared with numbers extracted from analysis of the received signals at Malden. Secondary quantities computed by the program (Figure A-6) are the ray's phase velocity, the angle it makes with the horizontal when it is launched, and the maximum height the ray reaches before it turns back towards the ground. The program also lists the complete trajectory for that ray; range and height versus time. Also listed is the effective atmospheric profile for the corresponding bearing angle (Figure A-7): U(Z) is the wind speed component blowing parallel to vertical plane of ray towards Malden, S(Z) is the effective sound speed C(Z) + U(Z).

On the other hand, if the Malden site lies on the near side of the inner envelope line (typical for the type II secondary boom carpet), the smallest miss distance is an estimate of how far the site is from that line. The refined theory, in which geometrical acoustics is modified to include full-wave effects, predicts arrivals on the near side of the envelope line as well as on the far side, but predicts that such arrivals are weaker the further away from the line the listener falls. Consequently, the computed minimum miss distance should be negatively correlated with amplitudes.

An estimated time of arrival of type II secondary booms at Malden when the site lies between the two envelope lines (the usual case) is computed with the assumptions that: (1) the type II arrival has the same launch point and azimuth as does the type I arrival; (2) the time difference between type I and type II arrival times is independent of range and may therefore be extracted from computed ray arrival times at a point further on beyond Malden where both rays are actually received.

A.6 PRIMARY CARPET

The primary carpet generated by a supersonic flight consists of all points that receive direct rays from the aircraft trajectory without intervening excursions to the mesosphere. The rays generated at a given point on the flight trajectory that are proceeding obliquely downwards reach the ground only if

$$u(z) + c(z) \leq u_f + Mc_f \cos(\theta_B - \theta_H)$$

for all heights z that are below the height of the airplane. Here the various symbols are as defined in Section A.3; the right side of the inequality is also the phase velocity V_p.

A ray satisfying the criteria:

$$u_g + c_g = u_f + Mc_f \cos(\theta_B - \theta_H)$$
$$u(z) + c(z) < u_g + c_g; \quad 0 < z < z_f$$
$$(d/dz)\left(u(z) + c(z)\right) \leq 0; \quad z=0$$

is such that it propagates to the ground and there just grazes the ground. Its phase velocity marks the borderline between where rays reflect and where they bend back upwards before they touch the ground. The point at which it touches the ground should therefore lie on the border between where rays touch the ground and where they do not touch the ground; the former region is the *primary carpet*.

In the program's computation of the primary carpet border (see Figure A-8), the first of the three equations above is solved numerically for θ_B. The value of θ_B found (should more than one exist) is that corresponding to the smallest positive $\theta_B - \theta_H$ (or the northwest side of the primary carpet for inbound flights). The present version of the program does not test whether the other two criteria are met; the input meteorological data is such that the check need not be made.

Once θ_B is found, the program calculates the corresponding limiting ray, from aircraft trajectory to carpet edge. The tabulation (Figure A-8) lists, for each aircraft position, the ray launch time (hours, minutes, and seconds), which is the time the airplane passes through the point from which the ray under consideration was launched. The tabulation gives the bearing angle of the limiting ray and the distance (km) it travels before it touches the ground. The longitude and latitude of that point is also printed, as well as the time that it takes the ray to traverse that distance.

Other columns in the tabulation relate to the estimation of the properties of the ground wave that passes the Malden site. The ground wave is a very weak arrival that travels to the edge of the primary carpet along the geometrical acoustics limiting ray and that thereafter travels with the same bearing along the ground with speed $c_g + u_g$ Thus each limiting ray to the primary carpet edge generates a ground wave ray that travels along the ground in the same general direction. One (or more) such ground

wave ray passes through the Malden site. The tabulation in Figure A-8 consequently lists the distance by which each computed ground wave path misses Malden. Interpolation consequently will give the time at which the ground wave passing through the Malden site was launched.

An estimate of ground wave arrival time at the Malden site comes from an extended version of *Fermat's principle of least time.* The principle, which is founded on basic acoustical theory, states that, if one takes any given point on the flight trajectory and computes the ficticious arrival time FERMAT, equal to

$$\text{FERMAT} = \text{LNCHTM} + \text{RAYTM} + \text{EXTMN}$$

then FERMAT is later than the actual ground wave arrival time at Malden. Here LNCHTM is the time the grazing ray was launched, RAYTM is the transit time along the grazing ray to the primary carpet edge, and EXTMN is the time it would take sound to travel in a straight line (skewed with respect to the grazing ray) along the ground from the grazing ray touch-down point to the Malden site. The speed along the latter leg of the hypothetical path is that appropriate to the bearing angle from the touch-down point to Malden.

The minimum value of the computed value of FERMAT in the tabulation yields an estimate of the actual ground wave arrival time in Malden and also corresponds to the smallest miss distance.

```
6,20,1979,1,1,171,1
18
236.,16.,41.,7.
1598.,8.,37.,10.
3168.,-1.,33.,11.
5766.,-18.,6.,15.
7392.,-30.,358.,17.
9375.,-44.,349.,18.
10577.,-51.,341.,18.
12019.,-52.,336.,15.
13877.,-53.,333.,9.
16480.,-55.,25.,2.
18749.,-56.,349.,4.
20898.,-54.,6.,3.
24194.,-51.,51.,3.
31657.,-34.,55.,9.
36614.,-27.,83.,24.
43422.,-12.,84.,31.
48791.,-5.,78.,31.
55869.,-9.,77.,26.
18
548.,556.56,282.75,0.0,990.,92059.0
550.,550.00,280.50,0.0,990.,92123.0
552.,542.25,277.75,0.0,990.,92147.0
551.,500.12,263.37,0.0,990.,92411.0
552.,472.62,254.25,0.0,960.,92559.0
549.,467.31,252.06,0.0,950.,92623.0
538.,462.25,250.50,0.0,890.,92647.0
523.,457.25,249.06,0.0,880.,92711.0
515.,454.68,247.12,0.0,880.,92723.0
506.,452.31,247.12,0.0,870.,92735.0
495.,449.93,246.18,0.0,850.,92747.5
483.,447.50,245.75,0.0,800.,92759.0
467.,442.93,244.12,0.0,790.,92823.0
459.,440.56,243.37,0.0,790.,92835.0
451.,438.43,242.43,0.0,780.,92847.0
442.,436.25,242.00,0.0,770.,92859.0
432.,434.06,241.18,0.0,760.,92911.0
423.,432.06,240.56,0.0,750.,92923.0
```

FIGURE A-1. SAMPLE INPUT DATA FOR TSC SONIC BOOM COMPUTER PROGRAM

DATE OF FLIGHT= 6/20/1979
DESTINATION 1=JFK,2=DULLES 1
1=BRITISH AIRWAYS,2=AIR FRANCE 1
FLIGHT NUMBER 171
WEATHER DATA 1=BOSTON,2=WALLOPS 1

I	ALTITUDE(M)	HEIGHT(M)	WIND(M/S)	DIR(DEG)	SOUND(M/S)
1	336.	0.	7.1	4.	342.18
2	917.	651.	8.4	39.	339.34
3	1598.	1362.	9.9	37.	336.60
4	2383.	2147.	10.4	34.	333.61
5	3168.	2932.	11.1	29.	330.65
6	4467.	4231.	12.8	17.	325.55
7	5766.	5530.	14.9	2.	320.13
8	6579.	6343.	15.6	0.	316.54
9	7392.	7156.	17.7	358.	312.62
10	8384.	8148.	17.3	355.	308.29
11	9375.	9139.	17.0	353.	303.87
12	9976.	9740.	14.1	349.	301.59
13	10577.	10341.	11.3	341.	299.93
14	11298.	11062.	10.1	329.	298.86
15	12019.	11783.	10.4	317.	298.30
16	12942.	12706.	11.4	307.	297.91
17	13867.	13631.	9.1	298.	297.51
18	14779.	14543.	7.4	296.	296.97
19	16400.	16164.	2.7	327.	296.35
20	17615	17379.	1.1	1.	296.03
21	18749.	18513.	3.2	1.2	296.01
22	19824	19588.	1.4	1.	296.34
23	20891.	20655.	1.8	11.	296.90
24	22216.	21980.	1.1	31	299.14
25	23774.	23538.	1.8	72.	299.84
26	27952.	27690.	7.1	94.	304.63
27	33657.	33421.	7.8	87.	309.42
28	34456.	34220.	11.1	86.	313.40
29	36614.	36378.	13.2	78.	317.30
30	40016.	39780.	18.1	82.	319.39
31	41442.	41206.	19.1	87.	323.36
32	44107.	43871.	30.1	91.	325.70
33	48791.	48555.	50.3	77	326.87
34	52326.	52090.	39.3	76.	326.81
35	53879.	53643.	28.1	77.	326.16

FIGURE A-2. REDUCED METEOROLOGICAL DATA PRINTOUT

HEIGHT(M)	LON(DEG)	LAT(DEG)	HDG(DEG)	MACH	HRMINSEC
16703.	65.9483	42.7867	251.3	2.00	92059.0
16764.	66.1080	42.7455	251.3	1.96	92123.0
16793.	66.2642	42.7054	251.4	1.92	92147.0
16815.	67.1782	42.4724	251.4	1.74	92411.0
16778.	67.8182	42.3093	251.3	1.68	92559.0
16652.	67.9435	42.2769	251.2	1.62	92623.0
16358.	68.0579	42.2469	251.2	1.44	92647.0
15934.	68.1706	42.2164	251.7	1.37	92711.0
15687.	68.2258	42.2023	252.3	1.34	92723.0
15407.	68.2796	42.1892	253.1	1.31	92735.0
15068.	68.3352	42.1771	253.7	1.29	92747.5
14779.	68.3853	42.1656	253.7	1.28	92759.0
14234.	68.4905	42.1409	253.4	1.25	92823.0
13990.	68.5408	42.1285	253.3	1.23	92835.0
13736.	68.5905	42.1163	253.4	1.20	92847.0
13462.	68.6389	42.1045	253.6	1.18	92859.0

FIGURE A-3. REDUCED FLIGHT TRAJECTORY DATA PRINTOUT

FOOTPRINT OF RAYS FROM AIRPLANE TO STRATOSPHERE TO GROUND

SOURCE ALTITUDE=	15406.6	METERS
SOURCE LONGITUDE	68.28	DEGREES
SOURCE LATITUDE	42.19	DEGREES
AIRCRAFT HEADING	253.1	DEGREES
MACH NUMBER=	1.31	
TIME OF RAY GENERATION=	92735.	
BEARING TOWARDS MALDEN=	276.9	DEGREES
RANGE TO MALDEN=	234.41	KM

I	RANGE	BEARING	LONGITUDE	LATITUDE	TIME AP	TIME TRANS	MISS
1	377.664	276.765	72.801	42.722	94659.	1924.	143.259
2	337.276	276.932	72.316	42.503	94504.	1701.	102.869
3	258.297	277.099	71.370	42.476	94124.	1349.	23.906
4	254.365	277.265	71.322	42.479	94113.	1338.	20.010
5	250.100	277.432	71.270	42.480	94101.	1326.	15.852
6	245.372	277.598	71.212	42.481	94087.	1312.	11.345
7	239.926	277.764	71.146	42.481	94032.	1257.	6.571
8	233.258	277.930	71.065	42.479	94013.	1238.	4.347
9	223.105	278.095	70.943	42.472	93944.	1209.	12.264
10	213.671	278.261	70.829	42.465	93917.	1142.	21.404
11	212.899	278.426	70.819	42.470	93915.	1140.	22.313
12	212.144	278.591	70.809	42.474	93913.	1138.	23.212
13	211.387	278.755	70.798	42.479	93911.	1136.	24.119
14	210.647	278.920	70.789	42.483	93909.	1134.	25.015
15	209.913	279.084	70.779	42.487	93907.	1132.	25.909
16	209.205	279.248	70.769	42.492	93905.	1130.	26.783
17	208.550	279.412	70.760	42.496	93903.	1128.	27.611
18	207.955	279.576	70.752	42.501	93901.	1126.	28.387
19	207.491	279.739	70.745	42.505	93900.	1125.	29.046
20	207.310	279.902	70.742	42.510	93860.	1125.	29.452
21	208.107	280.065	70.750	42.516	93902.	1127.	28.988

FIGURE A-4. SAMPLE SECONDARY SONIC BOOM FOOTPRINT USED IN DETERMINATION OF TYPE I FOCUS LINE

```
RAY CLOSEST TO MALDEN.     LONGITUDE=-71.0852     LATITUDE=42.4427

JUST FINISHED  1-TH ITERATION
MISS DISTANCE IN METERS=                4347.3
AIRPLANE HEIGHT IN METERS=             15406.62
AIRPLANE LONGITUDE=                     68.2796
AIRPLANE LATITUDE=                      42.1872
AIRPLANE HEADING IN DEGREES=              253.1
AIRPLANE MACH NUMBER=                      1.31
TIME OF RAY LAUNCHING=                92735.0
BEARING TOWARDS MALDEN=                 276.90
DISTANCE IN METERS TO MALDEN=         234406.70
WESTWARD GROUND SPEED (M/S)=            372.36
NORTHWARD GROUND SPEED (M/S)=          -118.29


BEST RAY SO FAR WAS
 RANGE=          233258.1   M
 TRANSIT TIME=      759.0   SEC
 BEARING=           277.9   IN DEGREES


ESTIMATION OF LAUNCH POINT OF RAY REACHING MALDEN
```

FIGURE A-5. SAMPLE OUTPUT REGARDING AIRCRAFT POSITION AND FLIGHT PARAMETERS AT TIME OF LAUNCHING OF RAY THAT GOES TO MEASUREMENT SITE

```
RAY CLOSEST TO MALDEN,     LONGITUDE=71.0852     LATITUDE=42.4427

MISS DISTANCE IN METERS=              44672.1
AIRPLANE HEIGHT IN METERS=          15934.44
AIRPLANE LONGITUDE=                   68.1706
AIRPLANE LATITUDE=                    42.2164
AIRPLANE HEADING IN DEGREES=            251.7
AIRPLANE MACH NUMBER=                    1.37
TIME OF RAY LAUNCHING=                92711.0
BEARING TOWARDS MALDEN=                275.94
DISTANCE IN METERS TO MALDEN=      243050.75
WESTWARD GROUND SPEED (M/S)=           385.36
NORTHWARD GROUND SPEED (M/S)=         -131.85
GROOUP VELOCITY=                       298.35  M/S
PHASE VELOCITY=                        338.48  M/S
ANGLE BETWEEN RAY AND GROUND=           10.60  DEGREES
MAXIMUM HEIGHT OF RAY=              42802.31   METERS
TRANSIT TIME OF RAY=                  935.6    SECONDS



RAY PARAMETER=                         350.50  M/S
RAY BEARING ANGLE=                     281.73  DEGREES
RAY TYPE  1=UP,2=DOWN                       2
INITIAL ANGLE WITH HORIZONTAL=          32.68  DEGREES
```

FIGURE A-6. SAMPLE OUTPUT REGARDING RAY TOUCHING GROUND AT POINT CLOSEST TO MEASUREMENT SITE

ATMOSPHERE MODEL
SOURCE CORRESPONDS TO I= 18
RAY BEARING= 277.93 DEGREES

I	Z(M)	U(M/S)	C(M/S)	S(M/S)
1	0.0	3.9	342.2	346.0
2	681.0	4.3	339.3	343.6
3	1362.0	4.6	336.6	341.2
4	2147.0	4.5	333.6	338.2
5	2932.0	4.0	330.7	334.6
6	4231.0	2.1	325.5	327.6
7	5530.0	-0.2	320.1	320.0
8	6343.0	-1.6	316.5	314.9
9	7156.0	-2.9	312.8	309.9
10	8147.5	-4.4	308.3	303.9
11	9139.0	-6.0	303.9	297.9
12	9740.0	-6.9	301.6	294.7
13	10341.0	-7.6	299.9	292.4
14	11062.0	-7.8	298.9	291.1
15	11783.0	-7.5	298.3	290.8
16	12712.0	-6.2	297.9	291.7
17	13641.0	-4.6	297.5	292.9
18	14724.6	-2.5	297.0	294.5
19	14942.5	-2.1	296.9	294.8
20	16244.0	-0.7	296.3	295.7
21	17378.5	-0.3	296.0	295.7
22	18513.0	-0.5	296.0	295.5
23	19587.5	-0.4	296.3	295.9
24	20662.0	0.2	296.9	297.1
25	22310.0	1.5	298.1	299.6
26	23958.0	2.7	299.8	302.5
27	27689.5	5.7	304.6	310.3
28	31421.0	10.3	309.4	319.7
29	33899.5	14.9	312.4	327.3
30	36378.0	20.1	315.3	335.4
31	39782.0	25.5	319.4	344.8
32	43186.0	28.5	323.4	351.9
33	45870.5	29.2	325.7	354.9
34	48555.0	28.8	326.9	355.7
35	52094.0	27.6	326.8	354.4
36	55633.0	26.2	326.2	352.3

FIGURE A-7. SAMPLE OUTPUT GIVING EFFECTIVE SOUND SPEED PROFILE FOR PROPAGATION OF RAYS FROM FLIGHT TRACK TO MEASUREMENT SITE

PRIMARY CARPET AND GROUND WAVE

LNCHTM= TIME OF GRAZING RAY LAUNCH
GWBRG= BEARING IN DEGREES OF GRAZING RAY
GWRNG= RANGE IN NM OF GRAZING RAY
LON= LONGITUDE OF CARPET EDGE
LAT= LATITUDE OF CARPET EDGE
RAYTM= TIME GRAZING RAY TOUCHES GROUND
EXTTM= EXTRA TIME REQUIRED TO REACH MALDEN
BRGTM= BEARING FROM TOUCHDOWN TO MALDEN
MISS= MISS DISTANCE IN KM OF GROUND WAVE
FERMAT= FERMAT PRINCIPLE PREDICTED ARRIVAL TIME

LNCHTM	GWBRG	GWRNG	LON	LAT	RAYTM	EXTMM	BRGTM	MISS	FERMAT
92059.	305.7	45.76	66.40	43.03	157.2	1134.3	260.5	-279.9	94230.
92123.	304.9	45.97	66.56	42.98	157.9	1092.8	260.9	-263.6	94214.
92147.	304.1	46.11	66.72	42.94	158.3	1052.6	261.3	-248.3	94158.
92411.	299.4	46.75	67.67	42.68	159.8	819.3	264.7	-161.8	94030.
92559.	293.5	47.51	68.34	42.48	161.5	655.6	269.0	-94.4	93936.
92623.	290.9	47.69	68.48	42.43	161.6	622.9	270.4	-79.6	93928.
92647.	287.1	47.79	68.61	42.37	161.1	593.0	272.1	-63.0	93921.
92711.	283.1	47.76	68.73	42.31	159.9	565.1	274.2	-30.2	93916.
92723.	281.4	47.64	68.79	42.29	159.0	552.2	275.2	-20.8	93914.
92735.	280.1	47.41	68.84	42.26	157.7	540.3	276.1	-13.1	93913.
92748.	278.6	47.12	68.90	42.24	156.1	528.4	277.0	-5.1	93912.
92759.	277.0	46.95	68.95	42.22	155.0	517.6	278.0	3.3	93912.
92823.	272.7	46.87	69.05	42.16	153.4	495.4	280.5	23.3	93912.
92835.	269.7	47.05	69.11	42.13	153.3	485.3	282.1	36.0	93914.
92847.	265.2	47.52	69.16	42.08	153.8	476.4	284.1	53.3	93917.
92859.	257.2	48.72	69.21	42.01	156.1	471.7	287.3	81.6	93927.

FIGURE A-8. SAMPLE OUTPUT DESCRIBING BORDER OF SONIC BOOM PRIMARY CARPET

REFERENCES

1. Grover, F.H., "Geophysical Effects of Concorde Sonic Boom", Quart. J. Roy. Astron. Soc., 14, (1973), p. 141-158.

2. Balachandran, N.K., W.L. Donn, and D.H. Rind, "Concorde Sonic Booms as an Atmospheric Probe", Science, 197, (July 1, 1977), p. 47-49.

3. Donn, W.L., "Exploring the Atmosphere with Sonic Booms", American Scientist, 66, (1977), p. 724-733.

4. Whipple, F.J., "The Propagation of Sound to Great Distances", Quart. Journ. Roy. Met. Soc., 61 (1935), p. 285-308.
Donn, W.L., and D. Rind, "Natural Infrasound as an Atmospheric Probe", Geophys. Journ. Roy. Astron. Soc., 26, (1971), p. 111-133.

5. Rogers, P.H., and J.H. Gardner, "Propagation of Sonic Booms in the Thermosphere", Journ. Acoust. Soc. Amer., (1980), 67, p. 78-91.

6. George, A.R., and Y.N. Kim, "High Altitude, Long-Range Sonic Boom Propagation", Journ. Aircraft, 16, (1979), p. 637-639.

7. Perkeris, C.L., "Theory of Propagation of Sound in a Half-Space of Variable Sound Velocity under Conditions of Formation of a Shadow Zone", Journ. Acoust. Soc. Amer., 18, (1946), p. 295-315.

8. Pridmore-Brown, D.C., and U. Ingard, "Sound Propagation into a Shadow Zone in a Temperature-Stratified Atmosphere above a Plane Boundary", Journ. Acoust. Soc. Amer., 27, (1955), p. 36-42.

9. Onyeonwu, R., "Diffraction of Sonic Boom Past the Nominal Edge of the Corridor", Journ. Acoust. Soc. Amer., 58, (1975), p. 326-330.

10. Pierce, A.D., Acoustics: An Introduction to Its Physical Principles and Applications, (New York, McGraw-Hill, in press), ch. 9.

11. Pierce, A.D., and D.J. Maglieri, "Effects of Atmospheric Irregularities on Sonic-Boom Propagation", Journ. Acoust. Soc. Amer., 51, (1972), p. 702-721.

12. Thompson, R.J., "Computing Sound Ray Paths in the Presence of Wind", SC-RR-67-53, Sandia Laboratory, Albuquerque NM, (February 1967).

REFERENCES (CONTINUED)

13. Thompson, R.J., "Ray Theory for an Inhomogeneous Moving Medium", Journ. Acoust. Soc. Amer., 51, (1972), p. 1675-1682.

14. Rickley, E.J., and A.D. Pierce, "Detection and Assessment of Secondary Sonic Booms in New England", DOT-TSC-FA953-PR-79-2, (October 1979).